Prediction of Travel Time and Development of Flood Inundation Maps for Flood Warning System Including Ice Jam Scenario. A Case Study of the Grand River, Ohio

by

Niraj Lamichhane

Submitted in Partial Fulfillment of the Requirements

for the Degree of

Master of Science in Engineering

in the

Civil and Environmental Engineering Program

YOUNGSTOWN STATE UNIVERSITY

May, 2016

Prediction of Travel Time and Development of Flood Inundation Maps for Flood Warning System Including Ice Jam Scenario. A Case Study of the Grand River, Ohio

Niraj Lamichhane

I hereby release this thesis to the public. I understand that thesis will be made available from the OhioLINK ETD Center and the Maag Library Circulation Desk for public access. I also authorize the University or other individuals to make copies of this thesis as needed for scholarly research.

Signature:

Niraj Lamichhane, Student Date

Approvals:

Suresh Sharma, Thesis Advisor Date

Tony Vercellino, Committee Member Date

Bradley A. Shellito, Committee Member Date

Dr. Salvatore A. Sanders, Dean of Graduate Studies Date

ABSTRACT

The flood warning system can be effectively used to reduce the potential property damages and loss of lives. Therefore, a reliable flood warning system is required for the evacuation of people from probable inundation area in sufficient lead time. Hence, this study was commenced to predict the travel time and generate inundation maps along the Grand River, Ohio for various flood stages. A widely accepted hydraulic tool, Hydraulic Engineering Center River Analysis System (HEC-RAS), was used to perform the hydraulic simulation. HEC-GeoRAS, an ArcGIS extension tool, was used to prepare geospatial data and generate flood inundation maps for various flood stages. A topographic survey was conducted to obtain the accurate elevation of river channels. The hydraulic simulations were carried out using six different elevation datasets and various ranges of Manning's roughness to quantify the uncertainties in travel time and inundation area prediction due to the resolutions of the elevation datasets and Manning's roughness. The study showed that the coarse elevation dataset, which was 30m Digital Elevation Model (DEM) without integration of survey data, provided higher travel time and inundation area. It over predicted (11.03%-15.01%) in travel time and inundation area (32.56%-44.52%) for various return period floods when compared with the results of Light Detection and Ranging (LiDAR) integrated with survey data. Moreover, Manning's roughness was found to be more sensitive in channel sections than that of floodplains. The decrease in travel time and inundation area was observed with the decrease in manning's roughness. The highest decrement of 21.38% and 8.97% in travel time and inundation area was observed when roughness value was decreased in channel sections, while the decrement in travel time and inundation area was 3.45% and 1.49% when roughness value was decreased in floodplains. The difference in predicted travel time and

inundation area, while using LiDAR integrated with survey data, was not considerably different from 10m DEM integrated with survey data. However, LiDAR with survey data predicted conservative travel time which would be safe to consider for the evacuation planning from probable inundation areas. Therefore, LiDAR integrated with survey data was used for the calculation of travel time and generation of flood inundation maps for 12 different selected flood stages. The estimated travel time can be used for the evacuation of the people. Similarly, the rating curve and the flood inundation maps can be used to issue flood warning. More than 100 houses, many roads, bridges and parks along the Grand River are susceptible to 500 year return period flood. Therefore, it is suggested to install the siren system in various locations of the river.

In addition, winter flooding due to ice jams is one of the major problems as it has caused severe damages along the Grand River and nearby bridge structures frequently. Therefore, the effects of ice cover and ice jams on the river level near bridges were investigated. The increase in river stage and inundation area was observed, when ice cover and ice jam was considered in the simulation. The average increase in river stage was approximately 2 ft for maximum winter discharge. Likewise, the increase in inundation area varied from 24% to 52% for various winter flows resulting in the highest increment for the lowest winter discharge. In addition, the increase in river stage was noticed at the upstream section of bridges during winter when the model was simulated considering bridges. The effects of resolution of elevation datasets and ice jam/ice cover in flood travel time and inundations maps would be valuable assets for decision makers and planners for flood management and rescue operation in future.

ACKNOWLEDGEMENTS

First of all, I would like to convey my sincere thanks to my thesis advisor, Dr. Suresh Sharma, for his continuous guidance and encouragement while conducting this research. Also, I would like to express my sincere gratitude to thesis committee members, Dr. Tony Vercellino and Dr. Bradley A. Shellito for their willingness to serve in my thesis committee and provide valuable suggestions and feedbacks. Moreover, I am thankful to the Department Chair Dr. Anwarul Islam and Dr. Peter Kimosop for their worthful guidance and suggestions.

I would like to acknowledge for the grant support provided by Ohio Sea Grant to conduct this research. I would also like to extend my earnest thanks to Greg Koltun of USGS Ohio Water Science Center and Kirk Dimmick of Lake County Office, who provided the necessary research data for this study. Also, I am much obliged to Chrisopher R. Goodel, author of HEC-RAS User's and Hydraulic Reference Manuals, for providing ideas and suggestions to calibrate/validate the hydraulic model.

I am very much thankful to Linda Adovasio for her support and assistance at YSU. I am immensely grateful to all of my friends who helped and encouraged me at various stages during the research works and thesis writing.

Last but not the least, I am highly obliged especially to my father Hem Raj Lamichhane and my mother Pushpa Lamichhane, who inspired and motivated me to study and work on my thesis by taking all the family responsibilities and difficulties. Also, I would like thank to my sisters Nisha Lamichhane and Nita Lamichhane for their continuous support and encouragement to complete this research.

Table of Contents

LIST OF FIGURES

LIST OF TABLES

LIST OF ABBREVIATIONS

AFDD	Accumulated Freezing Degree Days
ALERT	Automated Local Evaluation in Real Time
CRREL	Cold Regions Research and Engineering Laboratory
DEM	Digital Elevation Model
FEMA	Flood Emergency Management Agency
GIS	Geographic Information System
GOES	Geostationary Operational Environmental Satellite
GPS	Global Positioning System
HEC-RAS	Hydraulic Engineering Center River Analysis System
HUC	Hydrologic Unit Code
LiDAR	Light Detection and Ranging
NCDC	National Climatic Data Center
NLCD	National Land Cover Database
NOAA	National Oceanic and Atmospheric Administration
NRCS	National Resource Conservation Service
NSE	Nash-Sutcliffe Efficiency
NWS	National Weather Service
ODOT	Ohio Department of Transportation
OGRIP	Ohio Geographically Referenced Information Program
PBIAS	Percent Bias
RMSE	Root Mean Square Error
SFIP	Standard Flood Insurance Policy

TDD	Thawing Degree Days
USD	United States Dollars
USGS	United States Geological Survey
USDA	United States Department of Agriculture
USACE	United States Army Corps of Engineers
USACE-HEC	United States Army Corps of Engineers-Hydrologic Engineering Center

Chapter 1. Introduction

Flooding is one of the most common natural disasters, which damages billions of dollars' worth of properties and takes the lives of many people each year (Wardsworth, 1999). Floods affect approximately 520 million people around the world, and global economic losses due to flooding are in between 50 to 60 billion USD annually (Van et al., 2011). In the United States alone, more than 75% of Federal disasters are associated with flooding, which leads to an annual average death of over 80 people and properties loss of approximately 8 billion USD (USGS, 2016). Potential losses due to flooding can be reduced by providing reliable information to the people about the risks of flood by means of flood warning system.

The Grand River is one of such rivers, which has flooded the City of Painesville and nearby cities in Northeastern Ohio time and again. Having experienced extremely wet June and July in Northeastern Ohio, the City of Painesville and adjoining cities were flooded by the Grand River due to incessant rainfall and thunderstorms of July 27-28, 2006. Property damages of worth 30 million USD were reported due to this flood. The United States Geological Survey (USGS) streamflow gage station at Grand River near Painesville, Ohio recorded a highest streamflow with an estimated recurrence period of approximately 500 years. Consequently, three counties, including Lake County of Northeastern Ohio were declared as Federal and State disaster areas. Flooding in the City of Painesville and the Lake Erie coastal zone was also experienced at various times of 2006, 2008 and 2011, with considerable damages and loss of the properties. Therefore, development of a flood warning system is essential for this region.

However, proper selection of input data, its resolution and modeling technique have been always crucial issues for the development of flood warning system. While significant advancement have been achieved in hydraulic and hydrologic modeling, the type of input data that would result the minimum error and accurate estimation of travel time in connection with flood warning system is still a matter of investigation. In addition, quantification of error, that will propagate while selecting the coarse resolution of the elevation datasets and selection of Manning's roughness, is equally important. Some research (Cook et al., 2009; Merwade et al., 2008) have been done in the past related to the effect of the resolution of elevation datasets in flood inundation areas. However, the effects of elevation datasets in flood travel time of various return periods have not been studied yet. Hence, the current study will quantify the error to the predicted travel time and inundation areas while using various resolutions of elevation datasets and various ranges of Manning's roughness.

Furthermore, river ice cover and ice jam processes are crucial during winter in Northern region of United States which might lead to dangerous flooding. Ice jams occur in the river during transitional time between freeze-up time and breakup time of winter period. Freeze-up time refers to the beginning time of ice season, whereas breakup time refers to the ending period of the ice season. Ice jams occur due to the complex interaction of climatic factors like weather, river geometry, streamflow and the type of ice in the river leading to complexities to forecast (Daly and Vuyovich, 2007). These jams have possibilities to increase the river stage suddenly with high chances of flooding creating economic and ecological impacts in the environments (Beltaos, 2010). In addition to the City of Painesville, many cities and towns in the Northern Ohio have been

flooded from time to time due to extreme weather patterns associated with ice jam. Flood prediction in this region is relatively complex because of the combined effect of ice jams and rainfall following after snowfall. Very few studies have been conducted pertaining to ice jam and its potential hazard using Hydraulic Engineering Center River Analysis System (HEC-RAS) especially in the United States. More importantly, evaluation of the impact of ice cover and ice jam flooding near hydraulic structure is essential to realize whether the ice jams near hydraulic structures have any additional impact on flood level or not. Therefore, development of a flood warning system, with frequently updated flood inundation maps incorporating careful analysis of ice cover and ice jams effect, is essential to ensure timely evacuation and reduction of the loss of lives and properties. For this, a reliable hydraulic model should be developed using appropriate sets of input data.

A widely accepted hydraulic model HEC-RAS 4.1 was used to setup the model and run the hydraulic simulation for the Grand River watershed in Northeastern, Ohio. HEC-RAS model was calibrated and validated to quantify the uncertainties involved in calculating flood travel time, generation of inundation maps and study the effects of ice cover and ice jam in river stage and near the hydraulic structures. All these scenarios have been described in subsequent chapters.

Scope and Objectives

Flood warning system and flood inundation maps are the necessary tools that can be used to reduce the human and property losses. Inundation maps are useful for preparedness before the occurrence of floods, timely response to future floods, damage assessment, mitigation and flood risk analysis. These tools act as an important guideline

for decision makers, policy makers and insurance agencies to plan accordingly for future probable flood disasters.

The main objectives of this research study are:

I. To quantify the effects of elevation data resolution and Manning's roughness in calculated travel time and inundation area prediction for generating reliable flood warning system;

II. To develop an approach for flood warning system and to generate flood inundation maps for a series of flood stages in the Grand River near the City of Painesville, Ohio;

III. To assess the potential impact in river stage and hydraulic structures due to winter ice cover and ice jams using one-dimensional HEC-RAS hydraulic model.

Methodology for Objective I

a. Collect input data like geospatial data, stage/discharge records, lake elevation records required for one-dimensional HEC-RAS modeling;

b. Prepare geospatial data using six different elevation datasets in HEC-GeoRAS, an ArcGIS extension, required for a hydraulic simulation;

c. Calibrate and validate the unsteady hydraulic model using field verified survey and United States Geological Survey (USGS) stage/discharge records;

d. Run the simulation to calculate travel time and export the simulated data to HEC-GeoRAS to generate flood inundation maps;

e. Compare travel time and inundation maps for various elevation datasets to quantify the effects of elevation data resolution and Manning's roughness.

Methodology for Objective II

a. Prepare flood discharges data for various flood stages (at streamgage 04212100, near the City of Painesville) as an input for steady hydraulic model;
b. Calibrate/validate for steady flow scenario using high-water marks of 2006 flood;
c. Run the simulation for 12 different flood stages to predict travel time and generate probable flood inundation maps as a part of the flood warning system.

Methodology for Objective III

a. Collect historical temperature, precipitation and ice jam location information and estimate ice thickness using modified Stefan's equation;
b. Prepare input data including winter discharge records and ice thickness information to simulate model;
c. Run the simulation for various scenarios including/excluding ice cover/ice jams and bridges;
d. Compare and analyze these scenarios and evaluate the difference in river stages for different scenarios.

Thesis Structure

This thesis is mainly divided into four chapters. Chapter 1 describes background, scope, objectives and thesis structure. Chapter 2 quantifies the error propagated with elevation data resolution and Manning's roughness values in channel and floodplains for the computation of flood travel time and inundation area. This chapter also gives the detail description of theoretical background, overall modeling approach, model input data and calibration/validation procedure of one-dimensional unsteady flow HEC-RAS model, which is crucial for further study.

Chapter 3 discusses the calculation of flood travel time and generation of flood inundation maps for various stages of floods along the Grand River. Additionally, it discusses an approach for the development of flood warning system. The same calibrated and validated unsteady flow model as discussed in Chapter 2 was used for this analysis. In addition, it further discusses the calibration of the model in steady flow using high-water marks of 2006 flood along the Grand River, near the City of Painesville as a part of the flood warning system development.

Chapter 4 discusses the effects of winter ice cover and ice jam in the flood level and inundation area along the Grand River. Additionally, the effects of ice cover and ice jam in hydraulic structures like bridge locations have been discussed. A comparative study has been done to see the differences in flood level and inundation area when ice jam occurs in the winter season in the Grand River.

In Chapter 5, the conclusions derived from this study and the recommendations for future work to develop more effective and automated flood warning system have been discussed.

Chapter 2 and Chapter 4 have been structured in journal paper format. These chapters will be developed as a full-length article after some additional work in the future. Since journal article should stand alone with sufficient background information, the readers may find some redundancies in these chapters.

References

Beltaos, Spyros. "Assessing Ice-Jam Flood Risk: Methodology and Limitations." 20th IAHR Inernational Symposium on Ice. 2010.

Cook, Aaron, and Venkatesh Merwade. "Effect of topographic data, geometric configuration and modeling approach on flood inundation mapping." Journal of Hydrology 377.1 (2009): 131-142.

Daly, Steven F. and Vuyovich, Carrie. “Ice Jam Formation Parameters in Selected U.S. Rivers” USACE, 2007

King, Rawle O. "National flood insurance program: Background, challenges, and financial status." Congressional Research Service, Library of Congress, 2009.

Merwade, Venkatesh, et al. "Uncertainty in flood inundation mapping: current issues and future directions." Journal of Hydrologic Engineering13.7 (2008): 608-620.

NOAA, 1981. Floods, Flash Floods and Warnings, Pamphlet, National Weather Service, NOAA, Washington, DC.

Sangwan, Nikhil. Floodplain mapping using soil survey geographic (SSURGO) database. Diss. PURDUE UNIVERSITY, 2014.

USGS, 2016. USGS Flood Inundation Mapping Science, Flood Inundation Mapping (FIM) Program (accessed March 2016) http://water.usgs.gov/osw/flood_ inundation/

Van Alphen, J., et al. Flood risk management approaches: As being practiced in Japan, Netherlands, United Kingdom and United States. IWR, 2011.

Wadsworth, G. 1999. Flood Damage Statistics. Public Works Department, Napa, CA.

Chapter 2. Effect of Elevation Data Resolution and Manning's Roughness in Travel Time and Inundation Area Prediction for Flood Warning System

Abstract

The flood travel time and possible area of inundation are two crucial issues in flood warning system to allow timely evacuation of people in sufficient lead time from the probable inundation area. Therefore, accurate travel time computation and floodplain mappings are essential to develop a flood warning system. While earlier research were more focused on the uncertainty of data resolution in floodplain mapping, the major objective of this study was to compute travel time for the timely evacuation and generate various return period floodplain maps, within the range of uncertainties associated with various resolutions of datasets and Manning's roughness. This was accomplished using one-dimensional hydraulic model, Hydraulic Engineering Center River Analysis System (HEC-RAS). Geospatial data required for HEC-RAS was obtained using various resolution Digital Elevation Model (DEM) datasets, which was pre-processed in HEC-GeoRAS. The hydraulic analysis was performed in HEC-RAS and post-processed in HEC-GeoRAS to produce flood inundation maps. The travel time and flood maps were analyzed using various Manning's roughness values with six elevation datasets: Light Detection and Ranging (LiDAR) data; 10m DEM; 30m DEM; integration of survey data with LiDAR data; integration of survey data with 10m DEM; and integration of survey data with 30m DEM. It was found that travel time and inundation area could be overestimated if coarser elevation datasets were used. The maximum difference in calculated travel time was 11.03%-15.01% and in predicted inundation area was 32.56%-44.52% for 30m DEM without integration of survey data. This error was based on the comparison of the result obtained with Light Detection and Ranging (LiDAR) data

modified with field verified survey data. The minimum difference in calculated travel time was 0.50%-4.33%, and predicted inundation area was 3.55%-7.16% while using 10m DEM along with survey data. The difference in travel time and possible inundation area generated from LiDAR with survey data was not significantly different from 10m DEM with survey data. However, LiDAR with survey data provided a conservative prediction in travel time which would be safe to plan for evacuation from possible flood prone areas. While 10 m DEM best represented the actual field survey section in channel compared to LiDAR data, the application of LiDAR data was pertinent as flood usually travels through the floodplain especially during high flow period and also provides elevation at high resolution. Since the topographical study was done for this study, LiDAR data with field verified cross sections were used to calculate flood travel time and generate inundation maps. Additionally, Manning's roughness of channel section was found to be more sensitive than that of floodplains while computing travel time and generating inundation maps. The decrease in inundation area was the highest (8.97%) while using the lower value of Manning's roughness (0.020).

Keywords: Floodplain mapping, Topographic dataset, River bathymetry, HEC-RAS, HEC-GeoRAS,

Introduction

Flooding is one of the most common forms of natural calamities in many countries across the world, which may damage millions of dollars' worth properties and may take the lives of thousands of people every year (Basha et al., 2007; King 2010; Lowe 2003). Flood caused more human lives and property losses (90% of all property losses) than any other forms of natural calamities in the twentieth century in the United States (Krimm 1996; Perry 2000). One of the ways to prevent from such calamities and

losses is to develop flood warning system and inform the people in the community for the evacuation in sufficient lead time. Therefore, the determination of flood travel (evacuation) time is essential for the timely evacuation of people from probable inundation area and to minimize the negative consequences of such hazards (Krzysztofowicz et al., 1994). On the other hand, it is equally important to make these floodplain maps easily accessible and comprehensible to the public without difficulties (Holtzclaw et al., 2005). Floodplain maps are very important tools, which represent the spatial variability of flood hazards and provide the direct and robust understanding of floods than any other forms (Merz et al., 2007; Leedal et al., 2010). While there has been a significant advancement in hydrologic and hydraulic models to generate floodplain maps, uncertainties associated with topography, vegetation/topography characteristics, flow discharge, techniques and methods of modeling still exist in floodplain mapping process (Marks and Bates, 2000; Crosetto et al., 2001; Smemoe et al., 2003; Merwade et al., 2008; Bales et al., 2009). Since the floodplain mapping process is not an exact science (Smemoe et al., 2003), probabilistic floodplain maps generated considering uncertainties in modeling are appropriate rather than deterministic maps while planning for the future rescue operation and quantification of flood insurance rates in probable affected areas (Di Baldassarre, 2012).

Some research has been previously conducted to study the uncertainties associated with flood inundation mapping process. Merwade et al. (2008) conducted a study in Strouds Creek, North Carolina in floodplain mapping and reported the uncertainties due to hydrologic flow including the complex interaction of individual inputs in hydraulic model. Similarly, another study was conducted in Strouds Creek in North Carolina and Brazos River in Texas (Cook and Merwade, 2009) to study the

effects of topographic data and the geometric configuration in flood inundation maps. The study concluded that the predicted area decreases with higher resolution of topographic data. Various other studies (Horrit & Bates, 2001; Bates et al., 2004; Domeneghetti et al., 2013; Dottoti et al., 2013) have been conducted to comprehend the uncertainties in flood inundation maps. However, to the best of my knowledge, no study has been conducted yet to quantify the potential uncertainties in flood travel time of various return periods when different elevation datasets and Manning's roughness values are used.

Therefore, the major objective of this research is to calculate the flood travel time and generate floodplain maps corresponding to different return period floods in the City of Painesville located along the Grand River of Lake County, Ohio. The uncertainties associated with flood travel time and the extent of flood inundation maps while using various resolutions of elevation datasets and different values of Manning's roughness are also reported. For this, the HEC-RAS model was developed for flood magnitude of different return period. Finally, the effects of elevation data resolutions and Manning's roughness have been reported for the appropriate representation of flood travel time and the flood extents.

Theoretical Description

The hydraulic modeling software, HEC-RAS, was used in this study for steady and unsteady flow analysis. HEC-RAS was developed by United States Army Corps of Engineers-Hydrologic Engineering Center (USACE-HEC), which has been widely used for steady flow analysis, unsteady flow simulation, movable boundary sediment transport computations and water quality analysis (Brunner, 1995). Usually, steady flow approach

is used for floodplain management and flood insurance studies, whereas unsteady flow approach is used for subcritical flow regime especially for dam break analysis and pressurized flow module (Brunner, 1995; Brunner, 2002). The effect of various obstructions such as culverts, bridges, dams and weirs can be considered in the analysis to see their impacts in the water surface profiles. HEC-RAS solves one-dimensional, Saint-Venant equations, using four-point implicit method developed for natural channels (Brunner, 2002) to simulate unsteady flow, which are derived from the continuity and momentum equations. The continuity and momentum equations have been listed as follows.

$$\frac{\partial A}{\partial t} + \frac{\partial Q}{\partial x} = 0 \qquad (2.1)$$

$$\frac{\partial Q}{\partial t} + \frac{\partial (\frac{Q^2}{A})}{\partial x} + gA\frac{\partial H}{\partial x} + gA(S_0 - S_f) = 0 \qquad (2.2)$$

Where A is cross-sectional area normal to the flow; t is any time; Q is discharge of river; x is longitudinal distance in the river; g is acceleration due to gravity; H is elevation of water surface in the river above assumed datum level; S_0 is slope of river bed, and S_f is energy slope of water.

The Saint-Venant equations are solved using the well-known four point implicit finite difference scheme in HEC-RAS. This scheme is completely non-destructive but marginally stable (Fread 1974; Ligget and Cunge, 1975) when it is run in semi-implicit form (weighting factor θ of 0.5). The value of θ in HEC-RAS varies from 0.6 to 1. The value of 1 provides the most stable form, whereas a value of 0.6 provides the greatest stability of the solution (Brunner, 2002).

In steady flow simulation, HEC-RAS solves energy equation as given below to calculate water surface elevations from one cross section to another cross section with an iterative procedure which is called as standard step method (Brunner, 1995).

$$Z_1 + Y_1 + \frac{\alpha_1 V_1^2}{2g} + H_e = Z_2 + Y_2 + \frac{\alpha_2 V_2^2}{2g} \qquad (2.3)$$

Where Z_1 and Z_2 are elevations of the main channel, Y_1 and Y_2 are depths of water, V_1 and V_2 are average velocities, and α_1 and α_2 are velocity weighting coefficients at section one and two respectively. Similarly, g is acceleration due to gravity, and H_e is energy head loss from section one to section two.

Materials and Methodology

Study Area

This study was conducted in the Grand River watershed, which consists of major three tributaries: Mill, Paine and Big Creek. The watershed which is located in Northeastern region of Ohio and has an area of 705 mi^2 with an elevation range from a minimum of 564 ft to maximum of 1385 ft (Figure 2-1). It has twenty-eight Hydrologic Unit Code (HUC)-14 watersheds and six HUC-11 watersheds, which spread out to five counties; Lake, Ashtabula, Trumbull, Geauga and Portage. The watershed is geographically surrounded within N 41° 22' to N 41° 51', E -80° 35' to E -81° 18'. The Grand River originates from the southern part of Middlefield and flows through Orwell, Rock Creek, Austinburg, Harpersfield, Madison, Perry, Painesville, Fairport Harbor and finally ends to the Lake Erie. The river is approximately 102.7 miles with an average slope of 1 in 900 and an average width of approximately 275 ft., varying from 150 ft to 500 ft at various locations. The mean annual precipitation in the watershed is found to be 38 inches based on the historical records. In this study, a river section of approximately

32.2 miles from Harpersfield to Fairport Harbor, which includes the City of Painesville, was considered as a study site to perform the hydraulic analysis.

The City of Painesville along the Grand River has been frequently threatened by several flooding that occurred from time to time (2006, 2008, and 2011). The disastrous flood of July 27-28, 2006 in Grand River caused by more than 11 inches of rainfall depth, led to the destruction of 100 homes and business, five bridges and 13 roads. Property worth of 30 million USD was damaged including one death in Lake County. Consequently, hundreds of people were evacuated and three counties including Lake, Geauga and Ashtabula were declared as Federal and State disaster areas (Ebner et al., 2007). This flood was reported to have a peak flow of 35,000 cfs (500 return year period) and highest historic stage of 19.35 ft (Ebner et al., 2007) as recorded by USGS gage station (04212100) near the City of Painesville.

Overall Modeling Approach

In order to calculate accurate flood travel time and generate floodplain maps, calibrated and validated one-dimensional hydraulic model, HEC-RAS, was developed by importing the geospatial data of river cross sections and bridges from HEC-GeoRAS. The HEC-GeoRAS is a tool that uses graphical user interface for preparing geospatial data in ArcGIS. Unsteady flow simulation for different flood events for the period of 1996-1998 was performed for model calibration and validation. Since steady flow simulation is typically performed during peak flood period (Hicks et al., 2005; Cook, A.C. 2008), peak flood was simulated in steady flow conditions to calculate the flood travel time and water surface elevations. These water surface elevations/extents were then exported back to HEC-GeoRAS to produce floodplain maps. Typically, elevation datasets such as National Elevation Datasets (NED) and Light Detection and Ranging (LiDAR) do not include the

river bathymetry leading to the requirement of field verification through the topographical survey. Therefore, the river was surveyed using highly accurate Global Positioning System (GPS) technology from Harpersfield to North St. Clair Bridge. For the remaining portion up to Lake Erie near Fairport Harbor, bathymetry survey using sounding method produced by National Oceanic and Atmospheric Administration (NOAA) and USACE was used. Six different topographical datasets including LiDAR derived DEM, 10m DEM, 30m DEM, and integration of field verified cross section with each datasets of LiDAR derived DEM, 10m DEM and 30m DEM were used in this study. The differences in the travel time and floodplain extents were compared and reported using such various resolution datasets.

HEC-GeoRAS/HEC-RAS Model Input

Elevation data sets are needed to generate geospatial data and perform hydraulic analysis in HEC-RAS. Therefore, high-quality datasets were used in this study in order to compute travel time and produce accurate flood inundation maps. LiDAR data was downloaded from Ohio Geographically Referenced Information Program (OGRIP) website. Similarly, Digital Elevation Model (DEM) of 10 m and 30 m resolutions were downloaded from National Resource Conservation Service-United States Department of Agriculture (NRCS-USDA), Geospatial Data Gateway. Land use data of 30 m resolution was downloaded from National Land Cover Database 2011 (NLCD 2011). The Grand River watershed includes forest (41.86%), cultivated land (24.57 %), waterbodies and wetlands (7.67%) and developed/urban land (10.21%). The remaining 15.70% are covered by other land such as Herbaceous (4.2%), barren land (0.08%), hay/pasture (9.29%) and shrub/scrub (2.13%) as per NLCD 2011 (Figure 2-2).

Geometric input features classes needed for HEC-RAS such as stream lines, cross sections, bank stations, storage areas were first created in HEC-GeoRAS and then exported to HEC-RAS. In order to represent the accurate cross section of the river, the topographical survey was performed at 77 different sections of the river (Figure 2-3). The cross sections were surveyed at an interval of half a mile to a mile depending upon the site conditions. The hydraulic model, HEC-RAS, developed for Grand River after incorporating river cross section is shown in Figure 2-4. Discharge and stage data for the station 04211820 (upstream gage station near Harpersfield) and 04212100 (downstream gage station near the City of Painesville) were obtained from USGS website to perform unsteady hydraulic analysis and calibrate Manning's roughness for study reaches in HEC-RAS. Peak discharge data for the recurrence interval of 10, 50, 100, and 500 years for Grand River were obtained from Koltun et al. (1990), which was determined based on log-Pearson Type III distribution. For other ungauged stream reaches including Mill, Paine and Big Creek, peak discharge from 10 to 500 years return periods were obtained from streamstat web application (Guthrie et al., 2008). The streamstat calculates the peak discharge based on different regression equations (Koltun et al., 1990) depending upon the river basin characteristics. There are altogether 10 bridges within the study area, and the data for these bridges were obtained from Lake County Office and Ohio Department of Transportation (ODOT). Similarly, the data for high flood levels for Lake Erie has been obtained from a report by USACE (USACE 2000). The summary of input data including their types and sources are presented in Table 2-1.

Model Calibration and Validation

The unsteady HEC-RAS model was calibrated by the iterative process to obtain the suitable value of Manning's roughness for river reaches by comparing simulated stage

and discharge with the observed data. The preliminary selection criteria of Manning's roughness has been recommended by various approaches including visual inspection, land use/land cover and optimization techniques rather than selecting it only from intuition approach (Kalyanapy et al., 2010). Channel roughness is highly variable as it depends on many factors like channel alignment, surface roughness, bed material, nature of sediments and obstruction present in the channel (Pappenberger et al., 2005; Timbadiya et al., 2011; Parhi et al., 2012). Chow et al. (1988) illustrates that the Manning's roughness varies from 0.035 to 0.065 for the main channel and 0.08 to 0.15 in the floodplains. Regardless, it needs to be calibrated using the known years flood data; therefore, eight different minor and major flood events from 1996-1998 were used in HEC-RAS simulation. Finally, the calibrated Manning's roughness values were used to calculate travel time and develop the flood inundation maps.

Model Evaluation Criteria

Various statistical parameters such as Nash-Sutcliffe efficiency (NSE), R-squared (R^2), percent bias (PBIAS) and root mean square error (RMSE) were used to test the accuracy and predictive power of the model (ASCE 1993; Gupta et al., 1999; Moriasi et al., 2007).

The NSE is a standardized statistic criteria that determines the relative magnitude of the residual variance ("noise") compared to the variance of measured data (Nash and Sutcliffe, 1970). NSE is recommended for model evaluation as it is found to be the best objective function for reflecting the overall fit of a hydrograph (Moriasi et al., 2007). Typically, it indicates the wellness of observed and simulated data fitting the 1:1 line. Its value ranges from $-\infty$ to 1, and values from 0 to 1 are acceptable. The NSE value of 1 is

rare and considered as a perfect value for an ideal model. NSE is calculated by using the following equation.

$$NSE = 1 - \left[\frac{\sum_{i=1}^{n} \left({Y_i}^{obs} - {Y_i}^{sim} \right)^2}{\sum_{i=1}^{n} \left({Y_i}^{obs} - {Y_{obs}}^{mean} \right)^2} \right] \quad (2.4)$$

Where ${Y_i}^{obs}$ is the i[th] value of observed data, ${Y_i}^{sim}$ is the i[th] value of simulated data, Y_{obs}^{mean} is the mean value of observed data, Y_{sim}^{mean} is the mean of simulated data, and n is the total number of observations.

R^2 measures the fitness of observed and simulated data. R^2 varies from 0 to 1, indicating 1 as a perfect fitness of data.

$$R^2 = \left(\frac{\sum_{i=1}^{n} \left({Y_i}^{obs} - Y_{obs}^{mean} \right) \left({Y_i}^{sim} - Y_{sim}^{mean} \right)}{\left[\sum_{i=1}^{n} \left({Y_i}^{obs} - Y_{obs}^{mean} \right)^2 \sum_{i=1}^{n} \left({Y_i}^{sim} - Y_{sim}^{mean} \right)^2 \right]^{0.5}} \right)^2 \quad (2.5)$$

RSR is the ratio of RMSE and standard deviation of the observed data. Lower the value of RSR, lower is the root mean square error and better is the model performance. The ideal value of RSR is 0. The RSR is calculated by using following equation.

$$RSR = \frac{RMSE}{STDEV_{obs}} = \frac{\sqrt{\sum_{i=1}^{n} \left(Y_i^{obs} - Y_i^{sim} \right)^2}}{\sqrt{\sum_{i=1}^{n} \left(Y_i^{obs} - Y_{obs}^{mean} \right)^2}} \quad (2.6)$$

PBIAS is the percentage deviation in simulated data from the observed data (Moriasi et al., 2007). PBIAS with value 0 is considered as a perfect model harmonizing with the observed data. Negative values of PBIAS specify overestimation bias, whereas positive values of PBIAS indicate underestimation bias. PBIAS is calculated using following equation.

$$PBIAS = \left[\frac{\sum_{i=1}^{n} \left({Y_i}^{obs} - {Y_i}^{sim} \right) X\ 100}{\sum_{i=1}^{n} \left({Y_i}^{obs} \right)} \right] \quad (2.7)$$

Uncertainties Associated with Floodplain Modeling

A large number of uncertainties accompanied with numerous variables including topography, Manning's roughness, flow discharge, techniques and methods of modeling are still associated with the floodplain mapping regardless the advancement in hydrologic and hydraulic modeling tools (Oegema and McBean, 1987; Merwade et al., 2008; Smemoe et al., 2003). Therefore, the accuracy of the floodplain maps depends on how these uncertain variables have been incorporated in hydraulic and hydrologic models (Merwade et al., 2008). Two important variables, which may impose errors in flood travel time and inundation area, have been discussed in this study.

Effect of Topography

The reliable elevation datasets are essential for the generation of accurate flood inundation maps. The use of high-resolution LiDAR data, somehow, might improve the accuracy of floodplain mapping as it provides highly accurate elevation data. However, it does not represent the exact river bathymetry, which may still pose serious errors in travel time calculation and flood inundation mapping. According to Merwade et al. (2008), the poor quality of terrain data can impose error in flood inundation mapping process in three ways. Firstly, it affects the streamflow generated from hydrological models. Secondly, it affects the river stage calculated from hydraulic models, and lastly, it affects the spatial extents of floods. So, the field verified cross sections of river reaches are absolutely essential to get the better bathymetry of the river for travel time computation and floodplain mapping.

Effect of Manning's Roughness

Since the complete characteristics of terrain are reflected by Manning's roughness, it plays a significant role in model calibration and floodplain delineation. The

roughness value varies spatially along the river depending upon the river bed material and surrounding floodplain characteristics. It is essential to adequately represent the roughness characteristics of the floodplain and channel in order to reduce the uncertainties involved in the flood travel time and floodplain mappings. The preliminary selection of Manning's roughness was based on the terrain properties of other similar rivers as presented in Arcement et al. (1989) and Barnes, (1849). The hydraulic model in this study was simulated for different values of channel roughness to study the uncertainties associated with it.

Effect of Discharge

River discharge is also considered as one of the uncertain variables that has to be considered in floodplain mapping (Oefema & McBean, 1987; Pappenberger et al., 2006b; Merwade et al., 2008; Di Baldassarre & Montanari, 2009). The discharge values for various return period floods were generated from the regression equation derived by USGS (Koltun et al., 1990). Error associated with discharge prediction for tributaries can be dissipated in water surface elevation and the flood extents calculated from hydraulic model (Merwade et al., 2008).

Results and Discussions

Simulation of Hydraulic Model

The performance of the model was good in calibration and validation based on the evaluation measured through different statistical criteria. The calculated value of all statistical parameters was higher than the recommended values (NSE > 0.50, PBIAS ±25% and RSR ≤ 0.70) by Moriasi et al. (2007). The detail results of calibration/validation for the stage at upstream gage station 04211820 are presented in Table 2-2. Similarly, the detail results of calibration/validation for discharge at

downstream gage station 04212100 are presented in Table 2-3. In this study, NSE for stage calibration/validation varied from 0.74 to 0.89 (Table 2-2), and NSE for discharge calibration/validation varied from 0.69 to 0.96 (Table 2-3) except for a period 2/26/1997 to 3/3/1997.

Furthermore, the performance of the model was also evaluated through the visual inspection using the graphical plot of observed and simulated stage/discharge. The calibration/validation of stage at upstream gage station 04211820 is shown in Figure 2-5. Similarly, the calibration/validation of discharge at downstream gage station 04212100 is shown in Figure 2-6. The model efficiency was assessed for several possible values of Manning's roughness, and the roughness value was calibrated based on the performance efficiency of simulated result with observed data. Overall, the model performance was well above the satisfactory range. The calibrated/validated value of Manning's roughness was adopted 0.035 for channels and 0.15 for banks/floodplain regions.

Effect of Topography

The effect of topography on flood inundation extents depends on the size of the river, bathymetry of the river, and the hydraulic modeling approach (Merwade et al., 2008). The elevation of rivers at different cross sections greatly varied when different sets of elevation datasets were used. The cross sections for 10 different locations generated from 4 different elevation datasets are shown in Figure 2-7. It was found that, in majority of those cross sections, the topographic data represented by 10 m DEM was better than LiDAR data particularly in channel sections indicating that cross section generated from 10m DEM was better representing to the actual cross sections. This is not surprising as airborne LiDAR cannot penetrate water (Allouis et al., 2007) especially in the channel

sections. However, LiDAR data are expected to represent the floodplain well, as these data are prepared in high resolution.

The study found out that the travel time of different return period floods varied based on the resolution of the datasets that were used in the hydraulic analysis. Travel time to reach the City of Painesville and Fairport Harbor for five different return period floods was calculated using six different elevation datasets. The graphical representation of travel time and percentage difference in travel time for various year return period floods to reach the City of Painesville is shown in Figure 2-8. The calculated travel time was found to be the highest for the most coarse elevation dataset (30m DEM without survey) and was on decreasing order for finer elevation datasets with an exception for LiDAR data. For example, the difference in calculated travel time for various return period floods was maximum (11.03% to 15.01%) for 30m DEM without integration of survey data and minimum (1.19%-3.35%) for 10m DEM while integrated with survey data. It was interesting to mention that 10 m DEM without integrating the survey data revealed small difference in travel time to the City of Painesville when compared to the travel time computed using LiDAR data without survey. The percentage difference for 10m DEM without survey was 3.67%-4.87%, whereas it was 10.24%-11.75% for LiDAR without survey. A similar pattern was detected for the case of travel time from Harpersfield to Fairport Harbor. The graphical representation of travel time and percentage error in travel time for different return period floods to reach Fairport Harbor is shown in Figure 2-9. There was the maximum difference of 13.29%-14.28% in calculated travel time for 30 m DEM without integration of survey data for various return period floods. However, the minimum difference of 0.50%-4.33% was detected for 10m DEM integrated with survey data (Figure 2-9). The calculated travel time for LiDAR data

without integration of survey data was relatively higher. One of the reasons for this could be due to the coarser elevation data in channel sections as airborne LiDAR data cannot penetrate water bodies to accurately portray the river bed elevation. Similarly, the water surface elevation and total flow area for LiDAR data without integration of survey data were also found to be higher than some other coarser elevation datasets. Consequently, the flow and computed velocity was relatively smaller resulting to higher travel time. Therefore, bathymetric data is absolutely needed for the appropriate representation of river profile. Since bathymetric LiDAR data were not available, the detail survey was conducted along the channel sections to modify the cross section and best represent the site conditions in the model. The river cross sections after detailed survey were incorporated in the LiDAR data in channel sections. This decreased the travel time to reach the City of Painesville by 10.24 % to 11.75% (Figure 2-8) and by 2.33% to 6.84% to reach Fairport Harbor for various return period floods (Figure 2-9).

Furthermore, inundation maps were also generated for five different return period floods using six elevation datasets. The graphical representation of inundation area including its percentage difference for different return period floods and different elevation datasets are shown in Figure 2-10. Similarly, the tabular details of inundation area for each return period floods calculated using various elevation datasets and the percentage difference are shown in Table 2-4. It was found that the inundation area increased with the coarser resolutions of elevation datasets. For example, the inundation area for 500 return year period flood using LiDAR data with survey was 4.10 mi^2 and using 30 m DEM without survey was 5.55 mi^2 with an area difference of 35.37%. The maximum difference in inundation was found to be 32.56%-44.52% for 30 m DEM without integration of survey data for various return period floods and the minimum

difference was 3.55%-7.80% for 10 m DEM while integrated with survey data (Table 2-4). The flood maps of 2006 flood period were generated using various elevation datasets to have a clear picture of inundation area difference. These flood maps were generated in HEC-GeoRAS and are shown in Figure 2-11. The importance of detail bathymetry data to generate inundation maps was clearly observed. When the bathymetry data (survey data) was incorporated in DEM, the decrease in predicted inundation area was observed. The average reduction in inundation area of five different return period floods was found to be the highest (17%) for 30m DEM and least (9%) for LiDAR (Table 2-5). This finding was consistent with the result presented by Merwade et al. (2008).

Also, we compared the top width and the flow area for 2006 flood at several locations of the river. In most of the cases, there was a decrement in top width and flow area after the integration of bathymetry data. The decrement percentage was higher for 30m DEM and least for LiDAR data. Moreover, there was an increase in channel velocity and total average velocity which resulted decreasing the travel time for various return period floods when survey data was incorporated.

Effect of Manning's Roughness

As stated earlier, the result showed the difference in travel time and inundation maps when series of different Manning's roughness values were used. In this study, five different return period floods in Grand River were analyzed in two different ways. First, we considered the constant value of roughness in the channel section while varying the roughness value in floodplains. Four different roughness values (0.15, 0.10, 0.09 and 0.07) within acceptable range were chosen to see the variation. The detail results of travel time to the City of Painesville for different values of Manning's roughness are presented in Table 2-6. The lower values of Manning's roughness in floodplains resulted in the

increased travel time even though the increment was not significant. The maximum increment was found to be 3.45% for 2006 flood when the roughness value was the lowest (0.07) among those four different values (Table 2-6). Secondly, a constant value of roughness was considered in floodplains and varied in channel sections. For this, four different possible roughness values (0.035, 0.030, 0.025, and 0.020) in channel were chosen. As the roughness value was lowered in channel section, there was significant decrease in travel time for different return period floods. The maximum decrement ranged from 20.72%-22.35% when roughness value was 0.020 at channel section (Table 2-6). The main reason for the decrement was an increase in channel flow velocity due to a decrease in roughness value.

Similarly, the effect of Manning's roughness was observed in inundation area as well. Floodplain maps were produced for different sets of roughness values in channel and floodplain regions. There was a decrease in flood inundation area for lower values of Manning's roughness than that of the calibrated/validated values. The percentage decrease in inundation area while using different values of Manning's roughness is shown in Figure 2-12. In the first case (roughness value was lowered in floodplain region but kept constant in channel), the percentage decrease in inundation area was less than 1.49 %. However, in the second case, (roughness value was lowered in the channel but kept constant in floodplains), the percentage decrease in inundation area was 8.97% (Figure 2-12). The sensitivity of roughness in floodplain mapping is found to be higher in the second case. The decrease in inundation area was noticed mostly in the flat regions along the river. Therefore, the appropriate calibration of Manning's roughness at channel sections is more crucial. The difference in predicted inundation area for different Manning's roughness is shown in Figure 2-13.

Conclusion

Accurate floodplain maps are essential tools for floodplain managers and insurance actuaries to make appropriate decisions to plan for rescue operation in affected areas during flooding periods. In this paper, the effects of the resolution of topographic datasets and Manning's roughness value in the prediction of flood travel time and inundation areas have been discussed. Five different return period floods including 10, 50, 100, 500 years and 2006 flood were considered for analysis. These different floods were simulated in a widely recognized hydraulic tool, HEC-RAS, using various topographic datasets wide ranges of Manning's roughness. A topographic survey was carried out to represent accurate elevation dataset in the river channel sections assuming that LiDAR data gives the correct elevation representation especially in floodplains. The surveyed elevation datasets were integrated with high-resolution LiDAR data.. Among all elevation datasets, the travel time was highest for the coarse data (30m DEM without integration of survey data) and had a decreasing trend for high resolution data. However, the calculated travel time obtained from 10m DEM without integration of survey data showed less difference than the result obtained from LiDAR without integration of survey. Therefore, it can be concluded that the elevation data in channel section is better represented by 10m DEM than LiDAR in case field survey data are not available. However, the predicted inundation area from LiDAR without survey had less area difference than that of 10m DEM without survey. Nevertheless, a topographic survey is required to get the actual representation of the land surfaces in channel sections.

In this study, LiDAR with the integration of survey data gave conservative travel time. Since, it is always safe to make a decision based on the worst case scenario, lesser travel time would be appropriate for evacuation planning from the possible inundation

areas. Similarly, the predicted area of inundation also increased as the coarser resolution of datasets was used, and the percentage difference was very high for 30m DEM without integration of survey. Therefore, it can be concluded that very coarse dataset considered in this study (30m DEM without integration of survey data) is not appropriate for the calculation of travel time and the generation of flood inundation maps. The differences in results were significant in 30m DEM even after the integration of survey. It was also found that there was a decrement in travel time, inundation area, flow area and top width and increment in the flow velocity when the bathymetry data was integrated to any resolution of dataset. Therefore, when coarse datasets are used for travel time computation and generation of flood inundation maps, some factor of safety should be considered to account these errors.

The effect of Manning's roughness was found to be more crucial in flood travel time computation and prediction of inundation area, especially in channel sections. As the value of roughness in the channel sections was decreased, there was significant decrease in flood travel time (up to 22.35%) and decrease in inundation area (up to 8.97%). The effect of Manning's roughness in flood travel time and inundation area was studied only for 2006 flood event in the City of Painesville assuming the similar effect in other flood events.

There might be many other uncertainties associated with travel time computation and floodplain mapping. From this perspective, it would be wise to use probabilistic flood plain maps as a part of flood mitigation strategies. Since flood travel time computation is essential to evacuate people from probable inundation areas, it will be better to calculate travel time using slightly lower value of Manning's roughness and higher resolution data to remain in conservative side for early evacuation. On the other

hand, it will be better to generate flood inundation maps based on a slightly higher value of roughness and higher resolution data so that the affected areas are not underestimated. Hence, slightly underestimated result in travel time and slightly overestimated result in inundation area mapping might be helpful while planning and making flood warning decisions.

It should be noted that the calibration of Manning's roughness for this study was performed based on the unsteady flow simulation. However, entire results of travel time and inundation maps were obtained based on the steady flow assumption in HEC-RAS model. The steady flow assumption made in this study particularly for high flow period is valid, and this is a general practice to simulate flows in steady state conditions during peak flow time. In future, unsteady flow model and two-dimensional hydraulic models can be developed if discharge/stage data for all creeks and time series data of Lake Erie level can be obtained. Some error is associated with the flows in tributaries as it was computed using regression equations. This error might be transferred to the hydraulic model resulting in dissipation of further errors in water surface elevation and flood extents.

References:

Allouis, Tristan, Jean-Stéphane Bailly, and Denis Feurer. "Assessing water surface effects on LiDAR bathymetry measurements in very shallow rivers: A theoretical study." Second ESA Space for Hydrology Workshop, Geneva, CHE. 2007.

ASCE Task Committee. "The ASCE task committee on definition of criteria for evaluation of watershed models of the watershed management committee Irrigation and Drainage Division, Criteria for evaluation of watershed models."J. Irri. Drain. Eng, ASCE 119.3 (1993): 429-442.

Arcement, George J., and Verne R. Schneider. "Guide for selecting Manning's roughness coefficients for natural channels and flood plains." (1989).

Baldassarre, G. Di, and A. Montanari. "Uncertainty in river discharge observations: a quantitative analysis." Hydrology and Earth System Sciences 13.6 (2009): 913-921.

Basha, Elizabeth, and Daniela Rus. "Design of early warning flood detection systems for developing countries." Information and Communication Technologies and Development, 2007. ICTD 2007. International Conference on. IEEE, 2007.

Bates PD, Horritt MS, Aronica G, Beven KJ. 2004. Bayesian updating of flood inundation likelihoods conditioned on flood extent data.Hydrological Processes 18: 3347–3370.

Bales, J. D., and C. R. Wagner. "Sources of uncertainty in flood inundation maps." Journal of Flood Risk Management 2.2 (2009): 139-147.

Barnes Jr, Harry H. "Roughness characteristics of natural streams." US Geological Survey Water Supply Paper (1849).

Brunner, Gary W. HEC-RAS River Analysis System. Hydraulic Reference Manual. Version 1.0. HYDROLOGIC ENGINEERING CENTER DAVIS CA, 1995.

Brunner, Gary W. HEC-RAS River Analysis System: User's Manual. US Army Corps of Engineers, Institute for Water Resources, Hydrologic Engineering Center, 2002.

Crosetto, Michele, and Stefano Tarantola. "Uncertainty and sensitivity analysis: tools for GIS-based model implementation." International Journal of Geographical Information Science 15.5 (2001): 415-437.

Chow, Ven T., David R. Maidment, and Larry W. Mays. Applied hydrology. 1988.

Cook, Aaron Christopher. Comparison of one-dimensional hec-ras with two-dimensional feswms model in flood inundation mapping. Diss. Purdue University West Lafayette, 2008.

Cook, Aaron, and Venkatesh Merwade. "Effect of topographic data, geometric configuration and modeling approach on flood inundation mapping." Journal of Hydrology 377.1 (2009):131-142.

Di Baldassarre, Giuliano, et al., "Flood-plain mapping: a critical discussion of deterministic and probabilistic approaches." Hydrological Sciences Journal–Journal des Sciences Hydrologiques 55.3 (2010): 364-376.

Di Baldassarre, G.: Flood trends and population dynamics, EGU Medal Lecture: HS Outstanding Young Scientist Award, EGU General Assembly 2012, Wien, 2012.

Domeneghetti, A., et al. "Probabilistic flood hazard mapping: effects of uncertain boundary conditions." Hydrology and Earth System Sciences17.8 (2013): 3127-3140.

Dottori, F., G. Di Baldassarre, and E. Todini. "Detailed data is welcome, but with a pinch of salt: Accuracy, precision, and uncertainty in flood inundation modeling." Water Resources Research 49.9 (2013): 6079-6085.

Ebner, Andrew D., et al. Flood of July 27-31, 2006, on the Grand River near Painesville, Ohio. No. 2007-1164. Geological Survey (US), 2007.

ENGINEERS, US ARMY CORPS OF. "River analysis system HEC-RAS: hydraulic reference manual." Institute for Water Resources, Davis, CA (2008).

ENGINEERS, US ARMY CORPS OF. “Revised report on Great Lakes Open-Coast Flood Levels.” MI, 2000

Gayl, Ilse Elizabeth. A new real-time weather monitoring and flood warning approach. 1999.

Gupta, Hoshin Vijai, Soroosh Sorooshian, and Patrice Ogou Yapo. "Status of automatic calibration for hydrologic models: Comparison with multilevel expert calibration." Journal of Hydrologic Engineering 4.2 (1999): 135-143.

Guthrie, J. D., Alan H. Rea, Peter A. Steeves, and David W. Stewart.StreamStats: a water resources web application. US Department of the Interior, US Geological Survey, 2008.

Hicks, F. E., and T. Peacock. "Suitability of HEC-RAS for flood forecasting."Canadian Water Resources Journal 30.2 (2005): 159-174.

Holtzclaw, Emily, Betty Leite, and Rick Myrick. "Floodplain modeling applications for emergency management and stakeholder involvement a case study: New Braunfels, Texas." (2005).

Homer, C.G., Dewitz, J.A., Yang, L., Jin, S., Danielson, P., Xian, G., Coulston, J., Herold, N.D., Wickham, J.D., and Megown, K., 2015, Completion of the 2011 National Land Cover Database for the conterminous United States-Representing a decade of land cover change information. Photogrammetric Engineering and Remote Sensing, v. 81, no. 5, p. 345-354

Horritt, M. S., and P. D. Bates. "Effects of spatial resolution on a raster based model of flood flow." Journal of Hydrology 253.1 (2001): 239-249.

Kalyanapu, Alfred J., Steven J. Burian, and Timothy N. McPherson. "Effect of land use-based surface roughness on hydrologic model output." Journal of Spatial Hydrology 9.2 (2010).

King, Rawle O. "National flood insurance program: Background, challenges, and financial status." Congressional Research Service, Library of Congress, 2009.

Koltun, G. F., and John W. Roberts. Techniques for estimating flood-peak discharges of rural, unregulated streams in Ohio. Department of the Interior, US Geological Survey, 1990.

Krimm, Richard W. "Reducing flood losses in the United States."Proceedings of international workshop on floodplain risk management. < The> Committee of International Workshop on Floodplain Risk Management, 1996.

Krzysztofowicz, Roman, Karen S. Kelly, and Dou Long. "Reliability of flood warning systems." Journal of water resources planning and management120.6 (1994): 906-926.

Leedal, David, et al., "Visualization approaches for communicating real-time flood forecasting level and inundation information." Journal of Flood Risk Management 3.2 (2010): 140-150.

Lowe, Anthony S. "The federal emergency management agency's multi-hazard flood map modernization and the national map." Photogrammetric Engineering & Remote Sensing 69.10 (2003): 1133-1135.

Marks, Kate, and Paul Bates. "Integration of high-resolution topographic data with floodplain flow models." Hydrological Processes 14.11-12 (2000): 2109-2122.

Merwade, Venkatesh, et al., "Uncertainty in flood inundation mapping: current issues and future directions." Journal of Hydrologic Engineering 13.7 (2008): 608-620.

Merz, Bruno, A. H. Thieken, and Martin Gocht. "Flood risk mapping at the local scale: concepts and challenges." Flood risk management in Europe. Springer Netherlands, 2007. 231-251.

Moriasi, Daniel N., et al. "Model evaluation guidelines for systematic quantification of accuracy in watershed simulations." Transactions of the ASABE 50.3 (2007): 885-900.

Nash, J. E. and J. V. Sutcliffe (1970), River flow forecasting through conceptual models part I -A discussion of principles, Journal of Hydrology, 10 (3), 282-290

Oegema, B. W., and E. A. McBean. "Uncertainties in flood plain mapping."Application of Frequency and Risk in Water Resources. Springer Netherlands, 1987. 293-303.

Pappenberger, F., et al. "Uncertainty in the calibration of effective roughness parameters in HEC-RAS using inundation and downstream level observations." Journal of Hydrology 302.1 (2005): 46-69.

Pappenberger, Florian, et al. "Influence of uncertain boundary conditions and model structure on flood inundation predictions." Advances in Water Resources 29.10 (2006): 1430-1449.

Parhi, Prabeer Kumar, R. N. Sankhua, and G. P. Roy. "Calibration of Channel Roughness for Mahanadi River,(India) Using HEC-RAS Model. "Journal of Water Resource and Protection 4.10 (2012): 847.

Perry, Charles A. Significant floods in the United States during the 20th century-USGS measures a century of floods. No. 024-00. US Geological Survey,, 2000.Smemoe, Chris, Jim Nelson, and Alan Zundel. "Developing a Probabilistic Flood Plain Boundary Using HEC-1 and HEC-RAS." World Water & Environmental Resources Congress 2003. ASCE, 2003.

Timbadiya, Prafulkumar V., Prem Lal Patel, and Prakash D. Porey. "Calibration of HEC-RAS model on prediction of flood for lower Tapi River, India." Journal of Water Resource and Protection 3.11 (2011): 805.

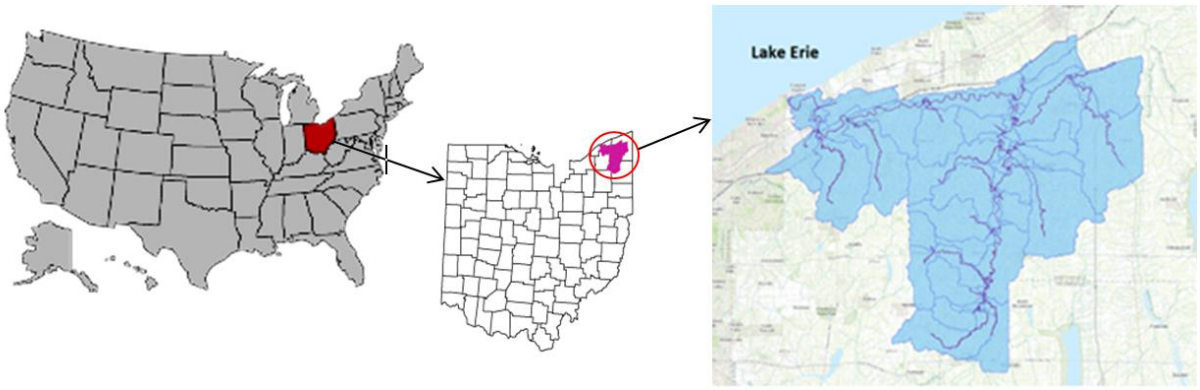

Figure 2-1: Study area of Grand River, Ohio (Grand River watershed)

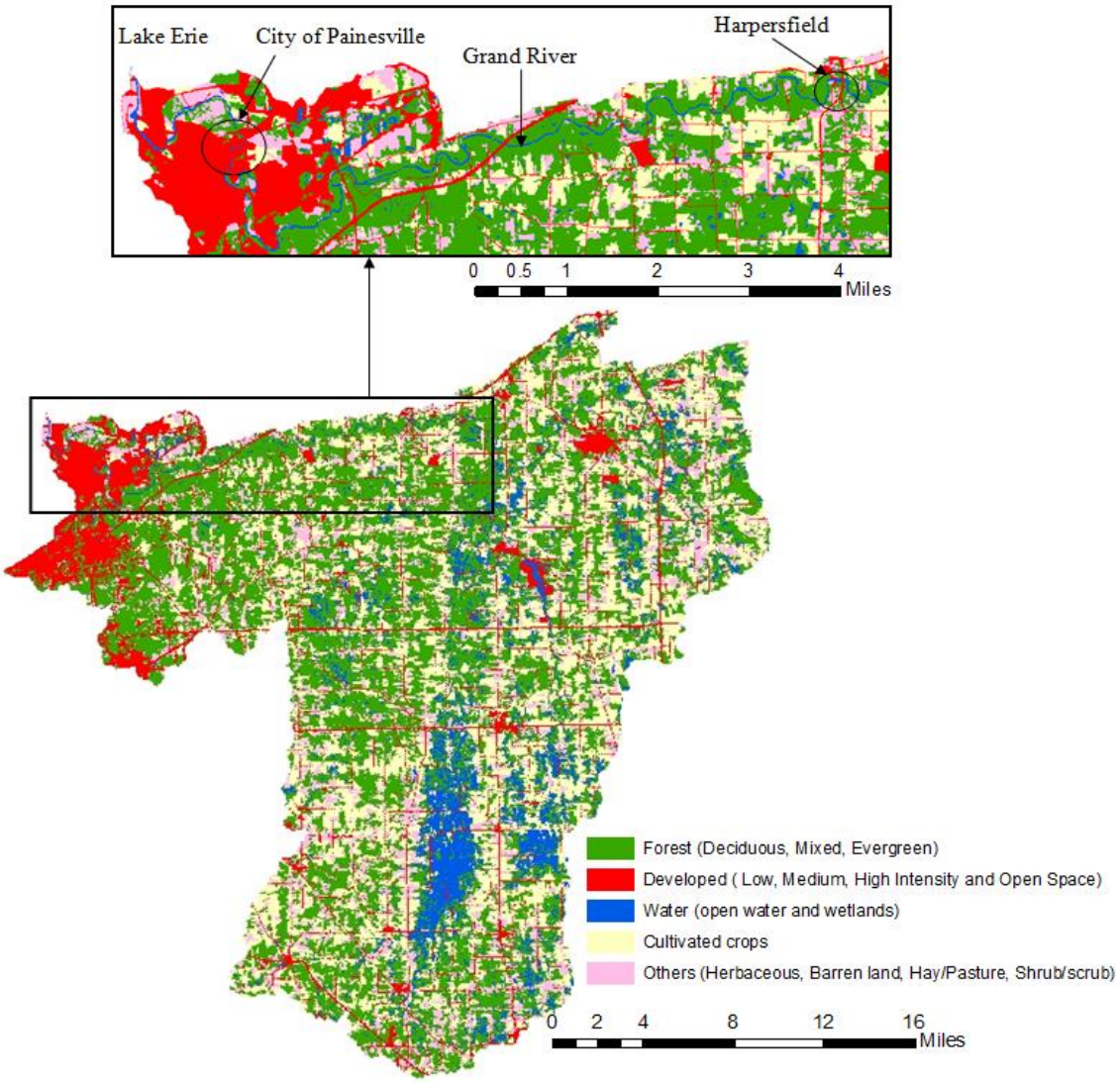

Figure 2-2: NLCD (2011) map of Grand River Watershed, Ohio

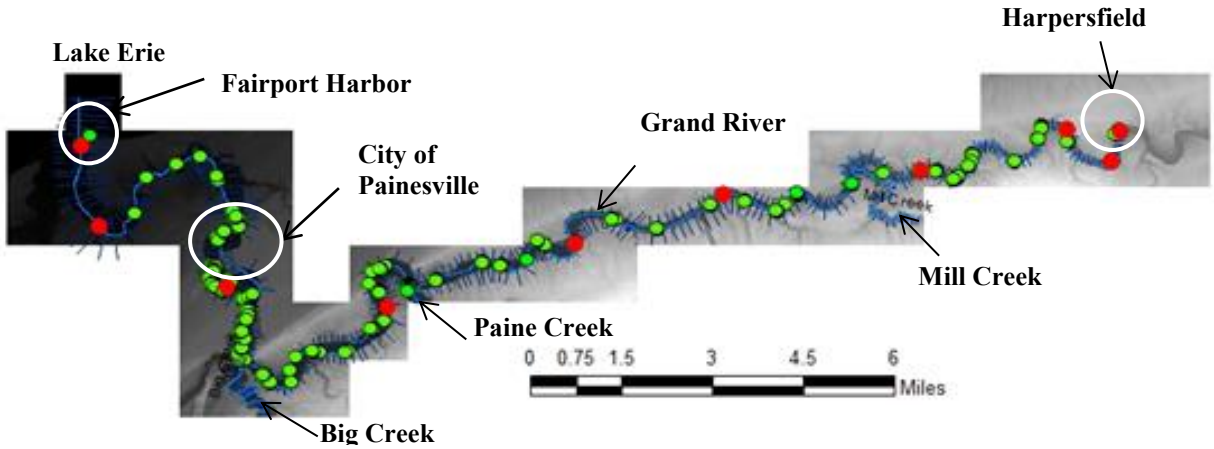

Figure 2-3: LiDAR DEM with cross section configurations of Grand River

(Note: Red dots show the places where cross sections from different elevation datasets are compared (Figure 2-7 a-j) and green dots show surveyed section along the Grand River)

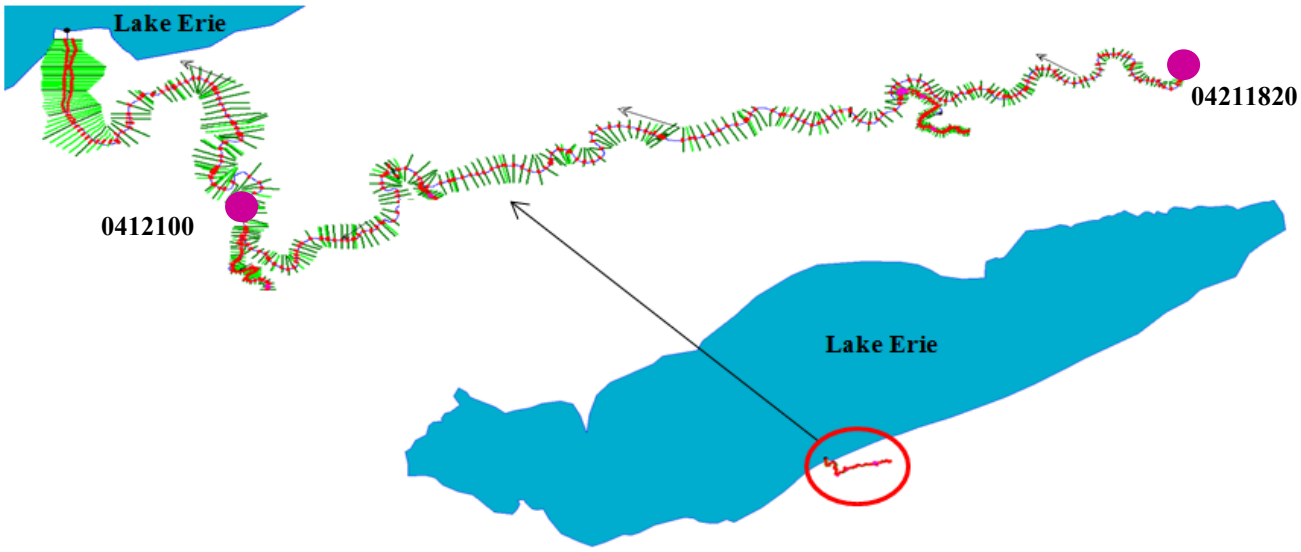

Figure 2-4: Hydraulic model of Grand River in HEC-RAS

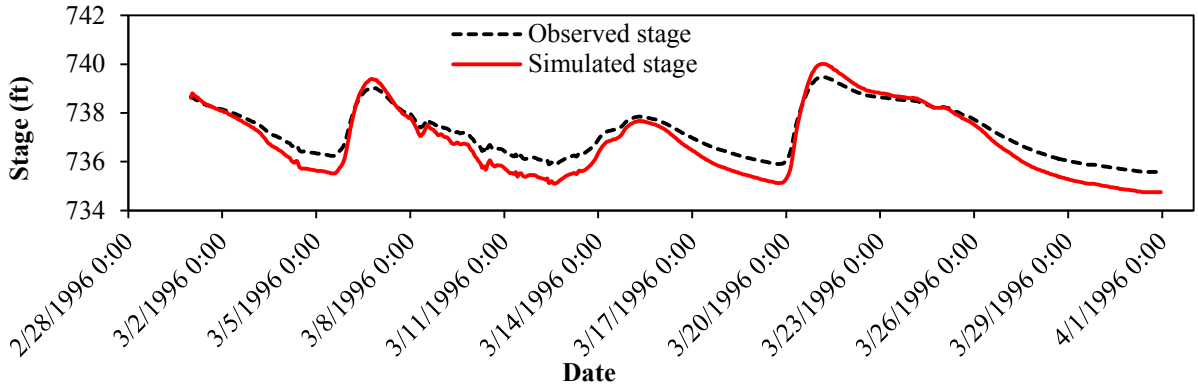

a) Calibration of stage from 3/1/1996 to 03/31/1996

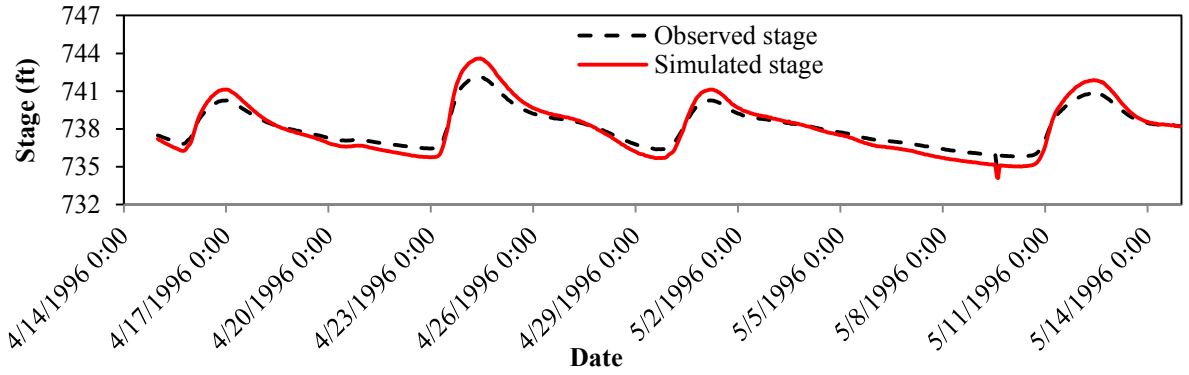

b) Calibration of stage from 4/15/1996 to 5/14/1996

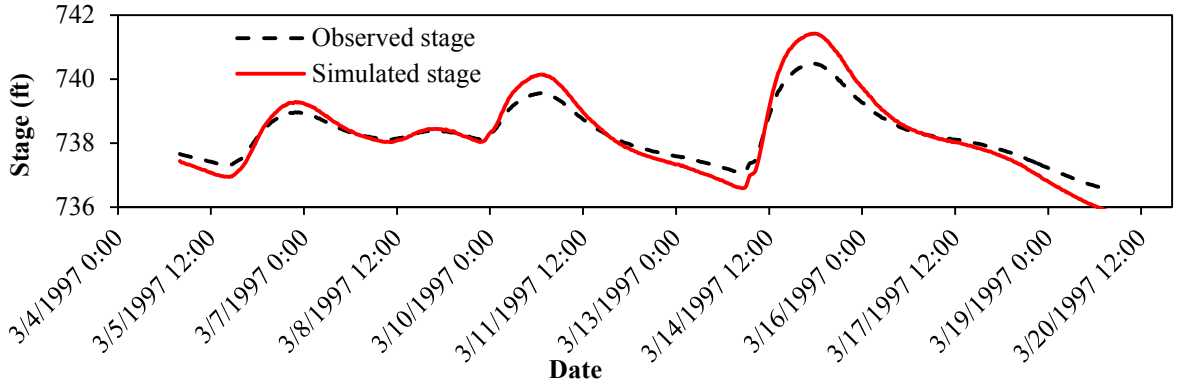

c) Validation of stage from 3/5/1997 to 3/19/1997

Figure 2-5: Calibration of stage from 3/1/1996 to 3/31/1996 (a), 4/15/1996 to 5/14/1996 (b), and validation from 3/5/1997 to 3/19/1997 (c) at upstream gage station 04211820

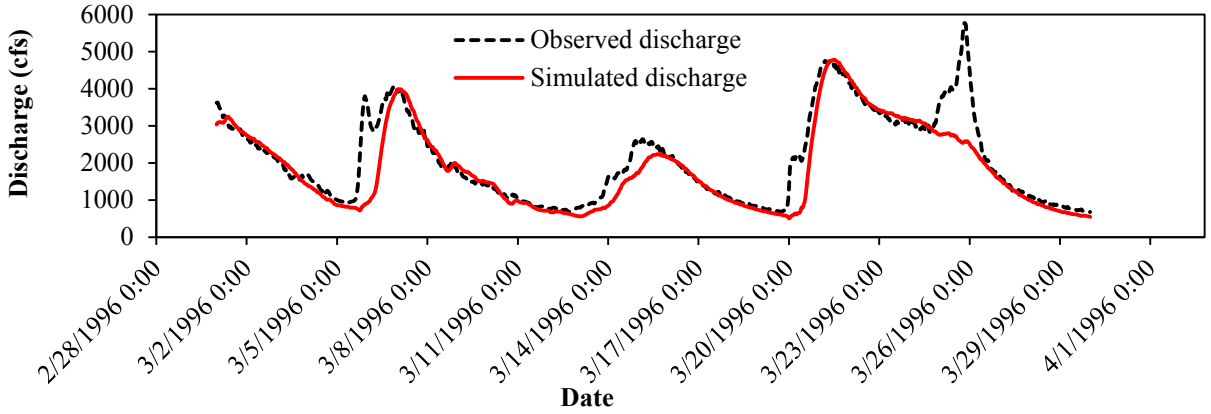

a) Calibration of discharge from 3/1/1996 to 3/31/1996

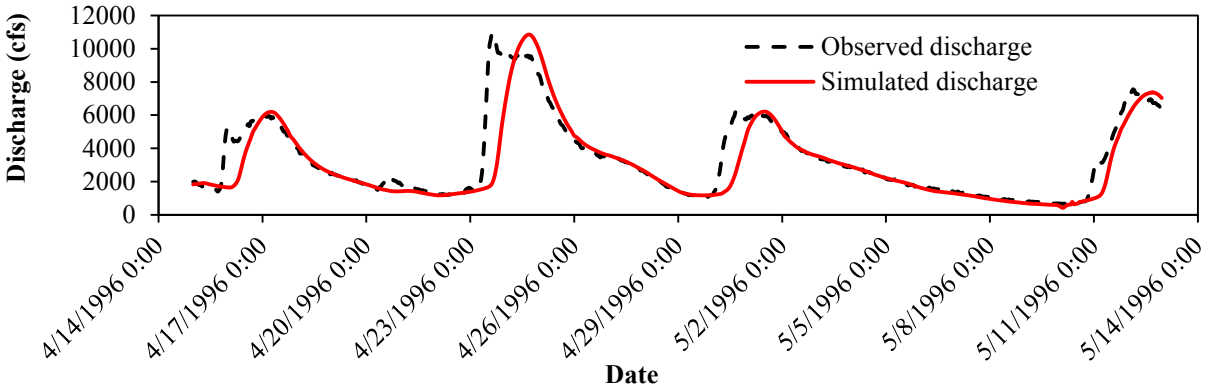

b) Calibration of discharge from 4/15/1996 to 5/14/1996

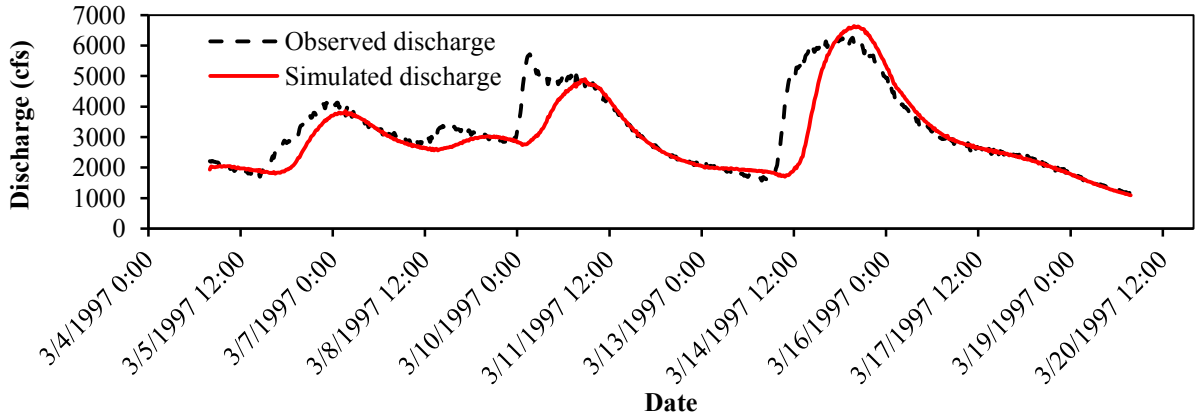

c) Validation of discharge from 3/5/1997 to 3/19/1997

Figure 2-6: Calibration of discharge from 3/1/1996 to 3/31/1996 (a), 4/15/1996 to 5/14/1996 (b), and validation from 3/5/1997 to 3/19/1997 (c) at downstream gage station 04212100

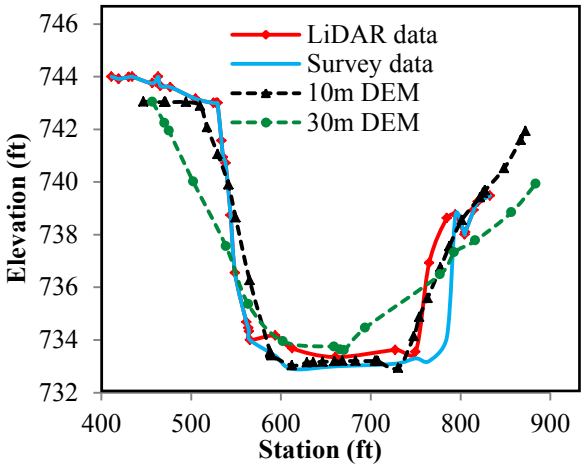

a) Cross section at 170766.4

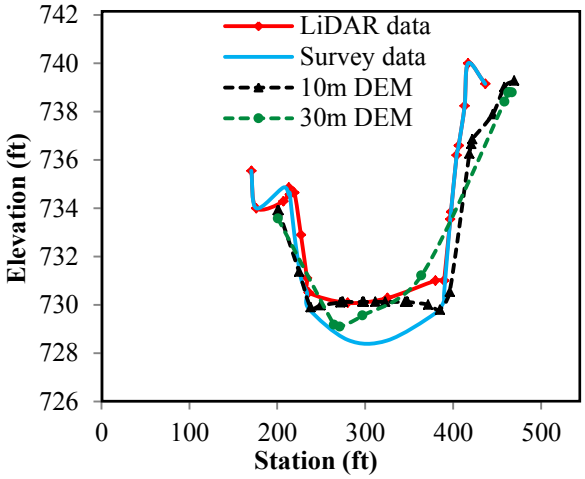

b) Cross section at167516.6

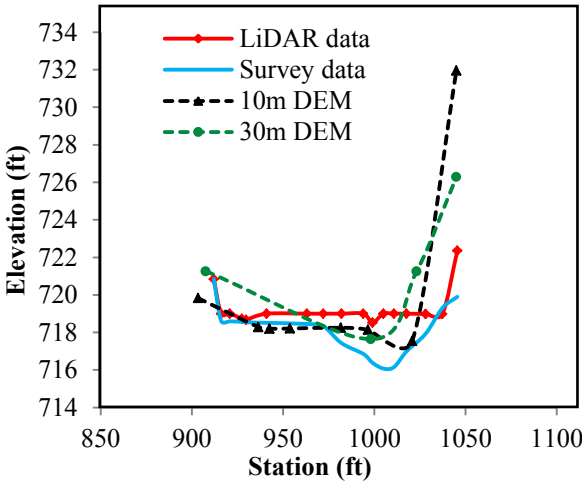

c) Cross section at 160741

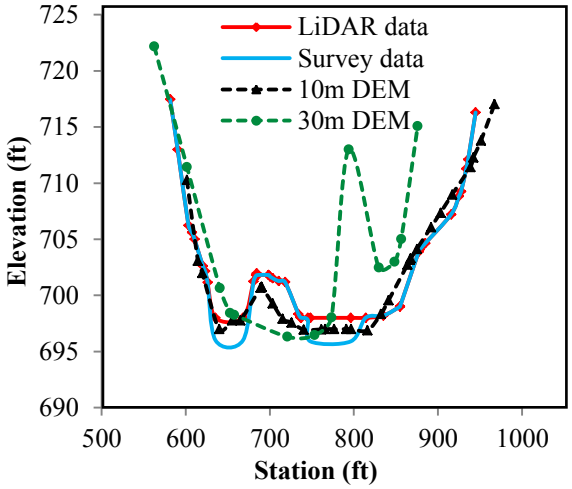

d) Cross section at 146411.3

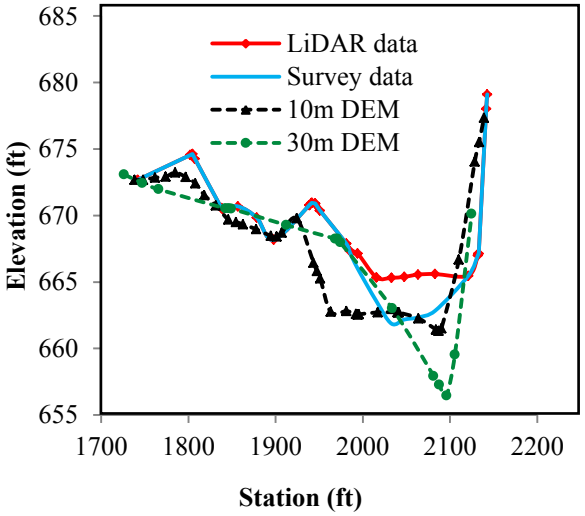

e) Cross section at 117638.8

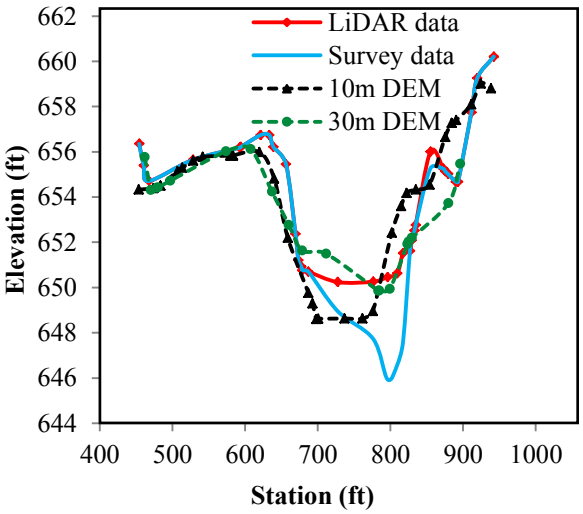

f) Cross section at 100566.7

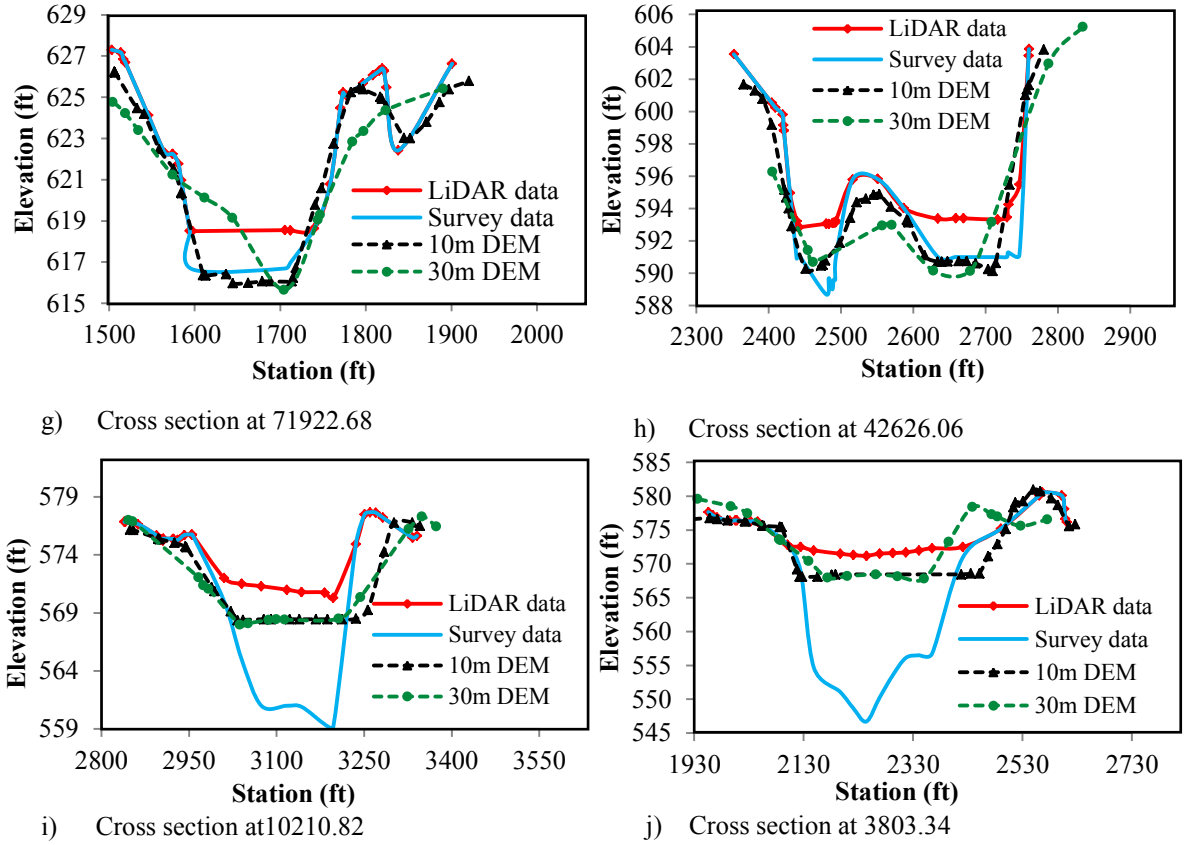

Figure 2-7: Cross section at different points along the Grand River (a)-(j)

(Note: Survey data for 10210.82 and 3803.34 cross sections have been taken from the survey documents of US Army Corps of Engineers Buffalo District. Survey was performed by sounding method)

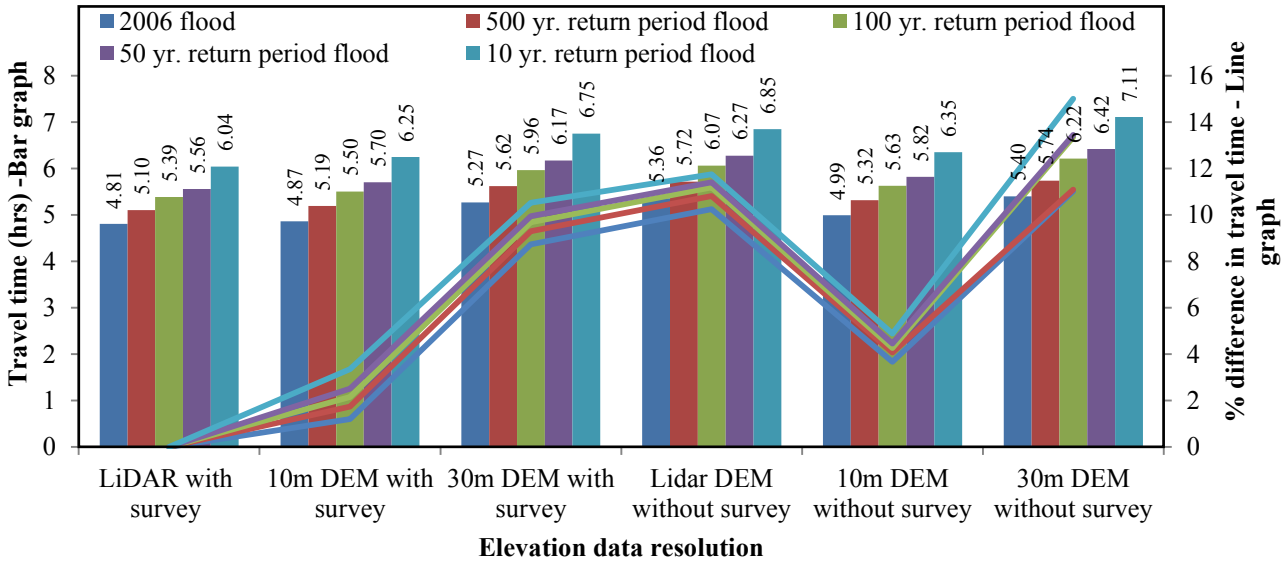

Figure 2-8: Travel time and difference in travel time for different return period floods to reach the City of Painesville using different elevation datasets[1]

([1] Percentage decrease/increase in travel time and inundation area for different elevation datasets has been computed by comparing with the results calculated using LiDAR with survey)

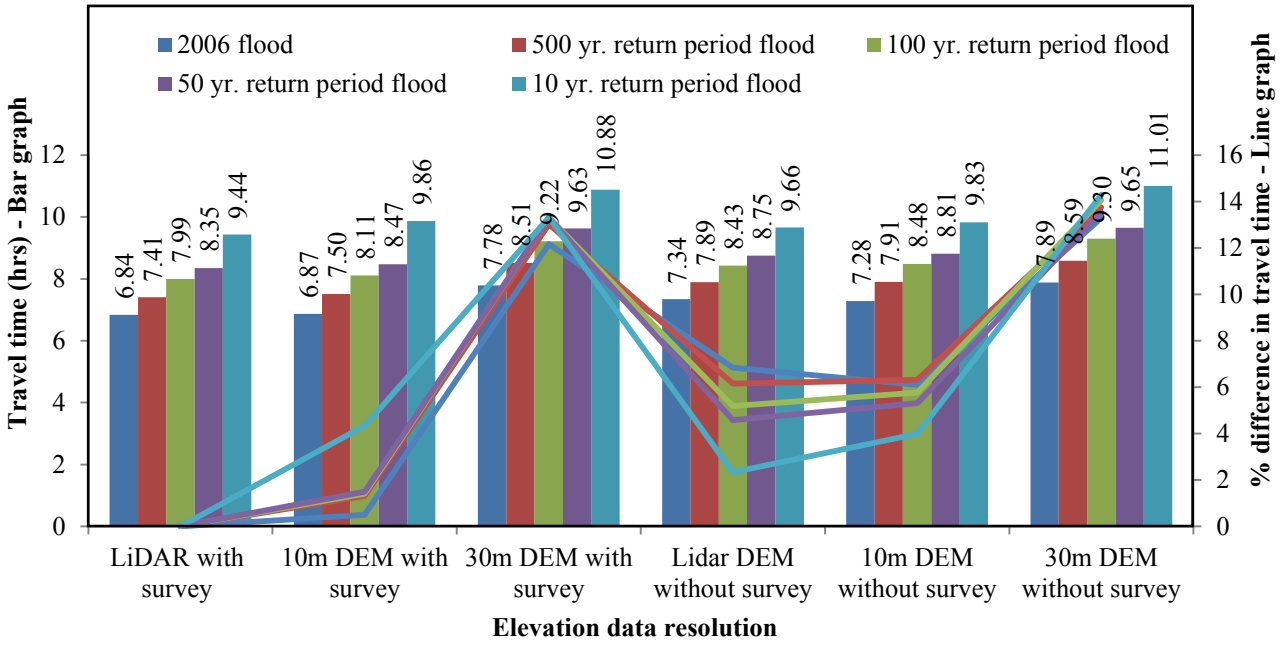

Figure 2-9: Travel time and percentage difference in travel time for different return period floods to reach Fairport Harbor using different elevation datasets[1]

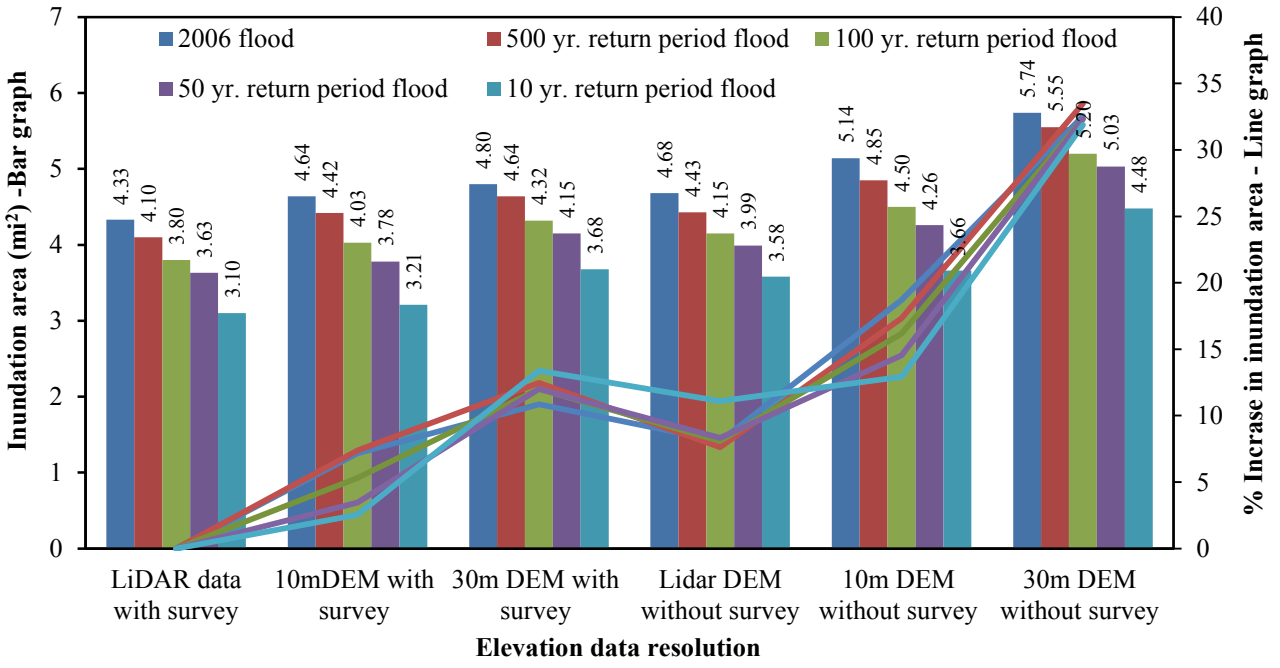

Figure 2-10: Inundation area and percentage difference in inundation area for different return period floods and different elevation datasets[1]

([1] Percentage decrease/increase in travel time and inundation area for different elevation datasets has been computed by comparing with the results calculated using LiDAR with survey)

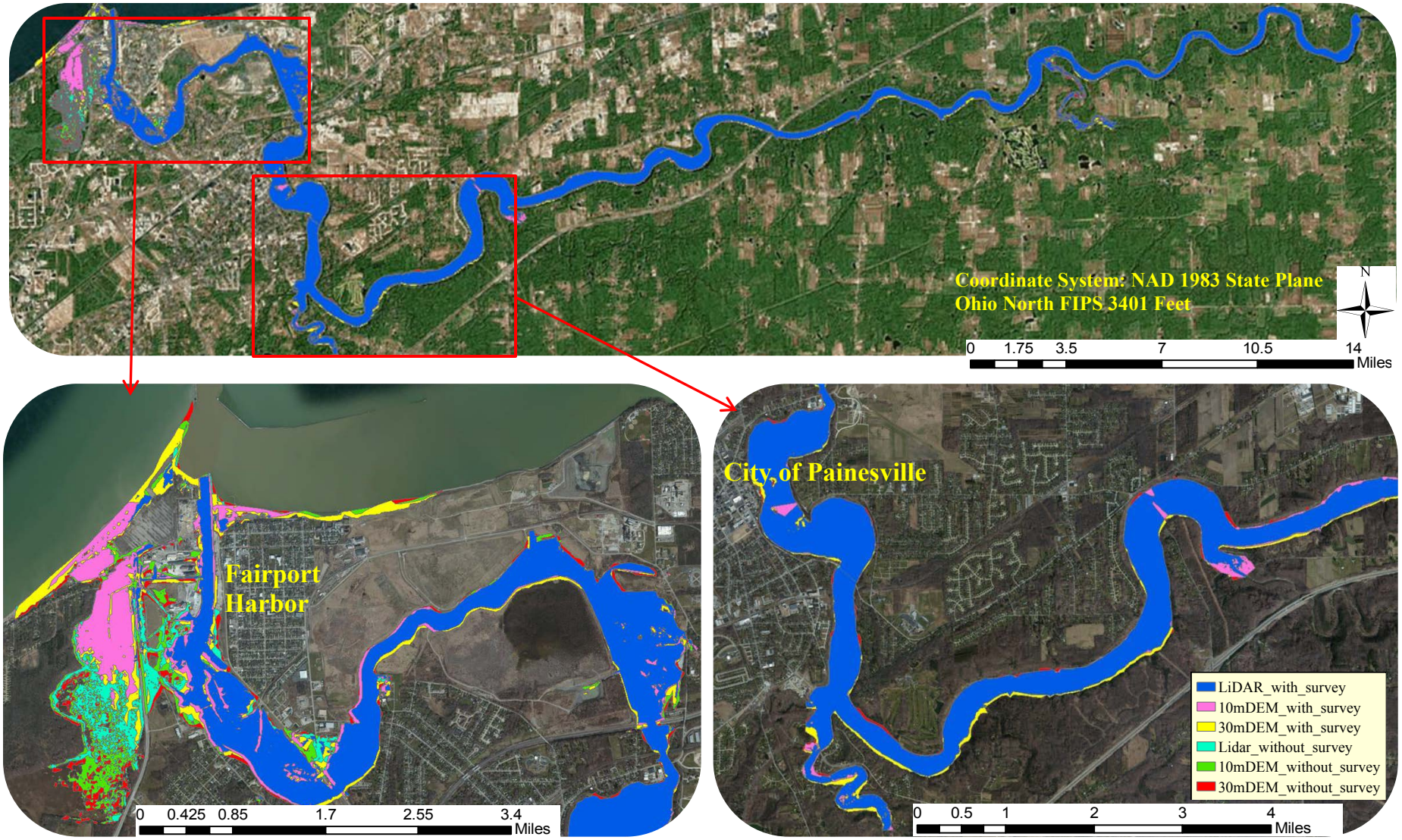

Figure 2-11: Difference in inundation area due to 2006 flooding in Grand River when generated using different sets of elevation dataset
(Note: It should be noted that pink color map covers all areas covered in pink as well as by blue. Similarly, yellow color map covers all areas in blue, pink and yellow. Likewise, red color map which represents 30mDEM without survey shows areas covered in red and all the areas that are included in all other cases.)

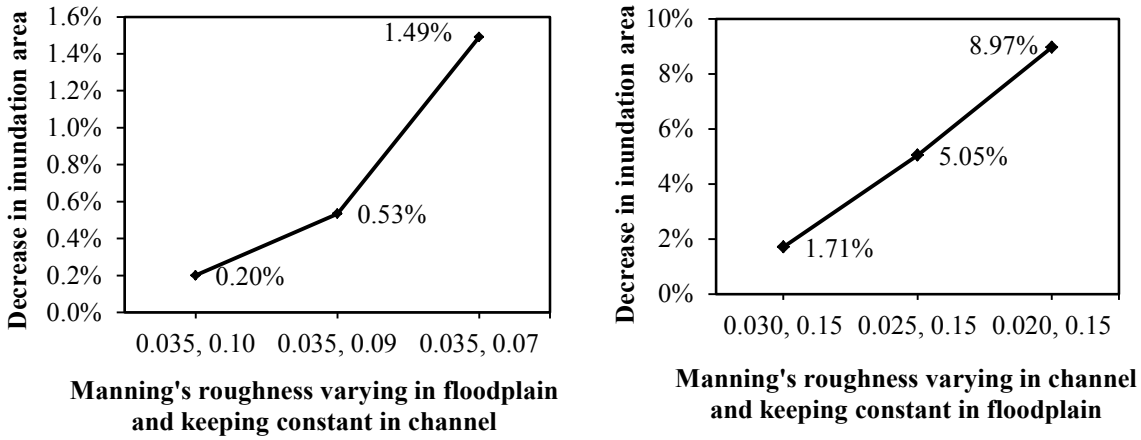

Figure 2-12: Percentage decrease in inundation area for different values of Manning's roughness

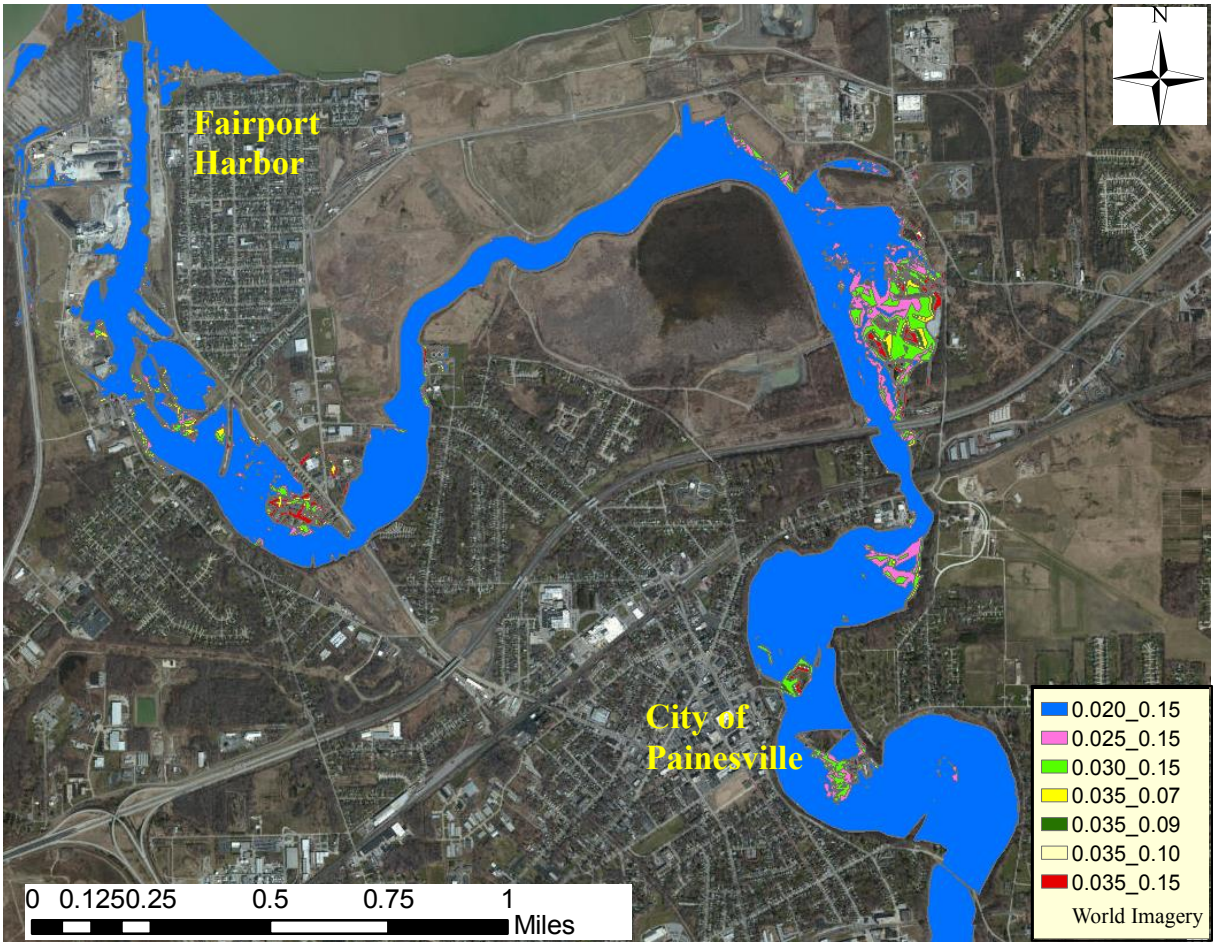

Figure 2-13: Difference in flood inundation maps for different roughness value

Table 2-1: Datasets used in the study

Types of data	Data	Source
GIS	Light Detection and Ranging (LiDAR) derived DEM	OGRIP http://gis3.oit.ohio.gov/geodatadownload/osip.aspx
	National Land Cover Datasets 2011	United States Department of Agriculture, Natural Resources Conservation Service (USDA, NRCS) Geospatial Data Gateway https://gdg.sc.egov.usda.gov/
	Digital georeferenced aerial photography	Ohio Statewide Imagery Program (Ohio Department of Administrative Services, 2007) http://ogrip.oit.ohio.gov/
	Digital Elevation Model (DEM) 10m DEM, 30m DEM	USDA, NRCS Geospatial Data Gateway https://gdg.sc.egov.usda.gov/
Hydrology	Stream flow (discharge) and water surface stage	United States Geological Survey (USGS) http://waterdata.usgs.gov/usa/nwis/uv?04212100 http://waterdata.usgs.gov/usa/nwis/sw
Climate	Precipitation and Temperature	NOAA/National Climatic Data Center (NCDC) http://www.ncdc.noaa.gov/cdo-web/
Bridge data	Engineering drawing of bridges	Lake County Office http://www.lakecountyohio.gov/ Ohio department of Transportation http://www.dot.state.oh.us/

Table 2-2: Calibration/validation for stage at upstream gage station 04211820

S.N.	Date		Statistical parameters			
	From	To	NSE	R^2	PBIAS	RSR
Calibration						
1.	3/1/1996 0:00	3/30/1996 0:00	0.74	1.00	0.05	0.51
2.	4/15/1996 0:00	5/12/1996 23:00	0.84	1.00	0.00	0.39
3.	10/20/1996 0:00	11/28/1996 23:00	0.84	1.00	0.03	0.40
4.	2/4/1997 0:00	2/10/1997 23:30	0.83	1.00	0.02	0.41
Validation						
5.	2/26/1997 0:00	3/3/1997 23:30	0.81	1.00	-0.07	0.43
6.	3/5/1997 0:00	3/19/1997 23:30	0.82	1.00	0.00	0.43
7.	5/15/1997 0:00	6/6/1997 23:00	0.85	0.99	0.02	0.39
8.	4/10/1998 0:00	4/30/1998 0:00	0.89	1.00	0.02	0.33

Table 2-3: Calibration/validation for discharge at downstream gage station 04212100

S.N.	Date		Statistical parameters			
	From	To	NSE	R^2	PBIAS	RSR
Calibration						
1.	3/1/1996 0:00	3/30/1996 0:00	0.74	0.88	11.04	0.51
2.	4/15/1996 0:00	5/12/1996 23:00	0.72	0.86	9.18	0.53
3.	10/20/1996 0:00	11/28/1996 23:00	0.90	0.96	8.85	0.31
4.	2/4/1997 0:00	2/10/1997 23:30	0.84	0.92	1.26	0.40
Validation						
5.	2/26/1997 0:00	3/3/1997 23:30	0.33	0.70	5.20	0.82
6.	3/5/1997 0:00	3/19/1997 23:30	0.69	0.85	7.37	0.56
7.	5/15/1997 0:00	6/6/1997 23:00	0.80	0.92	-3.34	0.45
8.	4/10/1998 0:00	4/30/1998 0:00	0.83	0.92	3.24	0.41

Table 2-4: Inundation area for different return period flood using various elevation datasets[1]

Return period floods	Inundation area (mi^2)						Percentage increase in inundation area				
	LiDAR with survey	10m DEM with survey	30m DEM with survey	LiDAR without survey	10m DEM without survey	30m DEM without survey	10m DEM with survey	30m DEM with survey	LiDAR without survey	10m DEM without survey	30m DEM without survey
2006 flood	4.33	4.64	4.80	4.68	5.14	5.74	7.16%	10.85%	8.08%	18.71%	32.56%
500 years	4.10	4.42	4.64	4.43	4.85	5.55	7.80%	13.17%	8.05%	18.29%	35.37%
100 years	3.80	4.03	4.32	4.15	4.50	5.20	6.05%	13.68%	9.21%	18.42%	36.84%
50 years	3.63	3.78	4.15	3.99	4.26	5.03	4.13%	14.33%	9.92%	17.36%	38.57%
10 years	3.10	3.21	3.68	3.58	3.66	4.48	3.55%	18.71%	15.48%	18.06%	44.52%

[1] Percentage decrease/increase in travel time and inundation area for different elevation datasets has been computed by comparing with the results calculated using LiDAR with survey

Table 2-5: Decrease in inundation area when survey data is incorporated

Return period floods	LiDAR data	10m DEM	30m DEM
2006 flood	7.48%	9.73%	16.38%
500 yr. return period flood	7.45%	8.87%	16.40%
100 yr. return period flood	8.43%	10.44%	16.92%
50 yr. return period flood	9.02%	11.27%	17.50%
10 yr. return period flood	13.41%	12.30%	17.86%
Average decrease	**9.16%**	**10.52%**	**17.01%**

Table 2-6: Travel time to City of Painesville for different Manning's roughness values

(Note: In percentage increase/decrease table first three column represents the result when Manning's roughness is varied in floodplain keeping constant in channel and in last three column represents the results when Manning's roughness is varied in channel keeping constant in floodplain)

Return Period Floods	Travel Time for n = 0.035, 0.15 (hrs)	Percentage increase or decrease in time travel time for different roughness value					
		n = roughness value in channel, roughness value in floodplains					
		n=0.035,0.10	n=0.035,0.09	n=0.035,0.07	n=0.030,0.15	n=0.025,0.15	n=0.020,0.15
2006 flood	4.81	1.52%	2.02%	3.45%	-7.48%	-14.32%	-20.72%
500 years	5.10	1.04%	1.55%	2.75%	-7.59%	-14.48%	-20.98%
100 years	5.39	0.95%	1.32%	2.27%	-7.61%	-14.60%	-21.12%
50 years	5.56	0.82%	1.13%	2.00%	-7.67%	-14.74%	-21.42%
10 years	6.04	0.60%	0.84%	1.48%	-7.77%	-15.19%	-22.35%

Note: Negative sign indicates percentage decrease

Chapter 3. Development of a Flood Warning System and Flood Inundation Mapping for the Grand River near the City of Painesville, Ohio

Abstract

Flooding is one of the most frequent natural disasters across the world, which damages properties and may take the lives of people. Flood warning system can play significant roles to minimize those effects by evacuating the people from the probable affected areas during the peak flood time. Therefore, the major objective of this research is to prepare flood warning system for the Grand River, Ohio to provide evacuation period for the people of probable affected areas with sufficient lead time. Flood warning system was developed by calculating flood travel time and generating the inundation mapping for 12 different selected flood stages, which were approximately 2 to 500 years in recurrence interval, ranging from 10.00 ft to 21.00 ft at gage station 04212100, near the City of Painesville. A one-dimensional model, Hydraulic Engineering Center-River Analysis System (HEC-RAS) was utilized for hydraulic modeling. Geospatial data required for HEC-RAS were obtained using Digital Elevation Model (DEM) derived from Light Detection and Ranging (LiDAR) datasets, which was pre-processed and post processed in HEC-GeoRAS to produce flood inundation maps. The flood travel time and flood inundation maps have been generated integrating LiDAR data with field verified survey and calibrated Manning's roughness value. The generated inundation maps estimate the aerial extent of flooding along the Grand River corresponding to the various flood stages at gage station 04212100 near the City of Painesville and 04211820 in Harpersfield. The inundation maps were overlaid on digital orthographic maps to visualize its aerial extents. The steady state hydraulic model was calibrated using available datasets. There are more than 100 houses, many roads, bridges and parks along

the Grand River are vulnerable to flooding during 500 year return period flood leading to the requirement of a flood warning system to be installed near the City of Painesville, Ohio.

Keywords: Flood Warning System, Inundation Mapping, HEC-RAS, HEC-GeoRAS, LiDAR datasets

Introduction

Flooding is a major natural hazard which greatly impacts different regions across the world (Yuan et al., 2011; Alfaro et al., 2013). Ludlum (1991) defines a flood as the presence of "too much water in areas that are not normally under water". Similarly, Standard Flood Insurance Policy (SFIP) defines flood as "A general and temporary condition of partial or complete inundation of two or more acres of normally dry land area of two or more properties (at least one of which is your property) from overflow of inland or tidal waters from any source, or from mudflow" (FEMA, 2001a). In the United States, flood takes the lives of more people than any form of other natural disaster (Krimm, 1996; Perry 2000). Among the various types of flood, flash floods are the most dangerous as these are the primary cause of deaths in the United States which kill more than 140 people each year (NWS, 2016). Flash flood is an abrupt flow of a large amount of water in a river within a few minutes or hours due to extreme rainfall, failure of a dam/levee or an abrupt release of water due to ice jam (NWS, 2016; Mwape, 2009).

The City of Painesville has been frequently threatened by flooding over different years such as in 1986, 1989, 2006, 2008, and 2011. The historical annual peak flow/stage and various flood stage level as per National Weather Service (NWS, 2016a) in the Grand River, Ohio is shown in Figure 3-1. The extensive flooding in Grand River, Ohio

was experienced on July 27-28, 2006 due to the intense rainfall of more than 11 inches depth that occurred within a short period of time. This was one of the highest historical flood occurred in the Grand River, near the City of Painesville. This flood led to the property damages estimated of 30 million USD and one fatality in Lake County. Several people (600) had to be evacuated due to which three counties (Lake, Geauga and Ashtabula) were declared as Federal and State disaster areas (Ebner et al. 2007). The flood destroyed more than 800 homes and 5 bridges in Lake County. Additionally, it disrupted traffic by closing 13 roads near the City of Painesville. The peak discharge and stage for that event was estimated to be 35,000 cfs and 19.35 ft. respectively (Figure 3-2) as recorded by USGS gauge station (04212100) near the City of Painesville. Therefore, the development of flood warning system in the Grand River is absolutely essential to protect the lives of people and reduce the property losses.

Flood warning system protects people's lives and prevents property damages from such disaster by providing the sufficient lead time for the evacuation (Krzysztofowicz et al., 1994). The formal UN report (ISDR, 2003) defines early warning system as "The provision of timely and effective information, through identifying institutions that allow individuals exposed to a hazard to take action to avoid or reduce their risk and prepare for effective response". Flood risk management should contain efficient actions of preparedness, response and recovery, which is essential for rescue operation during flood time (Borga et al., 2011). For the efficient management of flood risks, two important factors that should be taken into well are flood travel time and possible area of inundation. Flood travel time is the key element needed for the timely evacuation of people from probable flood prone areas. Likewise, flood inundation maps are also

important tools that represent spatial variability of flood hazard and provide the clear picture and robust understanding of floods than any other forms (Merz et al., 2007; Leedal et al., 2010). Therefore, these maps should be carefully prepared and made easily accessible to the public without any difficulties (Holtzclaw et al., 2005). Moreover, it is essential to have a proper communication and coordination among federal, regional, state and local bodies and the private sectors to establish effective flood warning system (Fukuoka, 1998).

There are some basic processes before and after the flood occurrence, which should be followed while developing the efficient flood warning system (Aliasgar, 2012; ISDR PPEW, 2006). The processes before the flood occurrence are: generation of flood inundation maps for various flood stages, quantification of thresholds in maps and identification of flood hazard areas for different flood scenarios. Similarly, the processes after the flood occurrence are: to inform concerned officials/authorities, issue warning system to the people of possible inundation areas, evacuate people from probable inundation areas, and rescue operation. However, both the citizens and concerned authorities should be able to understand the risks associated with the floods in order to minimize the effects of flood hazards in any area (Holtzclaw, 2005). Also, the communities should be involved in Federal Emergency Management Agency (FEMA) Map Modernization program (Holtzclaw, 2005) to understand the flood maps and warning system developed by FEMA.

The primary objective of this research was to develop a hydraulic model using HEC-RAS for the use by the National Weather Service and prepare all necessary digital files including rating curve to provide the evacuation time for flood warning system in

the Grand River, Ohio. A series of flood inundation maps for 12 different selected flood stages were generated using HEC-GeoRAS based on the steady state simulation performed in HEC-RAS. The basic processes needed for effective flood warning system before the occurrence of flood was accomplished and described in this study. The NWS has a legal responsibility for hydrologic forecast throughout the nation (Whitehead et al., 2009 and Ostheimer, 2012). The NWS Ohio River Forecast Center located in Wilmington, Ohio, forecasts the peak stage flows based on the precipitation gages and streamflow gages in Ohio. Based on the forecasted streamflow and stages, the flood travel time and possible inundation area can be estimated from pre-developed flood inundation maps and flood warning can be issued to probable affected areas.

Theoretical Description

The hydraulic modeling software, HEC-RAS, was used in this study for steady and unsteady flow analysis. The HEC-RAS model description has been described in detail in Chapter 2 under heading "Theoretical Description".

Flood travel time is calculated based on the flood velocity during the peak flood time. During the peak flood time, flood travels quickly in the channel section as area of flow is relatively less in channel section than in the floodplain region. The equations to calculate channel velocity and travel time are given below.

$$V_{ch.} = \frac{Q_{ch.}}{A_{ch.}} \qquad (3.1)$$

$$T = \frac{X}{V_{ch.}} \qquad (3.2)$$

Where $V_{ch.}$ is channel velocity in ft/sec; $Q_{ch.}$ is channel flow in cfs; $A_{ch.}$ is flow area in the channel; T is travel time in seconds that flood takes to travel from one cross section to the next; and X is a longitudinal distance between two corresponding cross sections.

Rating curve was used to calculate the streamflow for various stages. Rating curve equation was developed using the daily discharge data greater than 75 percentile for the period of 1988-2005. Since all the practical purposes of developing rating curve in this study was to estimate the streamflow during high flood time, rating curve was developed using 75 percentile flow in order to capture all high flood discharge values. It is noteworthy to mention that the rating curve developed for higher flow may not be applicable during low flow condition and vice versa.

Materials and Methodology

Study Area

This study was conducted in the Grand River watershed, which is located in the Northeastern region of Ohio. The City of Painesville along the Grand River is one of the most affected regions due to frequent flooding that occurred from time to time (2006, 2008, and 2011). The detail description of the Grand River watershed is already described in Chapter 2.

Overall Flood Warning Approach

Basically, an approach towards a better flood warning system was developed in this study. The following steps will be accomplished to develop fully functional flood warning system. This approach is the similar to the approach adopted in Findlay County (Whitehead, 2009) and Licking County (Ostheimer, 2012) of Ohio warning system has been developed.

Development of a Hydraulic Model

Fully functional HEC-RAS model was developed in this study. The calibrated/validated unsteady HEC-RAS model developed in Chapter 2 was used to run

the hydraulic simulation. The overall modeling approach for calibration and validation of Manning's roughness has been already described in Chapter 2 under heading "Overall Modeling Approach". The model was further calibrated for steady flow scenario using high-water mark profiles of 2006 flood. This hydraulic model will be shared with NWS so that they can utilize to simulate and generate inundation maps for other various flow scenarios.

Development of Rating Curve

Rating curve was developed for high flow periods for the streamgage 04212100 near the City of Painesville. The developed rating curve was utilized to predict the flood discharge for 12 different selected floods in the Grand River to be used in hydraulic model.

Preparation of Digital Flood Inundation Maps

The digital flood inundation maps for 12 different selected flood stages were generated using HEC-GeoRAS software based on the steady flow simulation performed in HEC-RAS. The digital flood inundation maps were generated based on the upstream and downstream gage height. These digital maps could be uploaded online in National Portal System or Regional Portal System after further refinement to provide the real time flood inundation to the people.

Installation of Siren System

For the effective flood warning approach, the siren system could be installed at various suitable locations near the City of Painesville to warn the people before the flood affects the probable areas along the Grand River.

Evacuation Time

The flood travel time for 12 different flood scenarios were calculated based on the hydraulic simulation in HEC-RAS. These flood travel time can be used for evacuation of people from probable inundation areas.

This approach provides the valuable information to the public regarding evacuation time and probable inundation areas for several flood stages. Hence, this information can be used to relocate people in safer places with sufficient lead time. However, in order to develop a fully automated flood warning system, streamgages in various required places with automated equipment are necessary to be installed, which will be discussed later in the recommendation section.

HEC-GeoRAS/HEC-RAS Model Input

The HEC-RAS model was developed using LiDAR with field survey data. The summary of input data and detail description of HEC-GeoRAS/HEC-RAS model inputs are discussed in Chapter 2.

Model Calibration and Validation

The unsteady HEC-RAS model was calibrated through the iterative process to obtain the realistic value of Manning's roughness, which was accomplished by comparing observed stage/discharge with the simulated stage/discharge. The model calibration and validation has been described in Chapter 2 under heading "Model Calibration and Validation".

Typically, steady HEC-RAS model is calibrated using high-water mark profiles obtained from the survey during the flood time (Dewberry & Davis, 2002). In this study, the high-water mark elevation points were compared with the modeled water surface

elevation points to evaluate the model efficiency. USGS conducted a survey to obtain high-water mark profiles along the Grand River using standard surveying technique during 2006 flood, and those high-water mark elevation points for this study were collected from Ebner et al. (2007). However, the surveyed data of high-water marks may not always be accurate especially debris and sediments may not be available during the time of the high flood (Ebner et al., 2007).

Model Evaluation Criteria

Various statistical parameters such as NSE, R^2, PBIAS, and RMSE were used to check the accuracy and predictive power of the model, which have been described in detail in Chapter 2 under heading "Model Evaluation Criteria".

Results and Discussions

Unsteady Flow Scenario

The unsteady model was calibrated and validated for both stage and discharge. The performance of the model was good in calibration and validation for different time periods of 1996-1998, which was evaluated using statistical parameter and visual inspection method. The detail calibration and validation of unsteady hydraulic model have been described in Chapter 2 under heading "Results and Discussion".

Steady Flow Scenario

The steady flow model was calibrated to match the high-water mark profiles of 2006 flood. The drainage area ratio method was used to estimate the discharge of all three creeks because of unavailability of gage readings. The streamflow data for all rivers that were taken in consideration are shown in Table 3-1. The high-water mark profiles were compared with simulated water surface elevation for 2006 flood in the Grand River in 19

locations, which are presented in Table 3-2. The errors associated with water surface elevation ranged from 0.02 ft to 1.75 ft. The errors were less than 1 ft in 12 different locations and within 1.36 ft for most of the locations.

Rating Curve

Rating curve for streamgage near the City of Painesville was developed using 75 percentile exceedance discharge values for the period of 1988-2005 in order to capture all the high flood discharge values (Figure 3-3). The equation of developed rating curve is given below.

$$Q = 166.67\, H^{1.7971} \qquad (3.6)$$

Where Q is flow discharge (cfs) and H is the stage (ft) of water in the river.

The developed rating curve was validated from the period of January 2006 to January 2015 with NSE of 0.91 (Figure 3-4). However, the rating curve developed using entire datasets under-predicted the high flow, especially during flood period. This is not surprising as the channel section representing the stage discharge relationship varies depending upon the flood stage; therefore, the rating curve developed for low flood stage may not necessarily true for the higher flood stage.

Calculation of Travel Time and Development of Profiles/Flood-inundation maps

The simulation was performed in steady state condition to generate the profile for 12 stages from 10 ft to 21 ft with 1 ft increment at the Grand River near the City of Painesville. However, 19.35 ft was selected instead of 19.00 ft. in order to represent the flood of July 2006, which approximately corresponds to the flood of 500 years return period. Discharge values corresponding to the selected stages were calculated using the rating curve developed at station 04212100. As there were no any recorded flows in

tributaries of the Grand River including Mill, Paine and Big Creek, discharges for various selected stages for those tributaries were estimated using simple drainage area ratio. The estimated streamflow data for selected stages are presented in Table 3-1. The water surface extents modeled in HEC-RAS were then transferred to HEC-GeoRAS for the development of flood inundation maps for those selected stages. The flood inundation maps were then superimposed onto digital imagery maps produced by Ohio Geographically Referenced Information Program (OGRIP) to see the aerial extents of flooding. The generated inundation maps for 12 different selected stages are presented in appendices section of this chapter.

Flood travel time to reach the City of Painesville and Fairport Harbor including the flood inundation areas were calculated for various flood stages at gage station 04212100, near the City of Painesville (Figure 3-5). The equations for calculated travel time and predicted inundation area were also developed so that they could be used to estimate travel time and inundation area for other flood stages (Figure 3-5).

Flood Damages along the Grand River

Many houses, apartments, roads, bridges and parks along the Grand River are more susceptible to flooding due to 500 years return period flood as shown in the study area. The flood inundation map corresponding to 500 year return period flood is shown in Figure 3-X in appendices section. Since this study was particularly focused in the City of Painesville, several houses, bridges and parks along the Grand River, beyond the study area, which are susceptible to flooding might have been excluded here. The detail information can be obtained from the flood map attached in appendices section for 19.35 ft stage at gage station 04212100. The major affected areas according to hydraulic

simulation are Hidden-Valley Park near South Madison Road, Helen Hazen Wyman Park near the junction of Grand River and Big Creek, Mill Stone Drive, Steel Avenue and Grand River Avenue near Main Street, Kiwanis Recreation Park, Huntington Road near Lakeland Freeway, Treatment Plant and Park near St. Clair St. bridge in the City of Painesville area. Similarly, other highly probable affected areas in Fairport are Western Reserve Yacht Club, Ram Island, Hidden Harbor Drive area, Fairport Harbor Yacht Club. There are more than 30 houses near Grand River Avenue and Steel Avenue, which are subjected to flooding. Almost all the areas of Kiwanis Recreation Park including more than 5 houses in Huntington Road could be expected to be inundated. Also, there are approximately 20 houses susceptible to flooding along the Big Creek and at the junction of Big Creek and Grand River. Moreover, there are approximately 35 houses near Hidden Harbor and Fairport Road in Fairport which are highly vulnerable to flooding. Based on our analysis, almost all the harbors along the Grand River in Fairport might be affected by the flood. Therefore, when the stage at gage station 04212100 near the city of Painesville exceeds above 19.35 ft, the situation might be worse compared to what was experienced in 2006 flood. The damages due to floods of various stages along the Grand River can be obtained from 12 different flood maps attached in the appendices section.

Likewise, the flooding effect was detected in bridges and roads in Painesville and Fairport. Flood levels for different bridges that might be affected during 500 year return period floods are shown in Figure 3-6. Bridges at Vrooman road, Lakeland freeway and Fairport road have the high likelihood of flooding during 500 year return period flood. Among those bridges, Vrooman Bridge was found to be more critical as water level significantly increased (> 3 ft.) average above the road level (Figure 3-6 a). Similarly, the

flood levels for other two bridges are shown in Figure 3-6 b and Figure 3-6 c. Therefore, the alternatives routes for those possibly affected bridges and roadways should be established.

In addition, the flash floods have higher chances to carry large amount of debris and sediments (Sene, 2008). The effects of debris and sediment in increased flood level and floodplain mapping have not been considered in this study. Large woody debris has the capability to affect the hydraulics and hydrology of channel and floodplain areas considerably (Jeffries et al., 2003) causing significant rise in water level at bridges, weirs and other control structures (Sene, 2008). So, the potential sites where debris jam could occur should be studied in order to simulate flood inundation maps accurately.

Conclusion

Flood warning system should be developed carefully and precisely to reduce the negative consequences of a hazard. There is an increasing need to develop reliable flood warning system to reduce the greater risks associated with flooding. In this study, an approach to flood warning system was made for the Grand River by estimating the flood inundation boundaries for 12 selected flood stages at gage station 04212100 near the City of Painesville. HEC-GeoRAS was used for pre-processing to prepare geospatial data required for hydraulic analysis and one dimensional hydraulic model, HEC-RAS, was used to perform hydraulic analyses for different flood stages. The unsteady flow model was developed to calibrate the Manning's roughness value. This unsteady flow model can be utilized in future for flood prediction in this region.

Rating curve was developed using the historical stage/discharge data and utilized to estimate the peak flood discharge for different flood stages. Due to lack of gaged

discharge/stage datasets, simple drainage area ratio method was used to calculate the peak flow for corresponding flood stages for three major creeks within the study area. Additionally, flows from other several ungagged minor creeks present in drainage area were not considered in modeling. The post-processing was performed again in HEC-GeoRAS to generate flood inundation maps for 12 different selected flood stages ranged approximately from 2 to 500 years recurrence period. Those generated inundation maps were overlaid with digital orthographic maps to see aerial extents of various floods. The generated flood inundation maps for 12 different flood stages could be refined and further calibrated considering all sources of streamflow in the model. Furthermore, reestablishing discontinued streamgage in Harpersfield and installing new streamgages each on Mill, Paine and Big Creek would help collect real time series data, which could be fitted to unsteady flow model to generate more accurate flood inundation maps.

Finally, it is expected that rating curve, digital files or flood inundation maps can be utilized to issue the flood warning in this region. In addition, the analysis will be useful resources to NWS, decision makers, emergency flood management agencies for the preparation and management of the situation before and after flooding time along the Grand River, near the City of Painesville.

Recommendation

Streamflow data of major reaches in every drainage basin have significant impact on accurate floodplain mapping. Therefore, reliable streamflow data should be available in order to generate accurate flood inundation maps. USGS developed automated flood warning system in Licking County and Blanchard River, Findlay in Ohio. USGS reestablished several discontinued streamgages and installed new streamgages in order to collect the actual stage and discharge data in various locations. Furthermore, they installed automated flood warning equipment to provide automatic warning about the flood stage. Since there is only one active streamgage in Grand River, installation of new streamgages will help to obtain time series data for the Grand River and develop reliable flood warning system. The summaries of streamgage information in the Grand River basin, Ohio are shown in Table 3-3. This approach is consistent with the method used by Whitehead (2009) in Findlay, Ohio and Ostheimer (2012) in Blanchard River, Ohio to develop automated flood warning system.

Therefore, the future direction to make a more effective automated flood emergency warning and management tool for the Grand River would be to:

1. Reestablish discontinued streamgage in Grand River at Harpersfield and install new streamgages for major creeks like Mill, Paine and Big Creeks;
2. Install automated warning system that contains a rain gauge station, Geostationary Operational Environmental Satellite (GOES) transmitter, Radio Frequency transmitter having Automated Local Evaluation in Real Time (ALERT) technology, and a voice model;

3. Collect high-water mark profiles during the peak flood time which could be used for further calibration and validation of steady flow model for different floods;
4. Couple hydrological and hydraulic model that might lead to improved warning system;
5. Develop two dimensional unsteady hydraulic models to understand the spatial flooding pattern more effectively.

References:

Alfaro et al., “Design of an early warning flood level indicator” October 2013.

Aliasgar, Kelly. "Developing a geoinformatics based early warning system for floods in the Caribbean, Trinidad and Tobago." (2012).

Borga, M., et al. "Flash flood forecasting, warning and risk management: the HYDRATE project." Environmental Science & Policy 14.7 (2011): 834-844.

Dewberry & Davis, LLC. “Floodplain Modeling Manual; HEC-RAS Procedures for HEC-2 Modelers” 2002; http://www.sciencedirect.com/science/article/pii/S0169555X02003252

Ebner, Andrew D., et al. Flood of July 27-31, 2006, on the Grand River near Painesville, Ohio. No. 2007-1164. Geological Survey (US), 2007.

FEMA. 2001a. Answers to Questions about the National Flood Insurance Program. Federal Emergency Management Agency, Washington D.C.

FEMA, 2001a- National Weather Service’s FLDWAV Computer Program;

FEMA, 2001b Full Equations (FEQ) Model for the Solution of Full, Dynamic Equations of Motion for One-Dimensional Unsteady Flow in Open Channels and Through Control Structures.

Fukuoka, Shoji. "Floodplain risk management. Proceedings of an international workshop, Hiroshima, Japan, 11-13 November 1996." Floodplain risk management. Proceedings of an international workshop, Hiroshima, Japan, 11-13 November 1996.. AA Balkema, 1998.

Jeffries, Richard, Stephen E. Darby, and David A. Sear. "The influence of vegetation and organic debris on flood-plain sediment dynamics: case study of a low-order stream in the New Forest, England." Geomorphology51.1 (2003): 61-80.

Holtzclaw, Emily, Betty Leite, and Rick Myrick. "Floodplain modeling applications for emergency management and stakeholder involvement a case study: New Braunfels, Texas." (2005).

ISDR (UN International Strategy for Disaster Reduction), 2003: Terminology: Basic terms of disaster risk reduction.

ISDR PPEW 2006, Basics of Early Warning, UNISDR, < http://www.unisdr.org/ppew/whats-ew/basics-ew.htm.>.

Krimm, Richard W. "Reducing flood losses in the United States."Proceedings of international workshop on floodplain risk management. < The> Committee of International Workshop on Floodplain Risk Management, 1996.

Krzysztofowicz, Roman, Karen S. Kelly, and Dou Long. "Reliability of flood warning systems." Journal of water resources planning and management120.6 (1994): 906-926.

Leedal, David, et al., "Visualization approaches for communicating real-time flood forecasting level and inundation information." Journal of Flood Risk Management 3.2 (2010): 140-150.

Ludlum, David McWilliams. National Audubon Society Field Guide to North American Weather. Vol. 18. Knopf, 1991.

Merz, Bruno, A. H. Thieken, and Martin Gocht. "Flood risk mapping at the local scale: concepts and challenges." Flood risk management in Europe. Springer Netherlands, 2007. 231-251.

Mwape YP (2009) An impact of floods on the socio-economic livelihoods of people: a case study of Sikaunzwe Community in Kazungula District of Zambia. M.Sc. Thesis, University of the Free State, South Africa

NWS, 2012; NOAA's National Weather Service Flood Warning Systems Manual, U.S. DEPARTMENT OF COMMERCE, NOAA-April, 2012

NWS, 2016. Flash Flooding-Flash Floods- The #1 Weather Related Killer in the United States. (Accessed March 2016, at URL) http://www.wrh.noaa.gov/psr/general/severe/ flashflood.php

NWS, 2016a. Advanced Hydrologic Prediction Service. (accessed March 2016) http://water.weather.gov/ahps2/hydrograph.php?wfo=cle&gage=PNVO1

Ostheimer, Chad J. Development of a flood-warning system and flood-inundation mapping in Licking County, Ohio. No. FHWA/OH-2012/4. US Department of the Interior, US Geological Survey, 2012.

Perry, Charles A. Significant floods in the United States during the 20th century-USGS measures a century of floods. No. 024-00. US Geological Survey,, 2000.Smemoe, Chris, Jim Nelson, and Alan Zundel. "Developing a Probabilistic Flood Plain Boundary Using HEC-1 and HEC-RAS." World Water & Environmental Resources Congress 2003. ASCE, 2003.

Sene, Kevin. Flood warning, forecasting and emergency response. Springer Science & Business Media, 2008.

United States Census Bureau, 2010 - http://quickfacts.census.gov/qfd/states/39/3959416.html).

White, Gilbert F. Human adjustment to floods: a geographical approach to the flood problem in the United States. No. 29. Chicago: University of Chicago, 1945.0

Whitehead, Matthew T., and Chad J. Ostheimer. Development of a Flood-Warning System and Flood-Inundation Mapping for the Blanchard River in Findlay, Ohio. 2009.

Yuan et al., “Floodplain Modeling in the Kansas River Basin Using Hydrologic Engineering Center (HEC) Models”. USEPA, NV, 2011

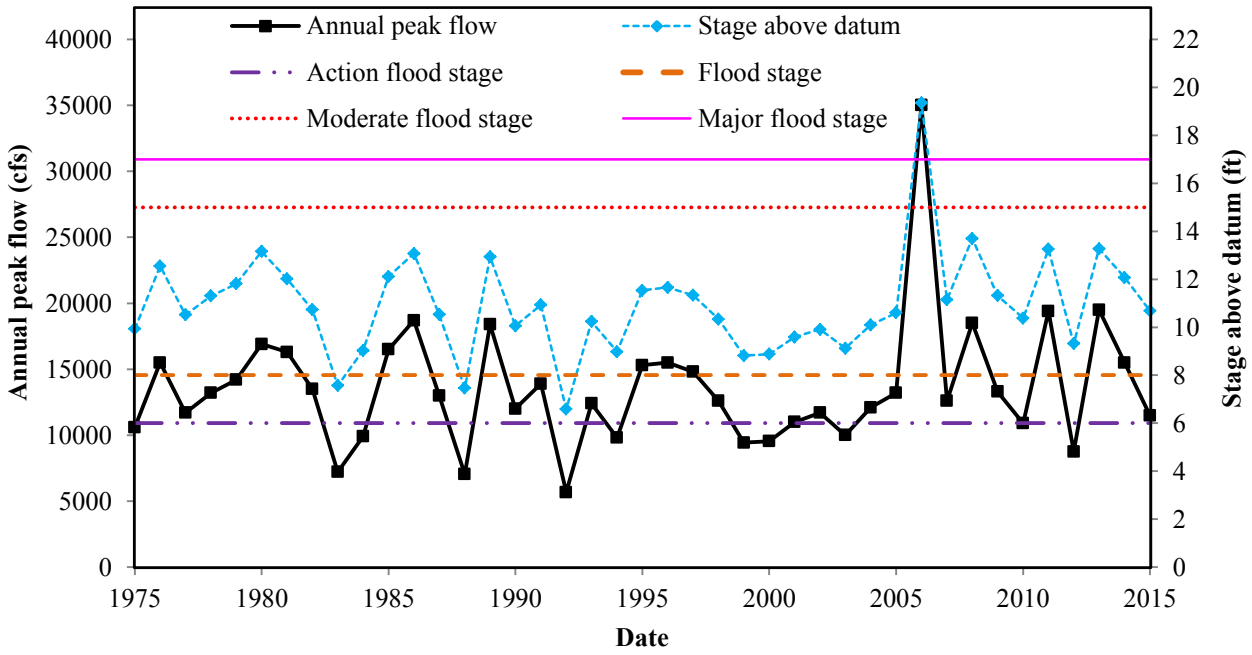

Figure 3-1: Historical annual peak flow/stage and various flood stage level (as per NWS) for the Grand River

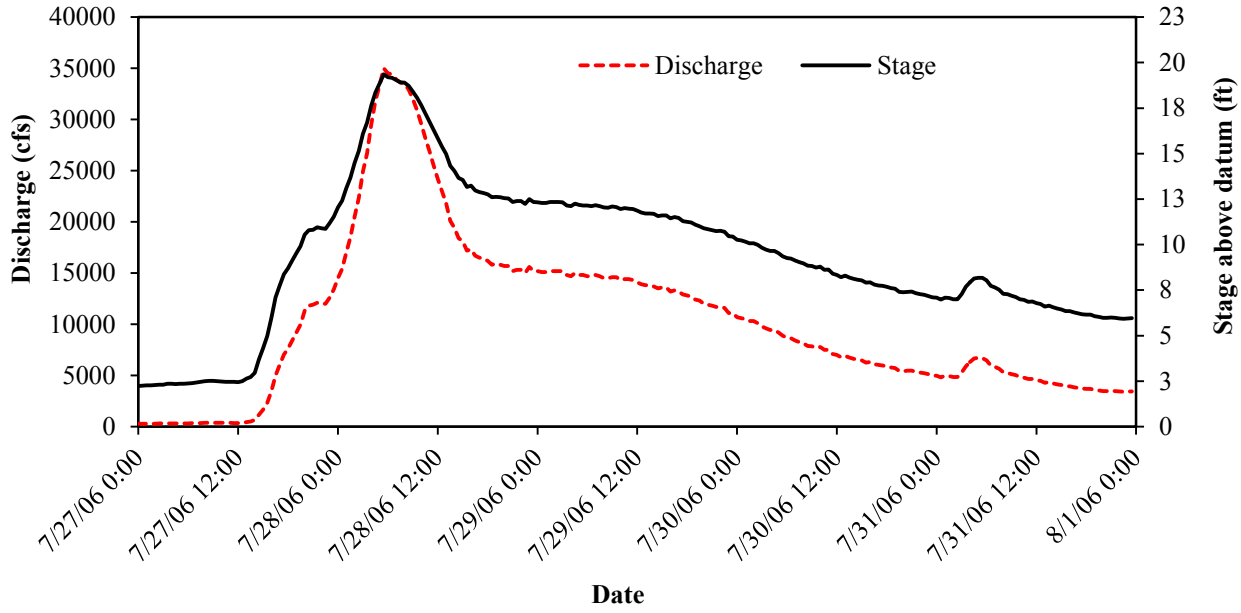

Figure 3-2: Half hourly hydrograph for July 28-29, 2006 flood of Grand River, near the City of Painesville

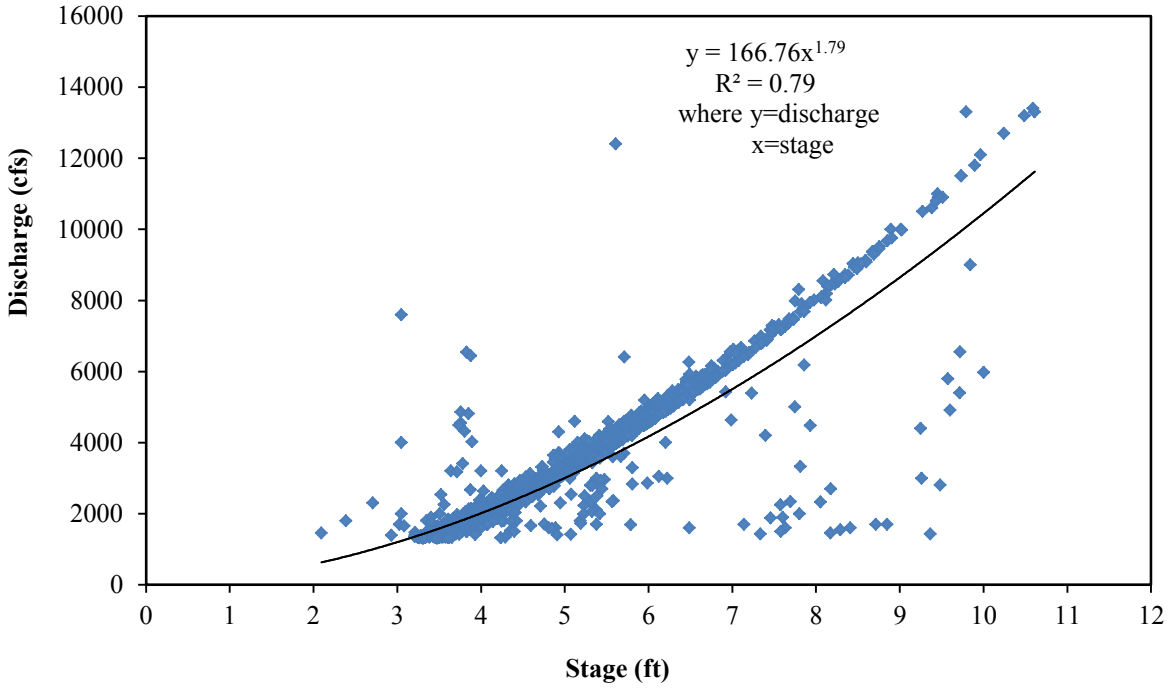

Figure 3-3: Rating curve (based on discharge greater than 75 percentile of discharge values) for Grand River (04212100) near the City of Painesville

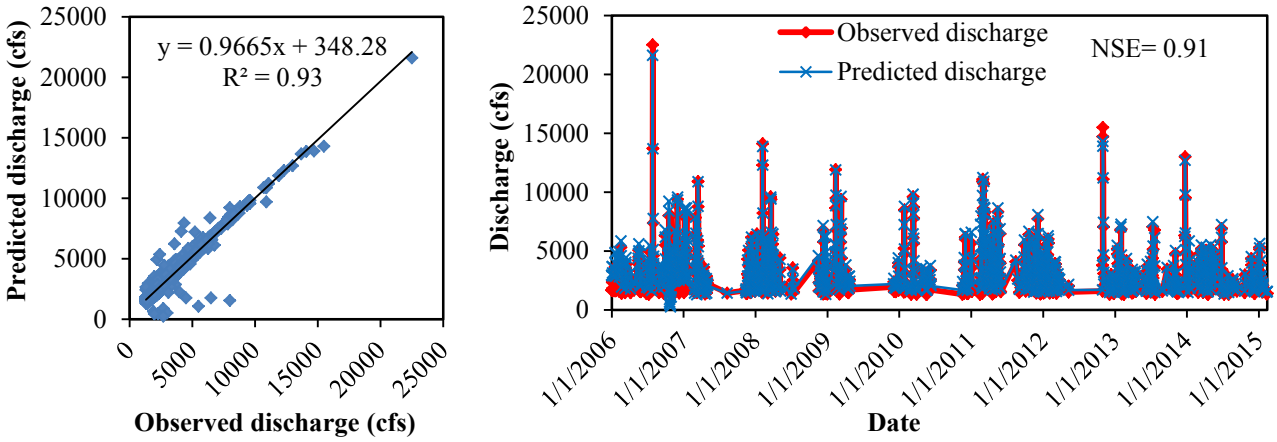

a) Predicted vs observed discharge

b) Validation of rating curve

Figure 3-4: Plot of predicted vs observed discharge (a), validation of the rating curve (b) for the period of 1/1/2006 to 1/1/2015

(Note: Only for discharge values greater than 75 percentile discharges)

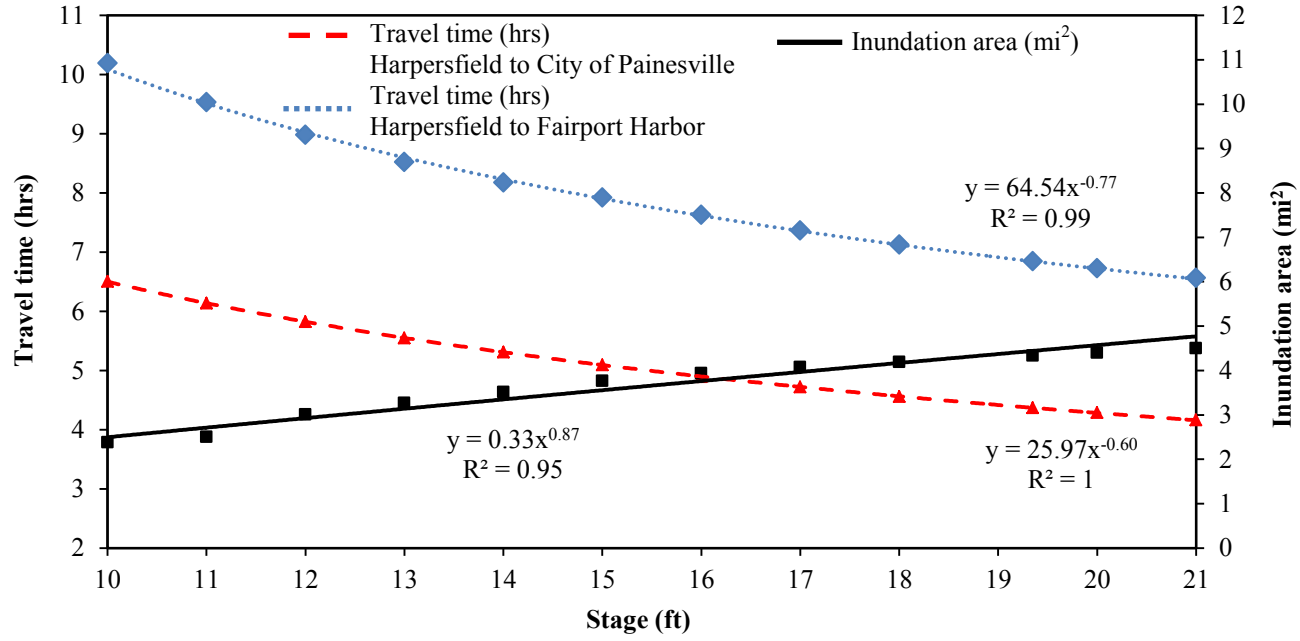

Figure 3-5: Travel time and flood inundation area for various flood stages at gage station 04212100 near the City of Painesville

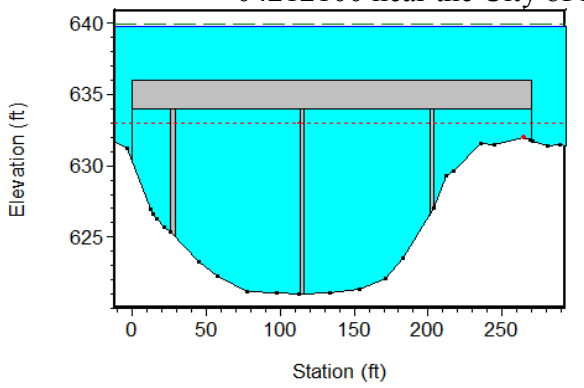

(a) Flood level at Vrooman bridge

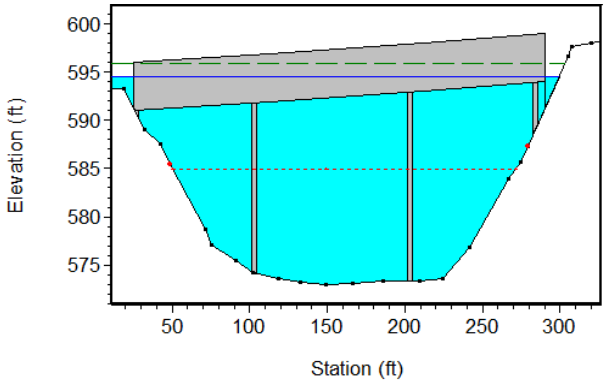

(b) Flood level at Lakeland freeway

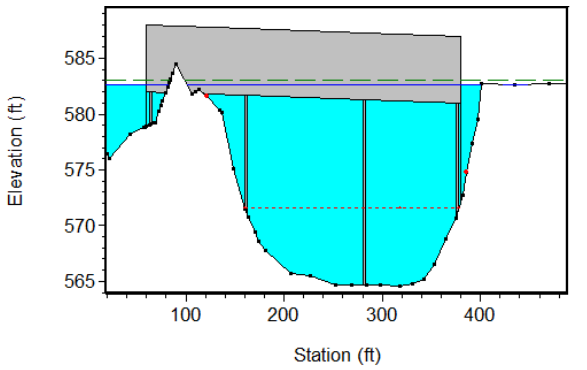

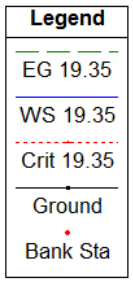

Where,
EG = Total Energy Level
WS = Water Surface Level
Crit = Critical Energy Level
19.35 = Stage of 19.35 ft at gage station 04212100
Ground = Ground Level

(c) Flood level at Fairport road bridge

Figure 3-6: Flood Level for the stage of 19.35 ft at gage station 04212100 at Vrooman bridge (a), Lakeland freeway bridge (b), and Fairport road bridge (c)

Table 3-1: Discharge values for various selected stage at 04212100 based on developed rating curve

Stage at USGS gage stations				Discharge (cfs)				
04211820 (datum level-733 ft)		**04212100 (datum level-595.59 ft)**		**Painesville (04212100)**	**Harpersfield (04211820)**	**Big creek**	**Paine creek**	**Mill creek**
Stage in ft above datum	Elevation (ft) in NAVD 88	Stage in ft above datum	Elevation (ft) in NAVD 88	**Drainage area**				
				685 mi^2	**552 mi^2**	**35.7 mi^2**	**27.3 mi^2**	**19.3 mi^2**
10.13	743.13	10.00	605.59	10451.82	8422.49	544.72	416.55	294.48
11.07	744.07	11.00	606.59	12404.48	9996.02	646.48	494.37	349.50
11.99	744.99	12.00	607.59	14504.02	11687.91	755.90	578.04	408.65
12.86	745.86	13.00	608.59	16747.87	13496.09	872.85	667.47	471.87
13.68	746.68	14.00	609.59	19133.68	15418.68	997.19	762.55	539.10
14.53	747.53	15.00	610.59	21659.35	17453.96	1128.82	863.21	610.26
15.35	748.35	16.00	611.59	24322.93	19600.38	1267.63	969.37	685.30
16.15	749.15	17.00	612.59	27122.62	21856.48	1413.54	1080.95	764.18
16.96	749.96	18.00	613.59	30056.76	24220.92	1566.46	1197.88	846.85
18.10	751.10	19.35	614.94	34228.37	27582.57	1783.87	1364.14	964.39
18.62	751.62	20.00	615.59	36322.26	29269.91	1893.00	1447.59	1023.39
19.42	752.42	21.00	616.59	39650.82	31952.19	2066.47	1580.24	1117.17

Table 3-2: Comparison of high-water mark profile and modeled profile for 2006 flood

S.N	Community (Location)	State plane coordinate system		High-water mark elevation (ft)	Simulated water surface elevation (ft)	Error (ft)
		Latitude	Longitude			
1	Leroy Township	2328226.99	752438.17	640.52	640.14	-0.38
2	Painesville Township	2315214.36	745057.64	622.12	621.31	-0.81
3	City of Painesville	2315591.23	750428.41	616.38	616.57	0.19
4	City of Painesville	2315665.58	750530.73	614.49	615.00	0.51
5	City of Painesville	2312665.85	753422.90	605.92	605.13	-0.79
6	City of Painesville	2312506.90	753926.77	602.84	603.80	0.96
7	Painesville Township	2314266.22	758102.79	596.14	594.97	-1.17
8	Painesville Township	2313812.87	757994.98	595.66	595.70	0.04
9	City of Painesville	2306518.39	759105.05	585.98	584.67	-1.31
10	City of Painesville	2305348.55	756051.50	582.82	582.44	-0.38
11	City of Painesville	2313981.20	751619.78	609.09	609.07	-0.02
12	City of Painesville	2313517.46	752220.45	606.70	606.91	0.21
13	City of Painesville	2313886.29	752934.42	605.79	605.13	-0.66
14	Painesville Township	2314792.43	758414.14	595.25	594.19	-1.06
15	Painesville Township	2308230.02	761356.54	589.25	587.89	-1.36
16	Village of Fairport Harbor	2306000.70	758186.61	585.64	584.36	-1.28
17	Village of Fairport Harbor	2304355.87	756543.63	581.64	581.19	-0.45
18	Village of Fairport Harbor	2305118.25	756250.70	580.93	582.21	1.28
19	Village of Fairport Harbor	2303675.01	756432.80	578.75	580.50	1.75

Table 3-3: Summary of streamgage information in the Grand River basin, Ohio
(Source: USGS-Streamstat and NWIS Web Interface)

Streamgage name	Stream gage number	Drainage area		Period of record	Datum of gage	Record type	Current status
		mi^2	km^2				
Grand River near North Bristol, OH	04209500	85.40	211.18	Mar 1942-Oct 1947	812 ft above NGVD29	Continuous	Inactive
Phelps Creek near Windsor, OH	04210000	25.60	66.30	May 1942-Jun 1959	803.7 ft above NGVD29	Continuous	Inactive
Hoskins Creek at Hartgrove, OH	04210100	5.42	14.03	1947-Nov 1985	997 ft above NGVD29	Peak flow, partial	Unknown
Bates Creek near Thompson OH	04212029	11.40	29.53	Jun 2003-Dec 2011	N/A	Peak flow, partial	Unknown
Montville Ditch at Montville OH	04210090	0.29	0.75	1966-Jul 1977	1185 ft above NGVD29	Peak flow, partial	Unknown
Grand River near Rome, OH	04210500	251.00	650.08	Mar 1942-Sept 1947	770 ft above NGVD29	Continuous	Inactive
Rock creek, OH	04211000	69.20	179.22	Apr 1942-Sept 1966	813 ft above NGVD29	Continuous	Inactive
Mill Creek near Jefferson OH	04211500	82.00	212.38	Apr 1942-Nov 1974	822.59 ft above NGVD29	Continuous	Inactive
Grand River at Harpersfield OH	04211820	552.00	1429.60	Mar 1996-Sept 1998	740 ft above NGVD29	Continuous	Inactive
Grand River near Madison, OH	04212000	581.00	1504.70	Oct 1922-Sept 1974	673.51 ft above NGVD29	Continuous	Inactive
Grand River near Painesville, OH	04212100	685.00	1774.10	Oct 1974-Present	595.51 ft above NGVD29	Continuous	Active

(Note: NGVD29-National Geodetic Vertical Datum of 1929, NWIS-National Water Information System, N/A-not available)

Chapter 4. Analysis of Winter Ice Cover and Ice Jam Effects in the Grand River Using One Dimensional HEC-RAS Model

Abstract

Ice jam events are very common in the Northern region of United States and cause frequent winter flooding leading to the damages of millions dollars' worth properties. Nevertheless, robust tools to forecast these ice jam events with sufficient lead time are not available yet. In addition, the effects of ice cover and ice jams in bridges and river flooding reviewing the historical ice jam information is a particular topic of research interest. Therefore, the major objective of this research is to observe the effects of winter ice cover/ice jams and evaluate ice jam flooding within bridge vicinity to make necessary preparation against ice jam flooding. This was accomplished by analyzing historical temperature, precipitation and ice jams information in Hydraulic Engineering Center River Analysis System (HEC-RAS) and using Light Detection and Ranging (LiDAR) data along with field verified survey data. The pre-processing of geospatial data required for hydraulic simulation and post-processing of flood inundation generation was performed in HEC-GeoRAS. The significant effect of ice cover and ice jam was noticed in most of the sections of the river including at the upstream of the bridges locations. The average increment in river stage, for highest winter flows, due to ice cover and ice jam in the Grand River was found to be approximately 2 ft. The maximum increment of 6.75 ft was detected at the upstream section of South Madison Bridge. Moreover, the increment in inundation area varied from 24% to 52% for various percentile winter flows. The percentage increase in inundation area was highest for 25 percentile flow than higher percentile flow when the same thickness of ice cover was used in the simulation.

Keywords: AFDD, Ice Jam, Flooding, Inundation Mapping

Introduction

River ice processes have significant effects in river hydrology and hydraulics during the winter time especially in cold regions (Hicks and Beltaos, 2008). Ice jams processes might lead to the extreme flood events and serious impacts on transportation and energy production (Prowse et al., 2002). The annual losses due to ice jam have been estimated to 100 to 135 million USD (Mahabir et al., 2006; White et al., 2007a) in United States alone, which includes potential losses of human lives, property, structural and environment damages. Furthermore, ice jam and its movement can severely erode river beds and banks resulting into adverse effects on aquatic lives (White, K.D., 1999).

Ice jam related flooding is one of the major problems during winter in Northern region of the United States. Therefore, this study was conducted in the Grand River, near the City of Painesville where ice jams have frequently occurred in the past at various locations (USACE, 2015). Most of the jams are occurred in the month of February, while some occurred in late January, and the rest in early March. These ice jams had led to closure of many roads and flooding of many properties in the past along the river. There was an extension of ice jam about a mile between the Richmond and St. Clair St. Bridges in 1978. Consequently, 150 people from Fairport harbor were evacuated and the estimated damage of 1.52 million USD was reported. Also, from the historical analysis of average freezing degree days (AFDD), the highest ice was formed in 1977/1989 period. Therefore, it is necessary to study the probable effects of ice jam flooding and generate flood inundation maps separately for winter season to protect human lives and reduce property damages. Appropriate representation of such flood hazards in this region can be accomplished by preparing flood maps for winter season as flood maps represent the

spatial variability of hazard and provide direct and robust understanding of flood extents (Merz et al., 2007; Leedal et al., 2010).

Ice jam is a situation of accumulation of fragmented or frazil ice that restricts the river flow (IAHR, 1986). Flooding is often frequently associated with ice jam in winter time as ice jam can lead to sudden increase in river stage, which can be much higher compared to open-water events (Ashton, 1986; White, 2003). Dynamic ice break up events lead to the greatest variation in river discharge and stage with time (Ferrick et al., 1992). Sudden increase in river stage and velocities are the result of ice break up events with a possibility to impose risk to houses, societies and aquatic lives in the downstream side of the river (Beltaos and Burrell, 2005). Also, there are several effects especially on bridge structures when the breakup event occurs due to higher river flow, velocities and hydrodynamic forces during breakup time (Beltaos et al., 2007). Although the discharge during the ice jam events is lower than that of the open water flow, the stage might become higher than the stage in open water flow (Lindenschmidt, 2015). Ultimately, this might bring the situation of potential disaster with socio-economic and environmental effects (Beltaos, 2011; Carlson, 1989; Brown et al., 2001). However, robust scientific tool is still not available at present that could be used to forecast the possible future flooding due to ice jams in advance (Mahavir et al. 2002). More importantly, it is challenging to predict the location and time of ice jam events as ice jam events are spatially variable, dependent on river discharge, hydraulics and river geo-morphology (Wuebben, J. L et al., 1995). Nevertheless, the probable future effects of ice jams can be found out by modeling the historical ice jam events because if an ice event occurs at the same location in the future, the database of pre-developed inundation maps can provide

quick access to information regarding probable inundation area needed for emergency response agencies (White, K.D., 1999). USACE Ice Cold Regions Research and Engineering Laboratory (CRREL) records and maintains for the historical records about the ice jam location and information all over the states, which can be utilized for exploring ice-related flooding. The prediction of ice jams and their effects is beyond the state of art, however, the possible damages and likelihood flooding pattern can be estimated by observing the historical data (Wuebben et al., 1995).

Therefore, the main objective of this study is to analyze the effects of ice jam in flood level of the Grand River, Ohio. The flood inundation maps were generated for various winter discharges incorporating ice cover and ice jam information. For this, the hydraulic HEC-RAS model was developed for different winter flood discharges considering ice cover and ice jam. Finally, the effects of ice jam in river and within the bridge vicinity were reported.

Theoretical Description

The hydraulic modeling software HEC-RAS was used to analyze the effect of ice cover and ice jam along the river especially in the bridge sections. The detail theoretical description of HEC-RAS is already discussed in Chapter 2.

HEC-RAS simulates wide river ice jams by modifying the jam thickness until the ice jam force balance equation and the standard step backwater equation are satisfied. This method of calculating ice jam in river is called global convergence (Brunner, 2010). The equations involved in ice jam simulation process are given below, which are obtained from Brunner (2010).

$$\frac{dt}{dx} = \frac{1}{2k_x Y_e}\left[\rho' g S_w + \frac{\tau_i}{t}\right] - \frac{k_0 k_1 t}{B} = F \qquad (4.1)$$

$$k_x = tan^2(45 + \frac{\Phi}{2}) \quad (4.2)$$

$$Y_e = 0.5\rho' g(1-s)(1-e) \quad (4.3)$$

$$k_0 = tan\,\Phi \quad (4.4)$$

Where t is accumulated thickness, x is longitudinal distance, Φ is angle of internal friction, e is the jam porosity, s is specific gravity of ice, ρ' is ice density, g is acceleration due to gravity, S_w is water surface slope, τ_i is shear stress applied to the underside of the ice by the flowing water, k_1 is coefficient of lateral thrust, B is accumulation width, and F is a shorthand description of the force balance equation.

Ice growth phenomenon depends upon many factors, which are not fully defined yet (White, K. 2004). However, ice growth and thickness can be predicted based on the climatic conditions and heat transfer mechanisms (Ashton, 1986). The transfer of heat from ice cover to the atmosphere helps thicken the ice cover but warming period in winter time leads snow and ice to melt. Carr et al. (2014) defines warming period as a period, when the average daily air temperature is above freezing temperature (32 ^{0}F) for at least 3 consecutive days. Even though ice thickness needs to be estimated considering many complex physical parameters like climatic variations, evaporation and snow cover radiations, it has been found that prediction of ice growth and thickness, for most of the engineering purposes, can be estimated by using simplified Stefan's equation (Ashton, 1986 and Beltaos, 1995) within a reasonable range. The modified Stefan's equation is given as follow.

$$t_i = \alpha\sqrt{AFDD} \quad (4.5)$$

$$AFDD = (32 - T_a) \quad (4.6)$$

Where, t_i is height of ice cover thickness in inches, α is a coefficient for wind exposure and snow cover, *AFDD* is Accumulated Freezing Degree Days and T_a is the daily average air temperature in ^{0}F.

AFDD is a term that provides an index of winter severity (Carr et al., 2014) and is calculated using the equation (4.6). The value 0.3 is typically used for α for small sheltered river. The values of coefficient "α" for different environmental conditions are listed in Table 4-2. It is worthwhile to note that its application is limited to calculate the ice thickness at the point of maximum annual AFDD (White, K. 2004). Beyond the point of peak AFDD, when thawing days start and ice starts to melt, these values of coefficients are not feasible to estimate the ice thickness (Bilello, 1980). Thawing degree days (TDD) is basically defined as negative freezing degree-days, which are taken as an indicator of ice thickness and rate of snowmelt (White et al., 2006).

The ice thickness at the downstream portion is typically calculated based on the user given upstream ice thickness (Brunner, 2010). The equations to calculate downstream ice thickness are given below.

$$t_{ds} = t_{us} + \bar{F}L \tag{4.7}$$

$$\bar{F} = \frac{F_{us}+F_{ds}}{2} \tag{4.8}$$

Where t_{ds} is thickness at downstream section, t_{us} is thickness at upstream section and L is the distance between sections. Similarly, F_{ds} and F_{us} are ice jam forces at downstream and upstream sections, respectively. The detail theoretical description of this phenomenon can be found in Brunner (2010).

The estimation of Manning's roughness values for the Grand River covered with a single layer of sheet ice was taken from the recommended values given by White (1999)

and Brunner (2010). The channel roughness value at a place where ice jam occurs depends on total depth of flowing water (Brunner, 2010). The roughness value is normally calculated using empirical relationship given by Nezhikovsky's (1964) as follows.

$$n_i = 0.0690H^{-0.23}t_i^{0.40} \text{ for } t_i>1.5 \text{ ft} \quad (4.9)$$

$$n_i = 0.0593H^{-0.23}t_i^{0.77} \text{ for } t_i<1.5 \text{ ft} \quad (4.10)$$

Where n_i is Manning's roughness value during ice jam, H is total water depth and t_i is the accumulated ice thickness.

Materials and Methodology

Study Area

The study was conducted in Grand River, which is located in Northeastern region of Ohio. The study area has been described in details in Chapter 2. Grand River has been frequently threatened by winter flooding due to ice jam in several sections along the river. The locations of occurrence of ice jam in the Grand River are presented in Figure 4-1 and the other details of ice jam are presented in Table 4-1.

Overall Modeling Approach

The HEC-RAS was used to study the effect of ice jam in the Grand River. Ice covered channel can be modeled in HEC-RAS by providing the ice thickness and ice jam information. However, the locations of jams have to be provided manually as HEC-RAS cannot identify the locations of ice jam in the river (Brunner, 2010). The detail description of overall modeling approach about model setup and its approach is described in Chapter 2 under heading "Overall Modeling Approach". Ice jam modeling approach in HEC-RAS is described in the following section.

At first, the AFDD was calculated for winter period of each year starting from 1949 to 2013. In the next step, the AFDD was used in modified Stefan's equation to estimate ice thickness. The maximum possible thickness of ice cover in the Grand River based on the historical data was selected for the hydraulic analysis. The estimation of Manning's roughness values for the Grand River covered with a single layer of sheet ice was taken from the recommended values given by White (1999) and Brunner (2010). The adopted value was 0.025. Furthermore, the hydraulic roughness of an ice jam was also calculated independently using Nezhikovsky's (1964) equation to provide the value in the sections where ice jam scenario was applied. The calculated Manning's roughness value for various ice jam places varied from 0.022 to 0.025 and the value of 0.025 was adopted. This was consistent with the adopted value by Wuebben and Gagnon (1995) to model ice jam flooding on the Missouri River, North Dakota. Since HEC-RAS simulation require separate set of manning's roughness for channel/flood plain and ice cover, the roughness values for river topography was adopted as 0.035 for channel sections and 0.15 for floodplains as discussed in Chapter 2. The estimated ice thickness was provided for each cross section in HEC-RAS model in order to model ice jams and evaluate its impact. The steady state HEC-RAS model was run for three difference scenarios: (a) simulation without ice cover and jam with bridges; (b) simulation with ice cover and ice jam with bridges; (c) simulation with ice cover and ice jam but without bridges. The ice jam locations were chosen based on the historical ice jam along the Grand River. The water surface elevation at the bridge sections was compared for three different simulation scenarios using five different discharge values. Similarly, separate flood inundation maps

were generated for three different scenarios to observe the difference in inundation areas due to ice jam especially in bridge locations.

HEC-GeoRAS/HEC-RAS Model Input

All types of data including elevation, streamflow/stage, land cover, bridge, and lake elevation data have been already described in Chapter 2 under heading "HEC-GeoRAS/HEC-RAS Model Input". Temperature data required to calculate AFDD were downloaded from NOAA-NCDC. Other data required for ice jam simulation like internal friction angle of jam, ice jam porosity, coefficient of lateral thrust (k_1), maximum mean velocity under ice cover, ice cohesion were adopted from the default values provided in HEC-RAS (Table 4-3). The ice thickness data needed for ice jam simulation in HEC-RAS was calculated using modified Stefan's equation. The steady flow data for winter simulation were obtained from the historical records. The historical winter discharge recorded in USGS was analyzed with different percentile values, which are presented in Table 4-4.

Model Calibration and Validation

The calibration and validation of Manning's roughness for river channel and flood plain has been described in detail under heading "Model Calibration and Validation" in Chapter 2.

Since there were no quantitative data of ice jam thickness for the Grand River, the model could not be calibrated for ice jam simulation. While the objective of the study was to make a comparison in water surface level with and without ice cover/ice jam, the calibration of the model would have little or no effect at all. Therefore, the comparative

studies in different flow scenarios were performed, and possible affected regions due to ice jam flooding were computed for three different scenarios.

Model Evaluation Criteria

The model performance for unsteady flow case was assessed using widely used statistical parameters such as NSE, R^2, PBIAS, and RSR as discussed in Chapter 2.

Results and Discussions

Simulation of Hydraulic Model

The performance of the model was found to be satisfactory in calibration and validation for different time periods of 1996-1998, which was evaluated based on the statistical criteria and visual inspection methods as discussed in Chapter 2. However, the model was not calibrated particularly for winter simulation considering the ice cover and ice jam scenario due to the lack of quantitative data for ice jam thickness.

AFDD and Ice Thickness Calculation

Since AFDD is the accumulation of freezing degree days, it increases as the temperature decreases. The maximum AFDD of 1068 degree days was encountered for 1977/1978 (Figure 4-2) based on the analysis of historical data for the period of 1949 to 2013. The ice thickness was estimated using modified Stefan's equation for winter periods for the entire period from 1949 to 2013. The value of coefficient "α" in modified Stefan's equation was adopted as 0.3. Since, ice thickness is directly proportional to AFDD, the estimated thickness (10 inches) was also the highest for 1977/1978 period (Figure 4-2). The maximum value of ice thickness was used to simulate winter discharge in HEC-RAS to quantify the effect of ice cover and ice jam in river stage and near bridge

structures. Additionally, flood inundation maps were generated considering ice jam conditions.

Ice Jam Flooding and Impacts

The relationship between the historical discharge of Grand River, AFDD and precipitation were studied. Some events of flooding were noticed due to the melting of ice and release of breakup jams in Grand River. This is consistent with the finding suggested by White, K.D (2006) as the ice jam events can bring several types of impact in the river such as increased river stage resulting in flooding due to freeze up jams and break up jams. The increase in the discharge of the river in winter periods likes 1976/1977, 1977/1978, 1978/1979, 1979/1980, 1984/1985, 2004/2005 and 2008/2009 were noticed. The increase in discharge during this period did not correspond to the precipitation event indicating the fact that melting of ice and ice jam breakup events were crucial to increase the discharge. These relationships are plotted in graphs which are shown in Figure 4-I to Figure 4-VIII in appendices section.

Lindenschmidit (2015) stated the river stage during ice jam events could be higher than the stage during open water flow without ice although the discharge is less during ice jam events. The river stage considering ice cover and ice jam in the river was compared with the stage during open water flow for five different flow conditions (Table 4-5). The average increment in stage for all sections of river was 2.02 ft, with the maximum increment up to 6.75 ft, just at the upstream of South Madison Bridge for the flow of 15,200 cfs (Table 4-5). The increment in the stage was higher mostly at the upstream section of the bridges.

Furthermore, this study found out the considerable effect of ice jam at the upstream section of the bridges. Based on the historical information of ice jam location, ice jam scenario was provided in seven different locations as shown in Figure 4-1 and run for various scenarios as discussed earlier. The river stage was highest for the scenario modeled with ice jam and bridge consideration in model. The increase in the stage due to ice jam was the highest for the South Madison Bridge, Madison. When South Madison Bridge was considered, the river stage just at the upstream of bridge was approximately 4.16 ft. higher for the highest flow than that of the stage without bridge. Similar trend of increase in stage were observed in other bridges as well even though the increase in stage in other bridges was not significant. The river stages for different scenarios near South Madison Bridge are shown in (Figure 4-3). The increase in river stage was consistently observed in all bridges for all flow scenarios, where ice jam scenario was considered. Even though significant increase in water surface level was detected near the bridge, it did not show significant effects in the overall inundation extents over entire river reach. Therefore, it can be concluded that the presence of hydraulic structures have the localized effect in increase in water level and flood inundation area. This result agrees with the conclusion drawn out by the study of Cook and Merwade (2009). The water surface levels for various other bridges using different flow scenarios are shown in Figure 4-4 and its detail increment in river stage are presented in Table 4-6.

The effect of ice jam in Vrooman Bridge was found to be crucial as the simulated water level crosses the bridge deck level for several different flow scenarios (Figure 4-5). Therefore, the Vrooman Bridge is more susceptible to flooding if the ice jam occurs in this location. The water level in Vrooman Bridge have increased to significant height due

to ice jam flooding several times in the past such as in 2007, 2010, 2011, and 2014 leading to the closure of the road. From the inundation maps, it can be concluded that winter flooding has significant impact near Grand River Avenue and Steel Avenue near Main Street in Painesville, Kiwanis Recreation Park including some houses and apartments near High Street in Fairport Harbor in appendix section. The graphical plot of inundation area for various winter flows including/excluding are shown in Figure 4-6. The increase in inundation area after incorporating ice covers and ice jam was the highest (52%) for 25 percentile flow (Figure 4-6). The percentage increase in inundation area decreased when the higher values of winter discharges were considered. The flood inundation maps for various winter flows were also produced to see the aerial extents of floods along the Grand River. The detail effects of flooding for various winter flows are presented in Figure 4-IX - Figure 4-XIII in appendices section.

The large volume of ice blocks was observed from the simulation where there was an ice cover and ice jam in some sections of the river. The blocks of ice jams at the upstream of South Madison Bridge and Vrooman Bridge can be seen in Figure 4-3and Figure 4-5, respectively. The result was based on the estimated ice thickness and historical jam information which can vary depending upon the variation in winter temperature and climatic conditions. When the temperature starts increasing above the freezing point after the mid-winter season, ice starts melting which might increase river discharge leading to ice break up events. This might bring the significant ice jam flooding and potentially disastrous condition.

Conclusion

The hydrological and hydraulic process of any river in cold regions is greatly affected by river ice processes. This might lead to the situation of potential ice jam flooding leading to property, structural and environmental damages. In this paper, the effects of ice cover/ice jam to the river stage and to the winter flooding pattern have been discussed. Additionally, the effects of ice jam to the river stage especially at the bridge locations have also been discussed using HEC-RAS. Various historical winter discharges with ice thickness and ice jam were analyzed to see the probable winter disaster and its effects. Due to the lack of gaged discharge/stage datasets for three tributaries, simple drainage area ratio method was used to calculate the winter flows. HEC-GeoRAS was used to generate the flood inundation maps for different percentile flow scenarios based on the historical winter flows, and generated inundation maps were overlaid with digital orthographic maps to observe the aerial extent of floods.

The significant effect of ice cover and ice jam was detected in most of the river sections. The average increment in river stage due to the presence of ice cover and ice jam in the Grand River was approximately 2 ft, with the maximum increment of 6.75 ft at the upstream section of South Madison Bridge. Furthermore, the effect of ice jam was also noticed considerably at the upstream section of bridge. The analysis was conducted with and without bridge. The river stage at the upstream of bridge was approximately 4.16 ft higher for 100 percentile flow than that of the river stage without considering bridge. While the discrepancies exist in the quantitative results of modeling study due to uncertainties associated with the data and modeling, the river stage is expected to increase due to ice cover and ice jam.

The hydraulic study of the presence of ice cover and ice jam in river gives useful information regarding inundation and increase in river stage during winter time. There are many places as discussed in the results that are vulnerable to winter floods which have to be considered while planning and preparing for emergency phase. Flood risk mapping including ice jam effects in the river would present more reliable flood risk estimation for policy makers and stakeholders to make decisions and plans accordingly for probable ice related flood disaster in winter time. Hence, it is anticipated that these information will be useful to decision makers and flood management agencies to plan, act and prepare for probable affected places during the winter flooding.

The generated flood inundation maps could be refined, and further calibration and validation for ice jam flooding could be carried out considering all sources of streamflow to generate accurate inundation maps and to quantify the increase in stage when ice cover and ice jam occurs in the river sections.

References

Ashton, G. D. (Ed.). (1986). River and lake ice engineering. Water Resources Publication.

Ashton, G. D. "Ice jam flooding on the Peace River near the Peace Athabasca Delta." Water Stewardship: How Are We Managing (2003): 11-13.

Beltaos, Spyros, ed. River ice jams. Water Resources Publication, 1995.

Beltaos, S. (2011). Alternative method for synthetic frequency analysis of breakup jam floods. CGU HS Committee on river ice processes and environment, 18-22.

Beltaos, S., & Prowse, T. D. (2001). Climate impacts on extreme ice-jam events in Canadian rivers. Hydrological Sciences Journal, 46(1), 157-181.

Beltaos, Spyros, and Brian C. Burrell. "Climatic change and river ice breakup." Canadian Journal of Civil Engineering 30.1 (2003): 145-155.

Brunner, Gary W. HEC-RAS River Analysis System. Hydraulic Reference Manual. Version 4.1. HYDROLOGIC ENGINEERING CENTER DAVIS CA, 2010.

Beltaos, Spyros, et al. "Hydraulic effects of ice breakup on bridges."Canadian Journal of Civil Engineering 34.4 (2007): 539-548.

Bilello, M. A. (1980). Maximum thickness and subsequent decay of lake, river and fast sea ice in Canada and Alaska (No. CRREL-80-6). COLD REGIONS RESEARCH AND ENGINEERING LAB HANOVER NH.

Brown, R. S., G. Power, and S. Beltaoa. "Winter movements and habitat use of riverine brown trout, white sucker and common carp in relation to flooding and ice break- up." Journal of Fish Biology 59.5 (2001): 1126-1141.

Beltaos, Spyros, and Brian C. Burrell. "Field measurements of ice-jam-release surges." Canadian Journal of Civil Engineering 32.4 (2005): 699-711.

Carr, Meredith L., and Carrie M. Vuyovich. "Investigating the effects of long-term hydro-climatic trends on Midwest ice jam events." Cold Regions Science and Technology 106 (2014): 66-81.

Carlson, Robert F., John P. Zarling, and Lewis E. Link. "Cold Regions Engineering Research-Strategic Plan." Journal of Cold Regions Engineering3.4 (1989): 172-190.

Ferrick, Michael G., Patricia B. Weyrick, and Susan T. Hunnewell. "Analysis of river ice motion near a breaking front." Canadian Journal of Civil Engineering 19.1 (1992): 105-116.

Hicks, Faye, and Spyros Beltaos. "River ice." Cold Region Atmospheric and Hydrologic Studies. The Mackenzie GEWEX Experience. Springer Berlin Heidelberg, 2008. 281-305.

IAHR, 1986. River ice jams: a state of the art report, working group on river ice hydraulics. Proceedings of the International Association for Hydraulics Research International Symposium on Ice. , vol 3, pp. 561–594 (Iowa City, IA).

Lindenschmidt, Karl-Erich, et al. "Ice jam flood hazard assessment and mapping of the Peace River at the Town of Peace River." 2015

Mahabir, C., Hicks, F. E., & Fayek, A. R. (2002, December). Forecasting ice jam risk at Fort McMurray, AB using fuzzy logic. In Proceedings of the 16th IAHR International Symposium on Ice, International Association of Hydraulic Engineering and Research, New Zealand, 2nd–6th December (pp. 91-98).

Mahabir, Chandra, Faye Hicks, and Aminah Robinson Fayek. "Neuro-fuzzy river ice breakup forecasting system." Cold regions science and technology 46.2 (2006): 100-112.

Merz, Bruno, A. H. Thieken, and Martin Gocht. "Flood risk mapping at the local scale: concepts and challenges." Flood risk management in Europe. Springer Netherlands, 2007. 231-251.

Leedal, David, et al., "Visualization approaches for communicating real-time flood forecasting level and inundation information." Journal of Flood Risk Management 3.2 (2010): 140-150.

Prowse, Terry D., and Spyros Beltaos. "Climatic control of river- ice hydrology: a review." Hydrological processes 16.4 (2002): 805-822.

USACE, 2015 CRREL Ice Jam Database for gage station 04212100 in Grand River, OH (accessed March 2015) http://rsgisias.crrel.usace.army.mil/apex/f?p=524:5:0::NO

WHITE, KATHLEEN D., ANDREW M. TUTHILL, and LINNZI FURMAN. "Studies of ice jam flooding in the United States." Extreme Hydrological Events: New Concepts for Security. Springer Netherlands, 2006. 255-268.

White, Kathleen D. "Review of prediction methods for breakup ice jams." Canadian Journal of Civil Engineering 30.1 (2003): 89-100.

White, K.D., Tuthill, A.M., Furman, L., 2007a. Studies of ice jam flooding in the United

States. Extreme Hydrological Events: New Concepts for Security. Springer, Netherlands.

White, Kathleen D. Hydraulic and physical properties affecting ice jams. No. CRREL-99-11. COLD REGIONS RESEARCH AND ENGINEERING LAB HANOVER NH, 1999.

White, K. (2004). Method to estimate river ice thickness based on meteorological data: ERDC. CRREL Technical Note TN-04-3, US Army Engineer Research and Development Center, Hanover, New Hampshire.

Wuebben, James L., and John J. Gagnon. Ice jam flooding on the Missouri River near Williston, North Dakota. No. CRREL-95-19. COLD REGIONS RESEARCH AND ENGINEERING LAB HANOVER NH, 1995.

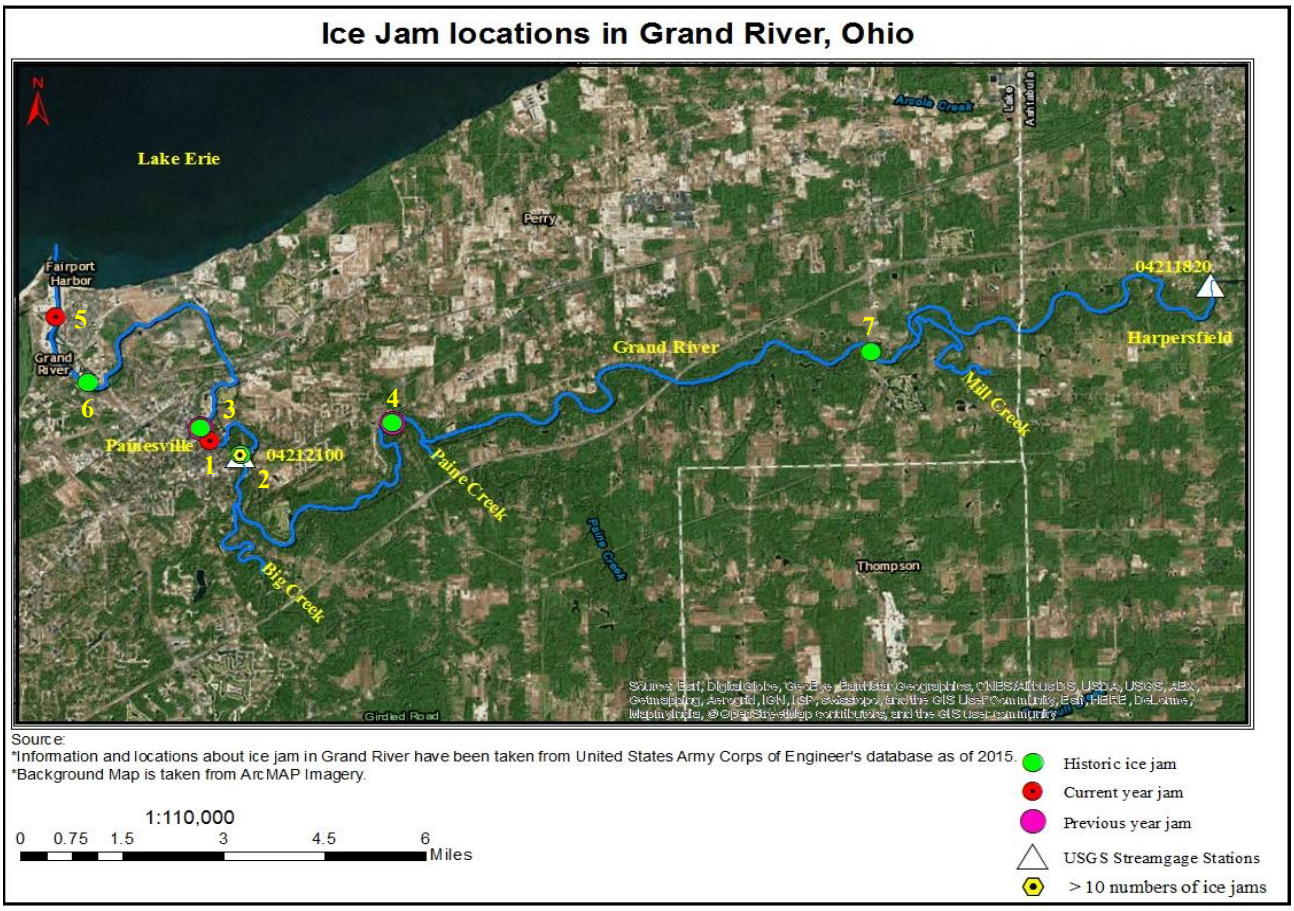

Figure 4-1: Ice jam locations in the Grand River as of CRREL Ice Jam Database, USACE (2015)
(Note: The details of these ice jam locations are given in Table 1)

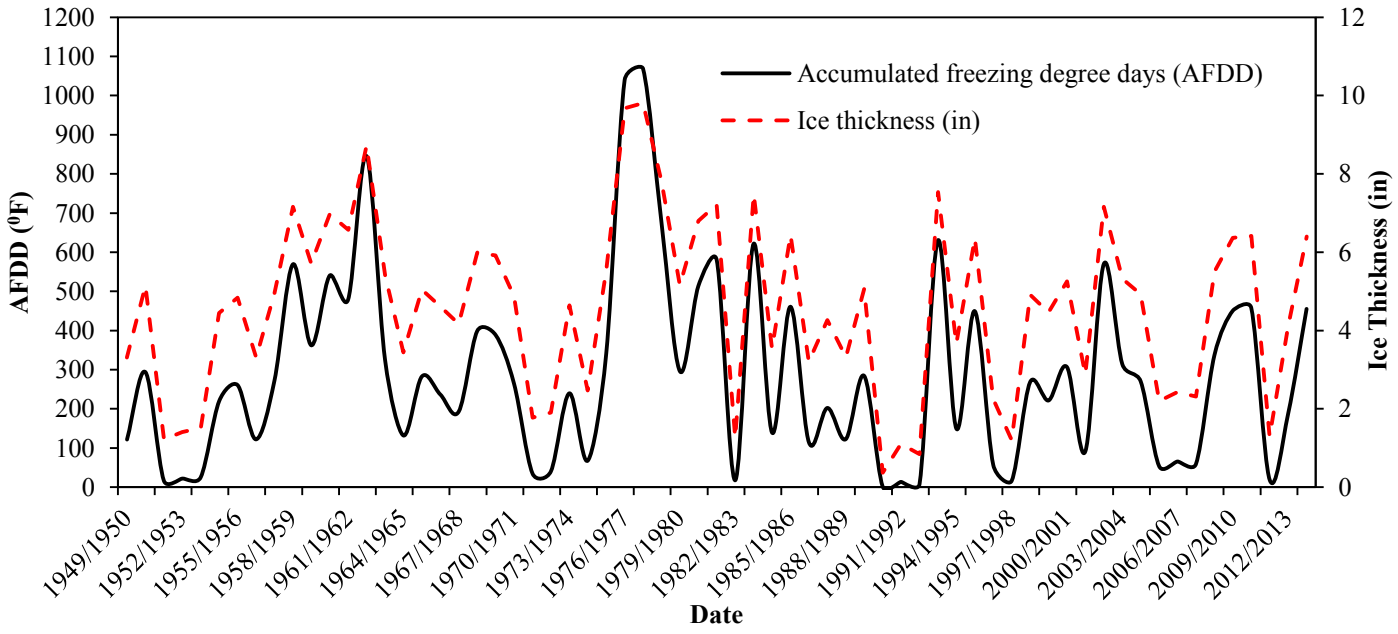

Figure 4-2: Calculated AFDD and estimated ice thickness for various winter periods

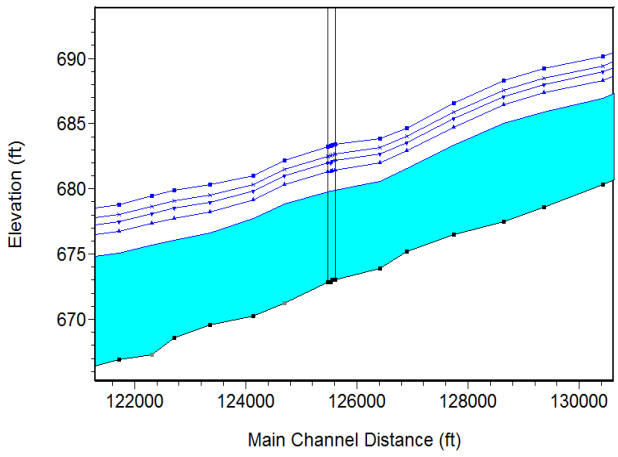

(a) Open water flow

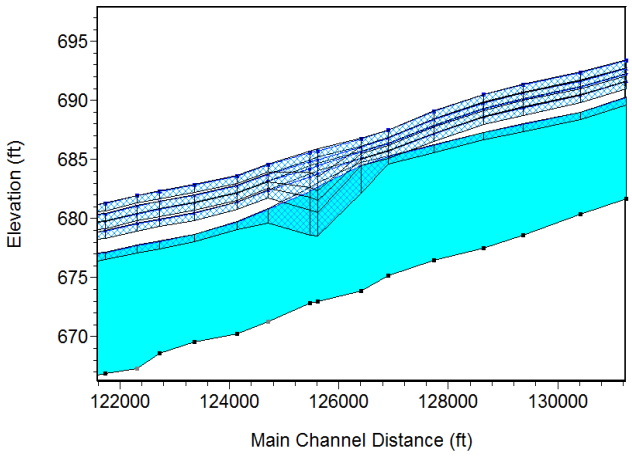

(b) Flow with ice jam without bridge

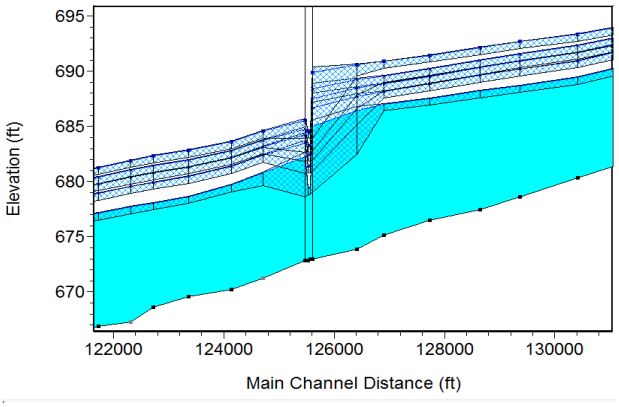

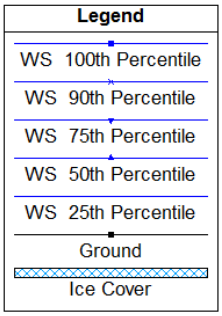

(c) Flow with ice jam and bridge

Figure 4-3: Water Surface level for various modeling scenarios near South Madison Bridge, Madison

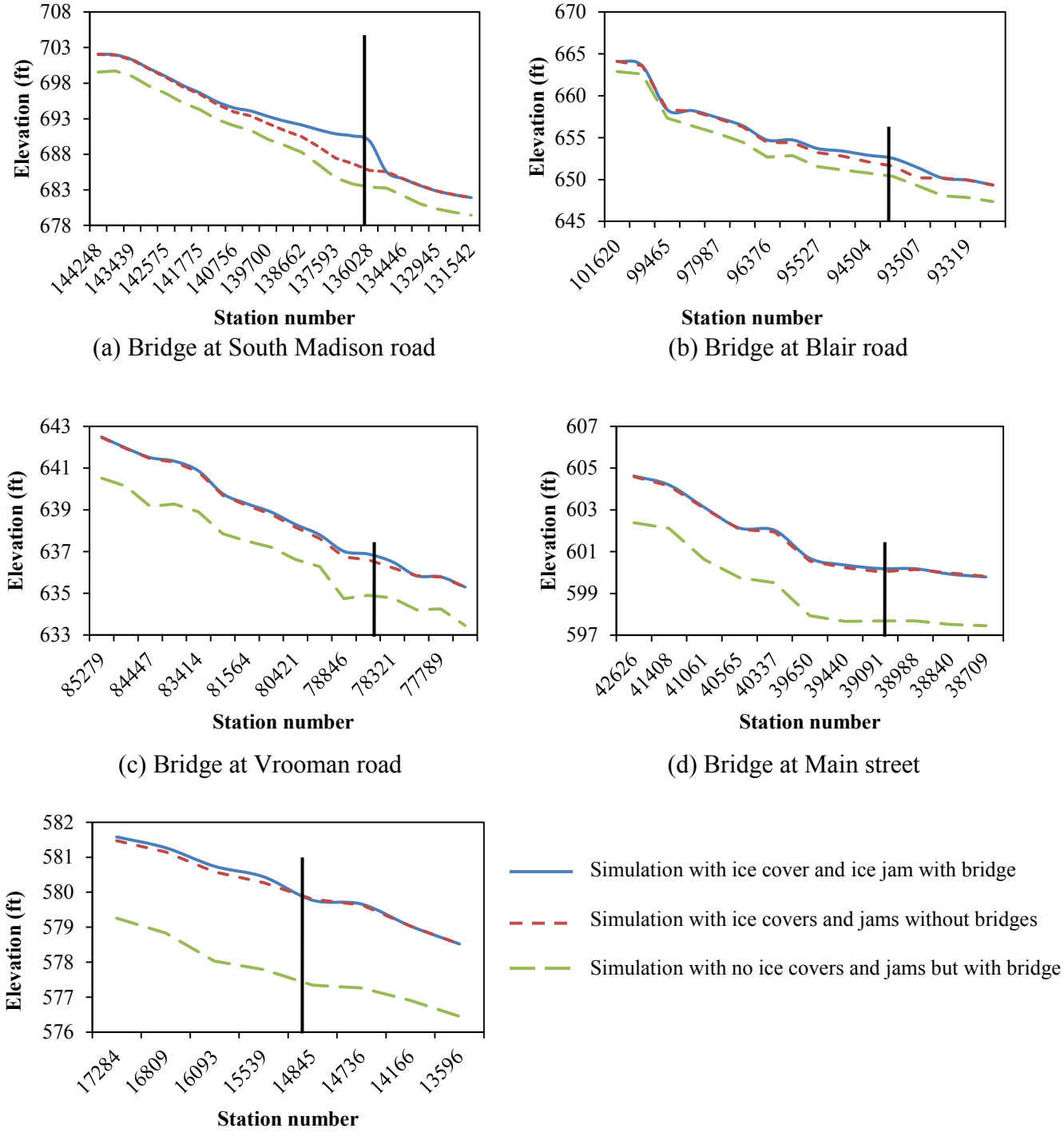

(a) Bridge at South Madison road

(b) Bridge at Blair road

(c) Bridge at Vrooman road

(d) Bridge at Main street

(e) Bridge at St. Clair street

Figure 4-4: Water surface elevation for various scenarios at South Madison road (a), Blair road (b), Vrooman road (c), Main street (d), and St. Clair street (e) along the Grand River

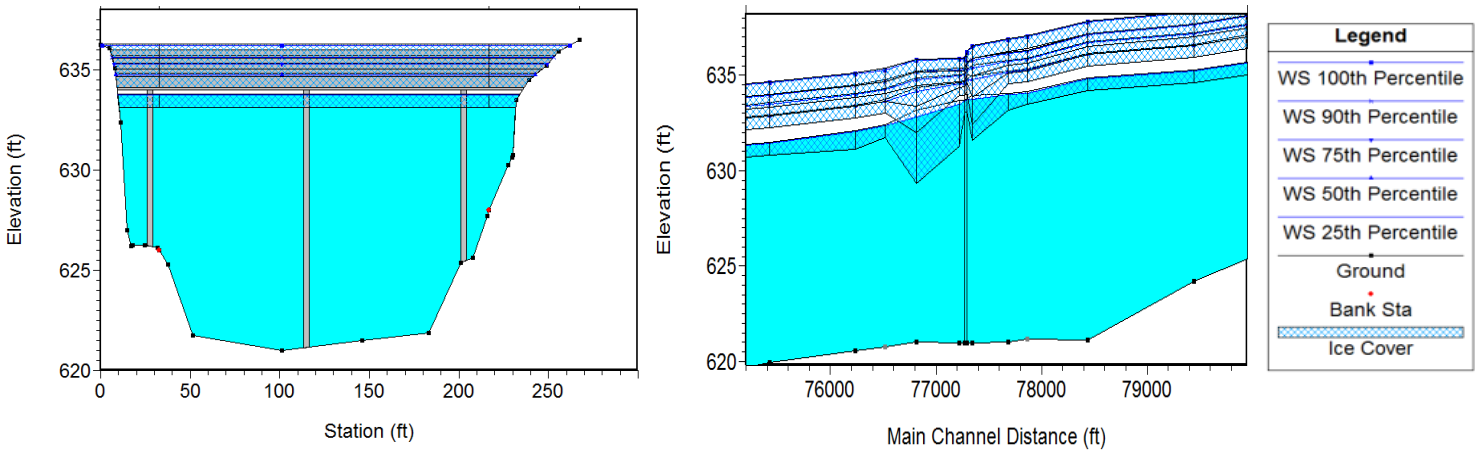

(a) Cross sectional view (b) Longitudinal view

Figure 4-5: Water surface level in Vrooman bridge for different flow conditions - cross sectional view (a), longitudinal view (b)

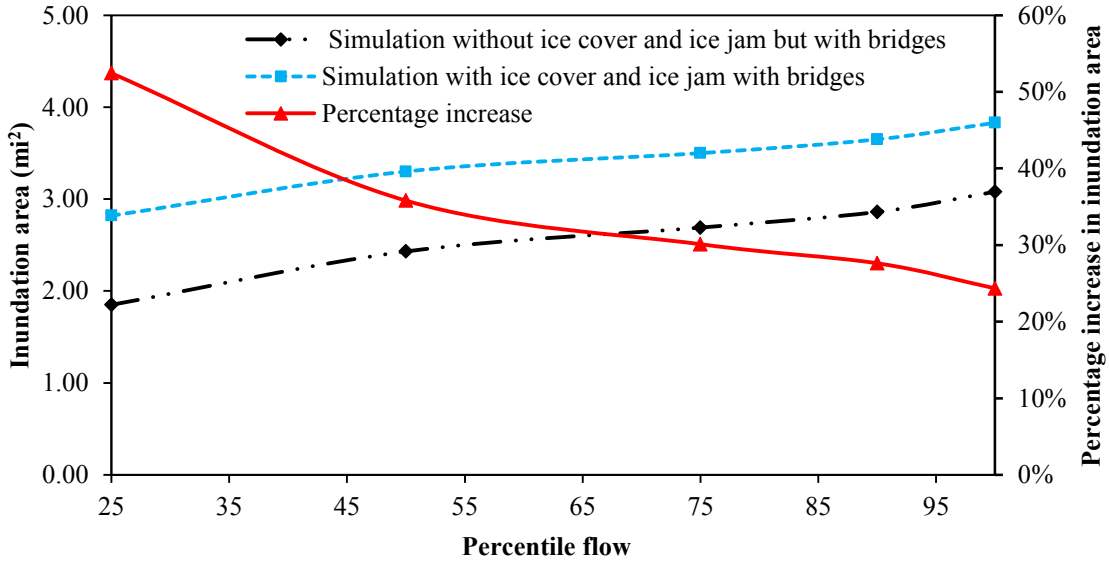

Figure 4-6: Inundation area and percentage increase in inundation area for various winter flows and various simulation scenarios

Table 4-1: Location, date and description of historical ice jam in the Grand River (Source: Map View and Query-Ice Jam Database, US Army Corps of Engineers)

S.N.	Locations	Dates of occurrence	Description
1.	0.1 mile upstream of Main street bridge, Painesville	02/22/2014	Breakup jam
2.	Upstream section of Grand River near East Walnut Ave.	1981, 1982, 1984, 1988, 2003, 2007, 2008, 2009, 2010, 2011	Most of them were breakup jams and some were releasing jams
3.	Near Main street bridge, Painesville	1961, 1978	
4.	Just upstream of Vrooman bridge, Vrooman road	2014	Blockage of Vrooman road
5.	Near Water street, Fairport Harbor	2014	-
6.	Near High street bridge, Painesville	-	-
7.	Near 4842 Bailey Rd, Madison, OH	-	-

(Note: The detail description of ice jam, location and damages due to ice jam related flooding can be found by using text query option in USACE CRREL online Ice Jam Database.)

Table 4-2: Values for α (coefficient that accounts wind exposure and snow cover) for different conditions taken from USACE, 2002

Condition	α (when AFDD is calculated using degree Celsius)	α (when AFDD is calculated using degree Fahrenheit)
Windy lake without snow	2.7	0.80
Average lake with snow	1.7 - 2.4	0.5 – 0.7
Average river with snow	1.7 – 1.7	0.4 – 0.5
Sheltered small river	0.7 – 1.4	0.2 – 0.4

Table 4-3: Default values of different parameters in HEC-RAS

Parameter	Value	Parameters	Value
Internal friction angle of jam	45^0	Maximum mean velocity under ice cover	5 fps
Ice jam porosity	0.40	Ice cohesion	0
Coefficient of lateral thrust (k_1)	0.33	Specific gravity	0.916

Table 4-4: Various winter discharge values obtained from historical data

Percentile Value	Approximate return periods	Discharge (cfs)
25	1	7598
50	2	10600
75	3	12175
90	4	13400
100	8	15200

Table 4-5: Increase in river stage due to the presence of ice cover and ice jamming

Percentile flow	Discharge (cfs)	Increase in river stage (ft)	
		Average	Maximum
25	7598	1.81	5.89
50	10600	1.93	5.73
75	12175	1.96	5.80
90	13400	1.99	6.08
100	15200	2.02	6.75

(Note: The increases in river stage were calculated by subtracting the stage of river analyzed excluding ice cover and jam from the stage of river analyzed including ice cover and ice jam)

Table 4-6: Increase in river stage when bridge is considered in ice jam location

Bridge location	Increase in river stage due to presence of bridge (ft)				
	25 percentile flow	50 percentile flow	75 percentile flow	90 percentile flow	100 percentile flow
South Madison Road	2.33	2.89	3.11	3.44	4.16
Blair Road	1.04	1.12	1.16	1.18	1.21
Vrooman Road	0.03	0.08	0.14	0.19	0.28
Main Street	0.06	0.13	0.15	0.16	0.15
St. Clair Street	0.27	0.39	0.45	0.35	0.17

(Note: The effect of ice jam near the bridge at East Walnut Avenue was not significant so it is not shown here in the table)

Chapter 5. Conclusion and Recommendations

In this study, an approach for flood warning system was introduced including digital map preparation and travel time computation. Furthermore, the effects of resolutions of elevation datasets and Manning's roughness in prediction of travel time and flood inundation areas were investigated. The study utilized a broadly accepted tool, HEC-RAS to perform the required hydraulic simulation. A HEC-GeoRAS, an ArcGIS extension, was used to produce flood inundations maps. The hydraulic model was calibrated and validated with satisfactory model performance for various periods from 1996 to 1998 using USGS discharge and stage data.

The hydraulic model was setup for various return period floods using different elevation datasets and a range of possible roughness values to observe the uncertainties involved in flood inundation mapping process. A topographic survey was conducted to get accurate elevation dataset in the river channel sections. The results obtained from LiDAR integrated with survey data, were considered the reference datasets to compare the results obtained using other elevation datasets. The predicted travel time and inundation area was highest, for the most coarse elevation dataset (30m DEM) without integration of survey data, and this was in decreasing trend while using finer elevation datasets. Since the predicted travel time, from 10m DEM without integration of survey data, showed less percentage difference than LiDAR without survey, it was concluded that elevation data in channel was better represented by 10m DEM than LiDAR data. However, this does not rule out the necessity of a topographic survey for accurate elevation datasets. Similarly, the selection of Manning's roughness in the channel sections and floodplains were found to be very important for the prediction of travel time and flood inundation areas.

However, the Manning's roughness value in channel sections was sensitive compared to the roughness values in floodplains. The maximum decrease in inundation area was 1.49%, when Manning's roughness was varied in floodplain and kept constant in channel. Similarly, the decrease in inundation area was 8.97%, when Manning's roughness was varied in channel section and kept constant in floodplain. Therefore, it is essential to consider those discrepancies while predicting flood travel time and generating flood inundation maps.

Furthermore, rating curve was developed using historical discharge and stage data to estimate the peak flood discharge for 12 different flood stages ranging from 10.00 ft to 21.00 ft, which were approximately 2 to 500 year return period floods. The digital flood inundation maps were generated for various flood stages based on the upstream and downstream gage heights. There are more than 100 houses and apartments, many roads, bridges and parks along the Grand River, which are vulnerable to 500 years return period flood within the study area. It is recommended to install the siren system at suitable locations to issue warning in sufficient time ahead. The predicted flood travel time from the study can be utilized to evacuate the people from probable inundation area.

The significant effect of ice cover and ice jam was found in most of the sections of the river during the winter period. There was an increase in river stage when the simulation was performed considering ice cover and ice jam along the river. Additional increase in river stage at the upstream section of bridges was found when bridges were considered in the model simulation. However, the flooding was limited to upstream and the increase in flooding extents was not realized along the entire river. The average increase in stage along the entire Grand River within study area was found to be

approximately 2 ft when ice cover and ice jam was considered. Flood inundation maps for several winter flows were produced to see the extents of ice jam induced flood.

While some discrepancies exist in input data and modeling techniques, it is expected that these results will be valuable for NWS, decision makers, flood insurance and emergency flood management agencies to plan and manage the situation before and after the occurrence of flood for effective rescue operation in affected areas. However, it is recommended for further calibration and validation of the model with detail recordings of the streamflow especially in tributaries and ice jam recordings in probable ice jam locations.

APPENDICES

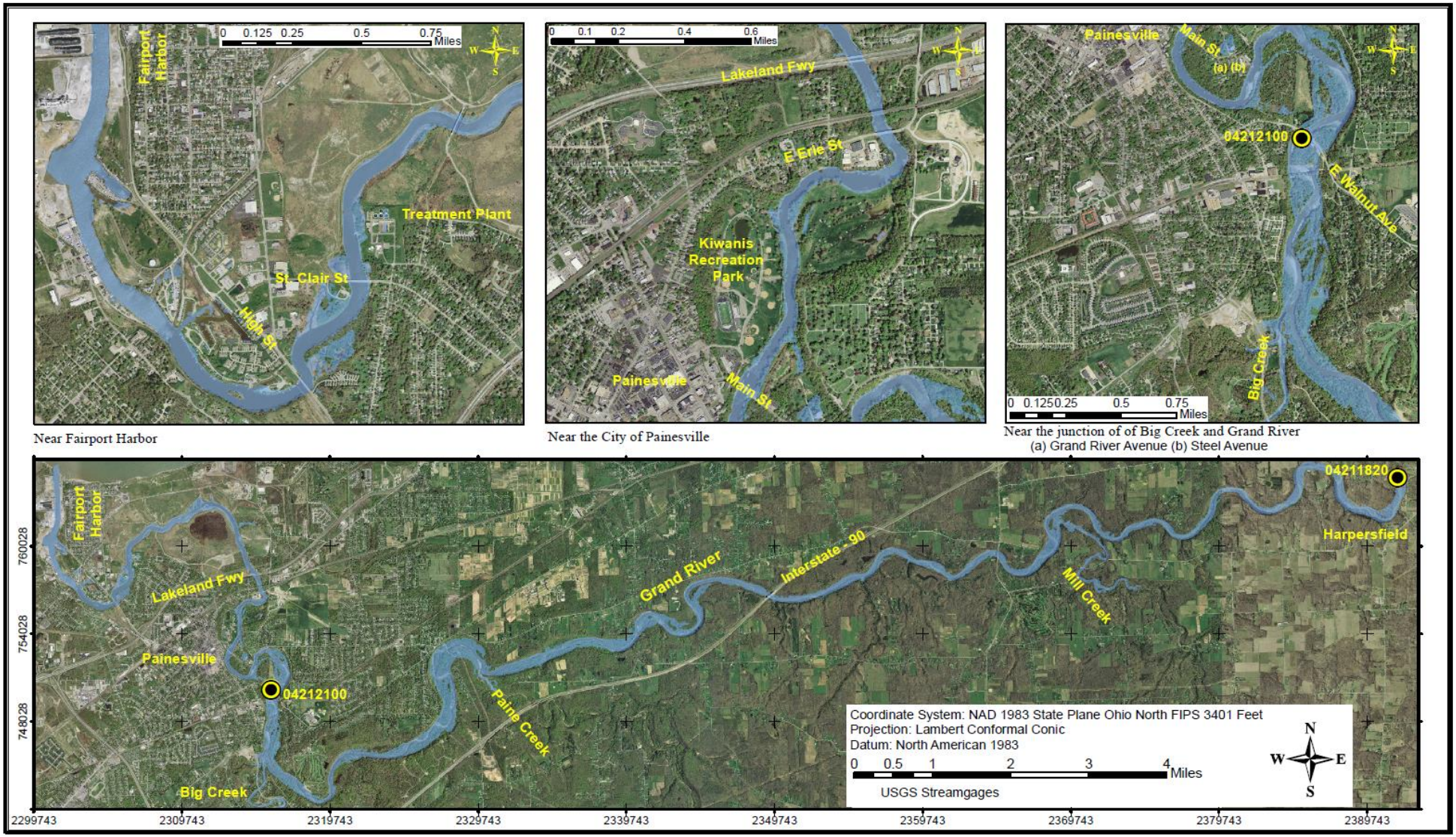

Figure 3-I: Flood inundation map along the Grand River, for the stage of 10.00 feet, 605.59 feet NAVD 88 at 04212100 and the stage of 10.13 feet, 743.13 feet NAVD 88 at 04211820

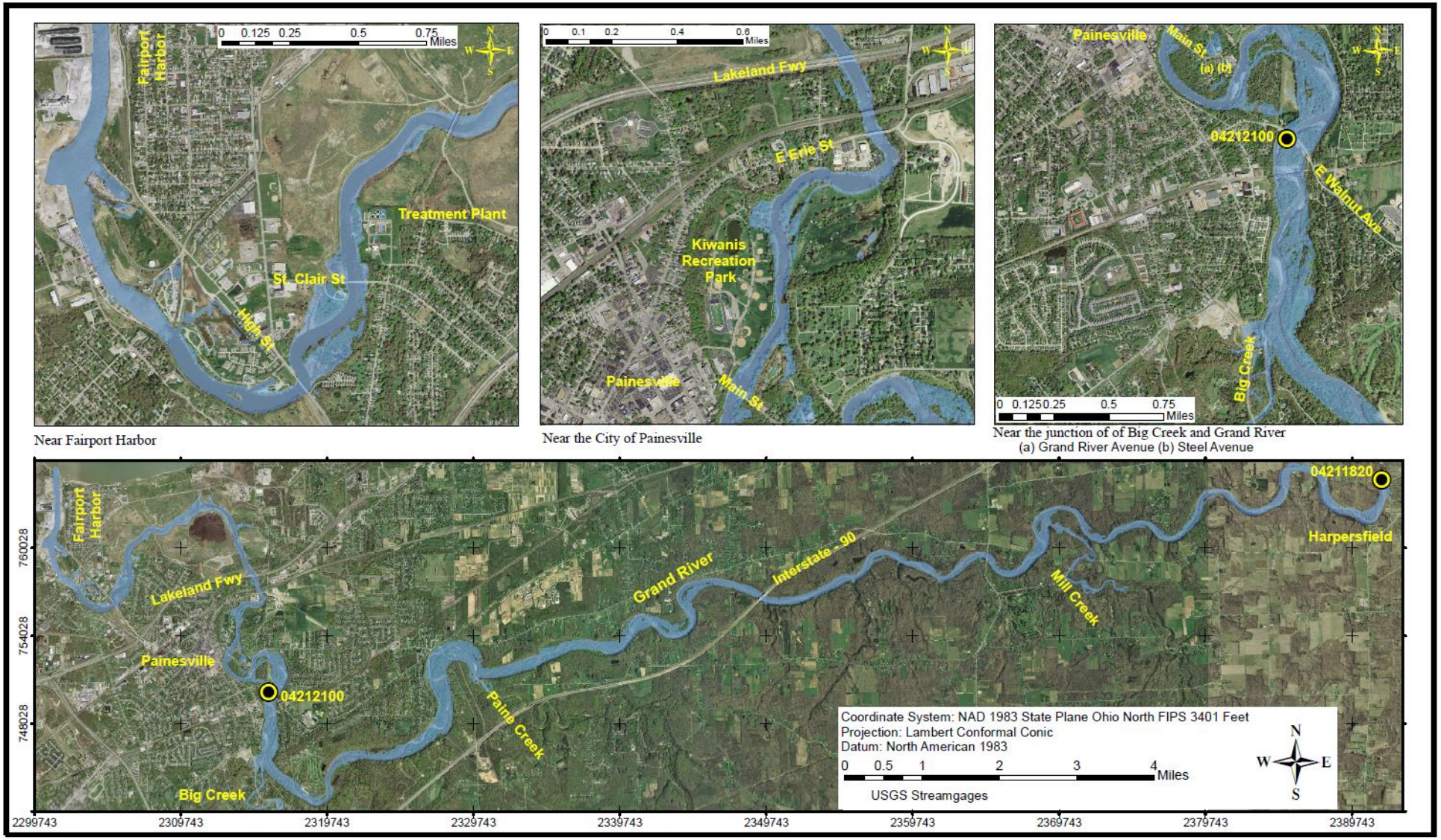

Figure 3-II: Flood inundation map along the Grand River, for the stage of 11.00 feet, 606.59 feet NAVD 88 at 04212100 and the stage of 11.07 feet, 744.07 feet NAVD 88 at 04211820

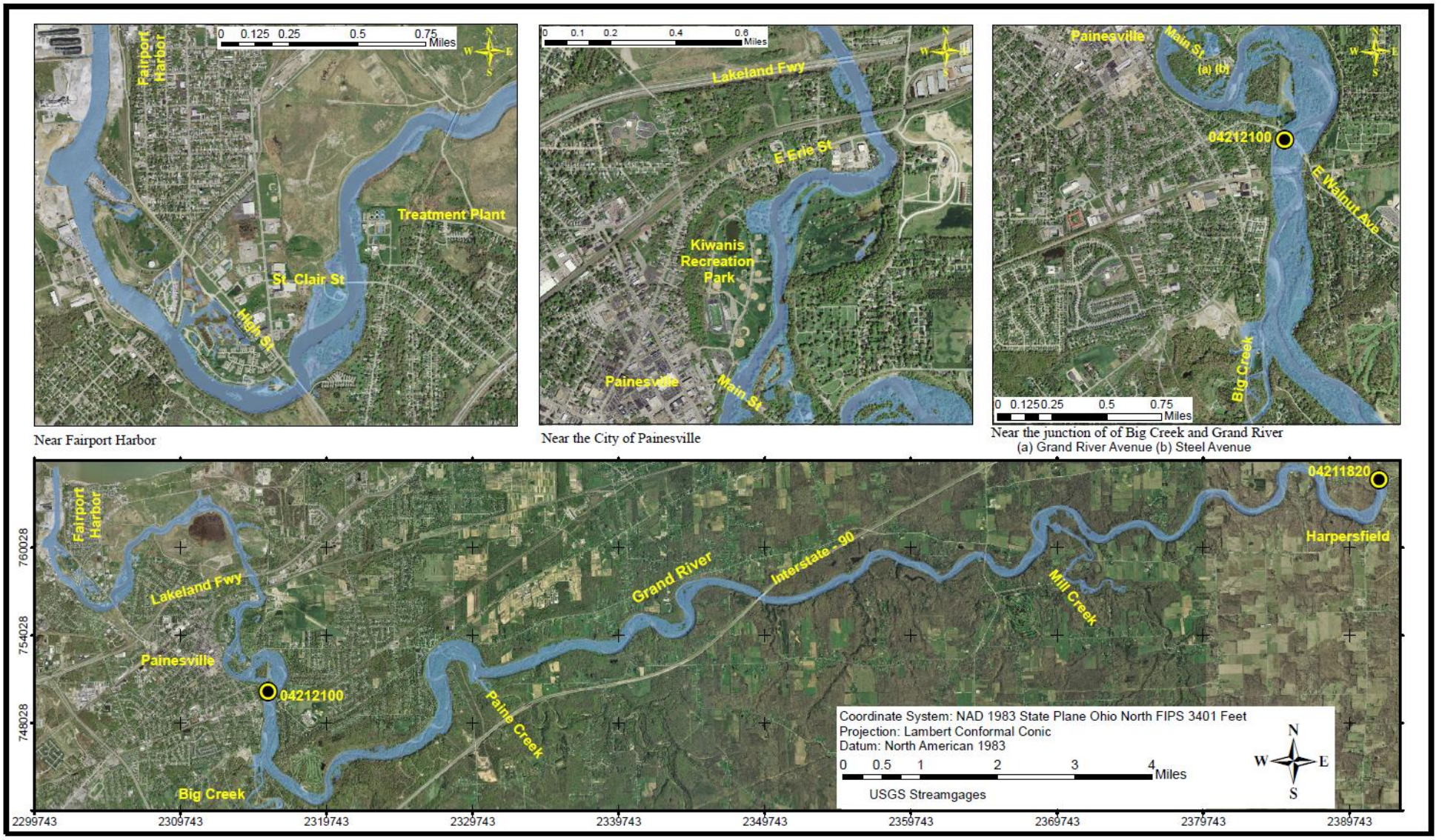

Figure 3-III: Flood inundation map along the Grand River, for the stage of 12.00 feet, 607.59 feet NAVD 88 at 04212100 and the stage of 11.99 feet, 744.99 feet NAVD 88 at 04211820

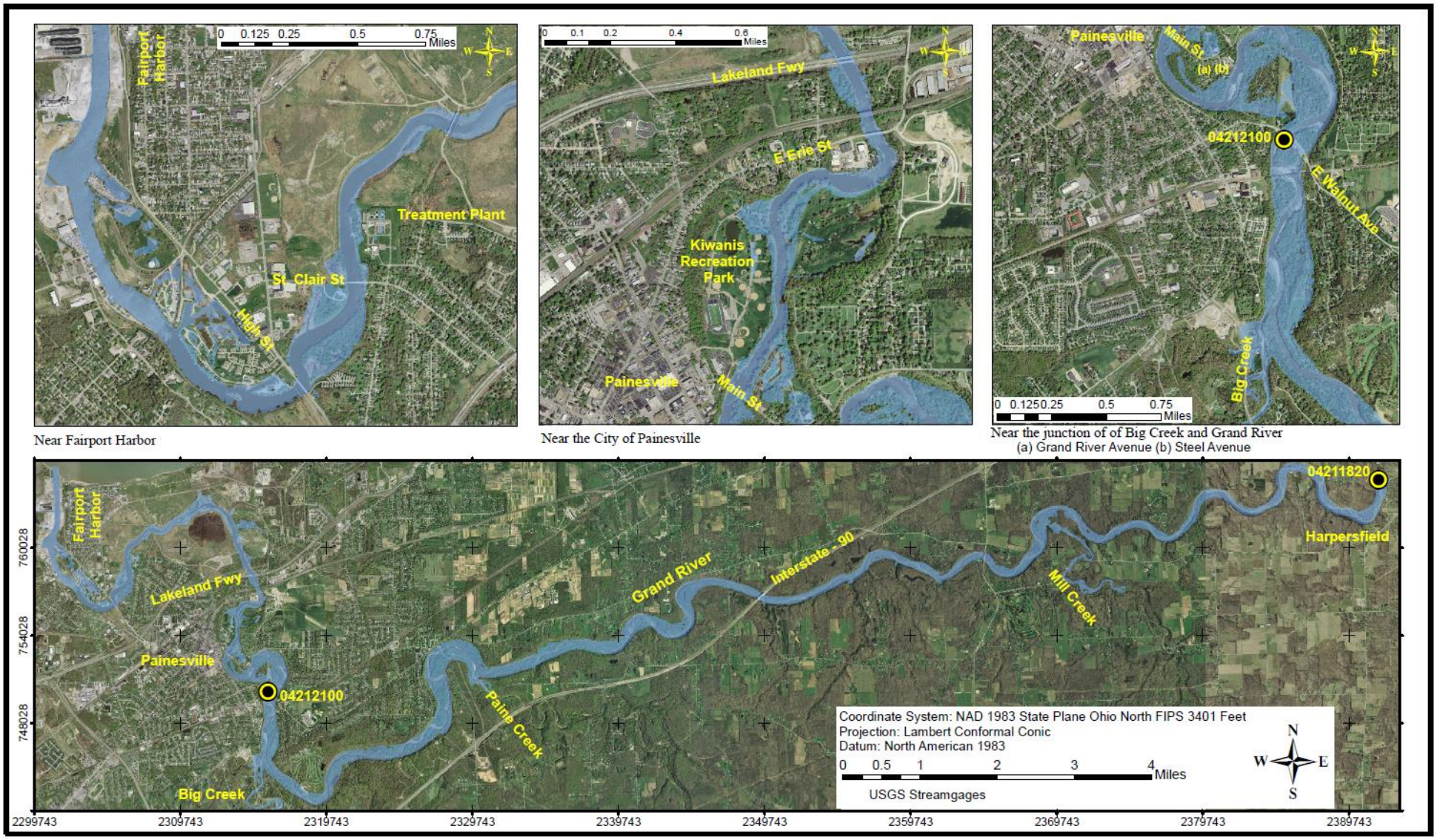

Figure 3-IV: Flood inundation map along the Grand River, for the stage of 13.00 feet, 608.59 feet NAVD 88 at 04212100 and the stage of 12.86 feet, 745.86 feet NAVD 88 at 04211820

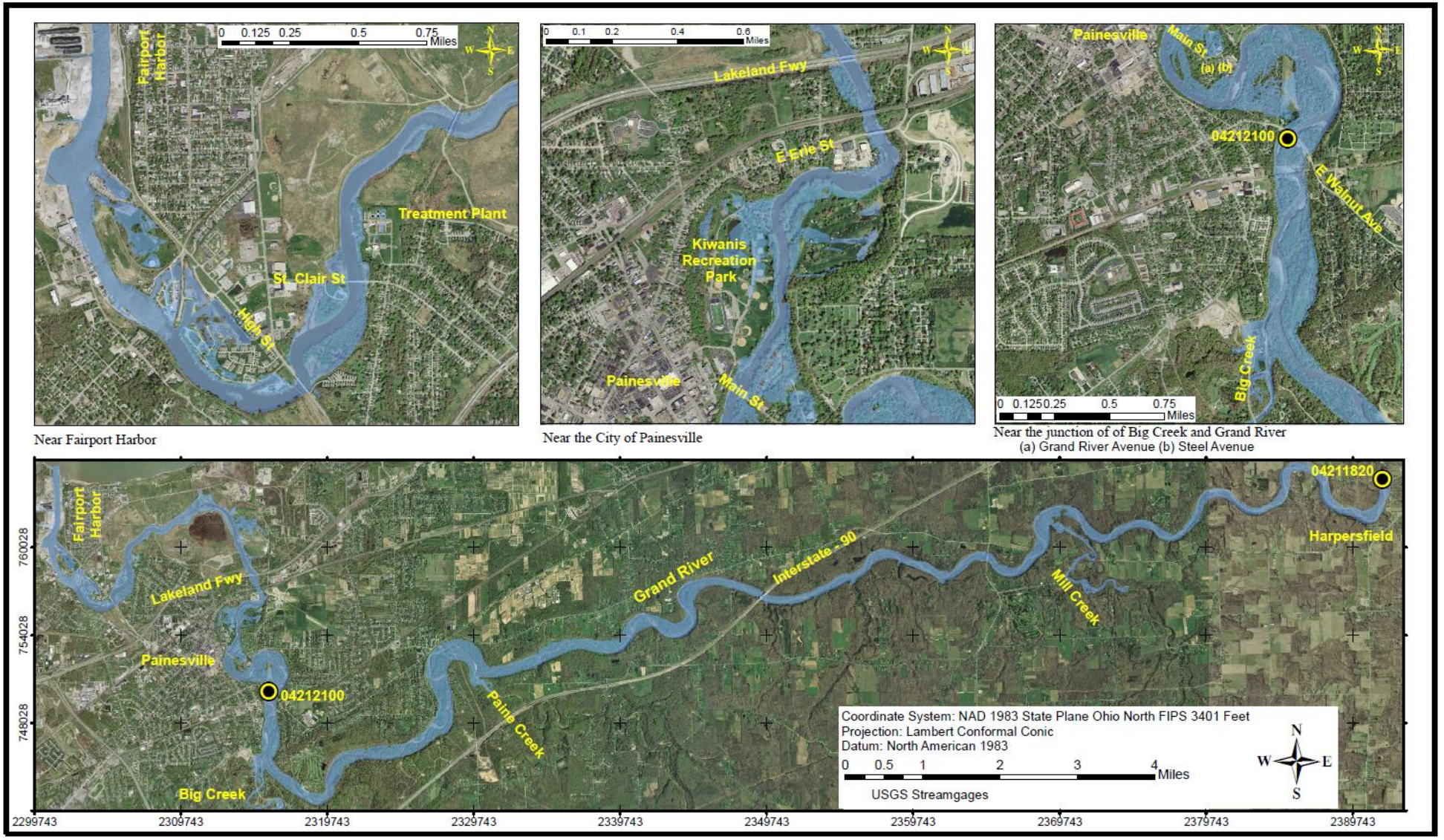

Figure 3-V: Flood inundation map along the Grand River, for the stage of 14.00 feet, 609.59 feet NAVD 88 at 04212100 and the stage of 13.68 feet, 746.68 feet NAVD 88 at 04211820

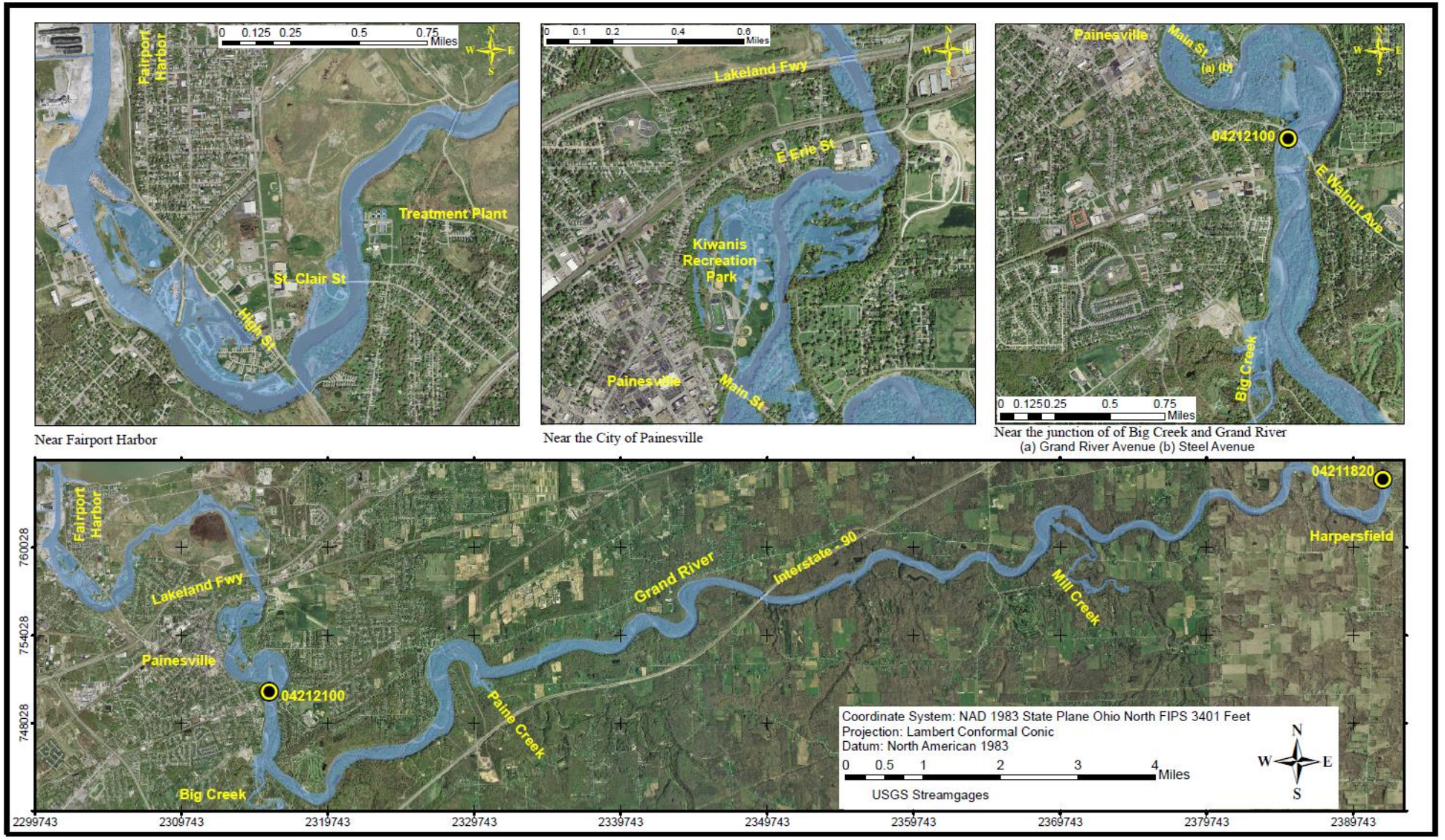

Figure 3-VI: Flood inundation map along the Grand River, for the stage of 15.00 feet, 610.59 feet NAVD 88 at 04212100 and the stage of 14.53 feet, 747.53 feet NAVD 88 at 04211820

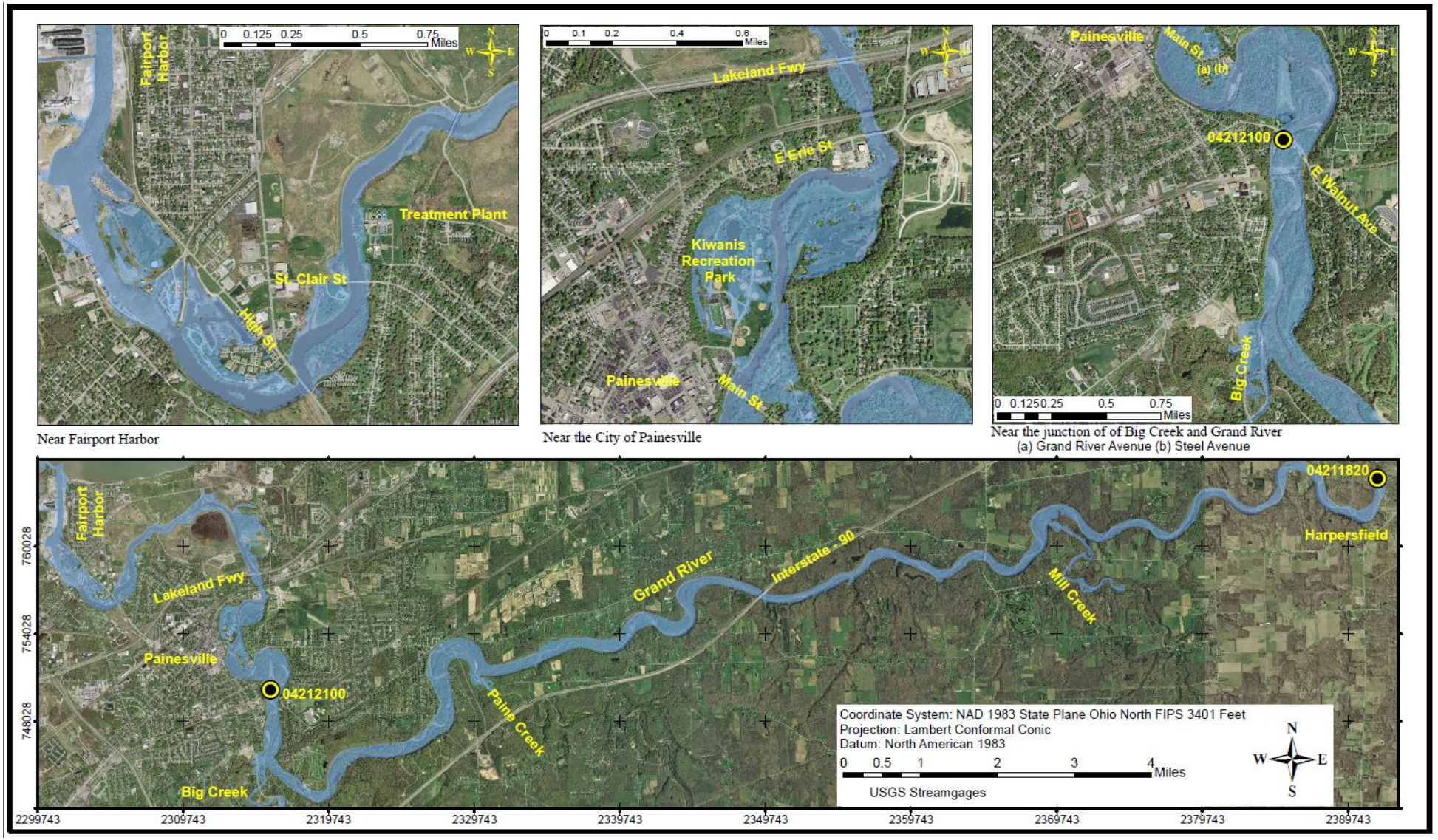

Figure 3-VII: Flood inundation map along the Grand River, for the stage of 16.00 feet, 611.59 feet NAVD 88 at 04212100 and the stage of 15.35 feet, 748.35 feet NAVD 88 at 04211820

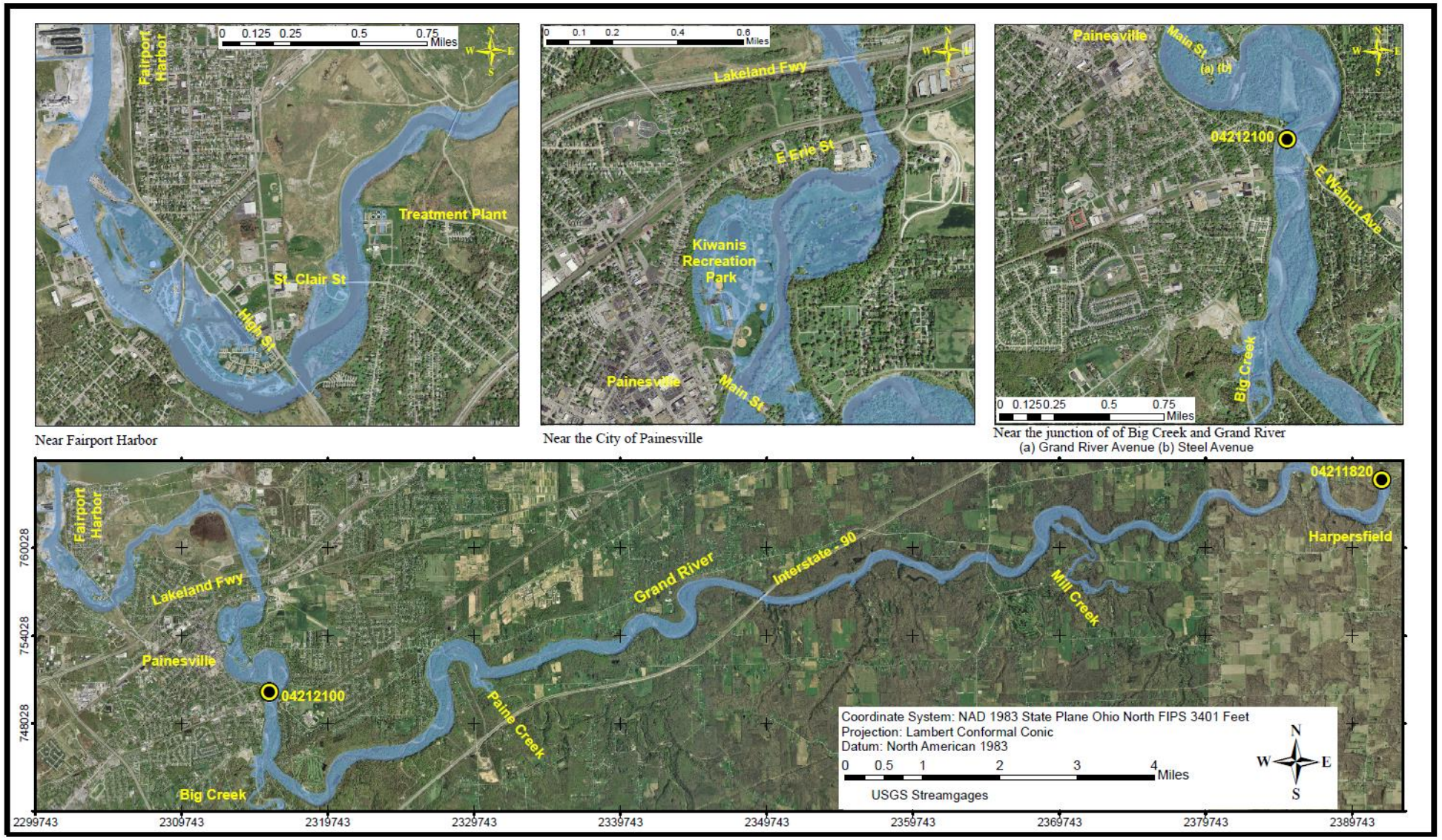

Figure 3-VIII: Flood inundation map along the Grand River, for the stage of 17.00 feet, 612.59 feet NAVD 88 at 04212100 and the stage of 16.15 feet, 749.15 feet NAVD 88 at 04211820

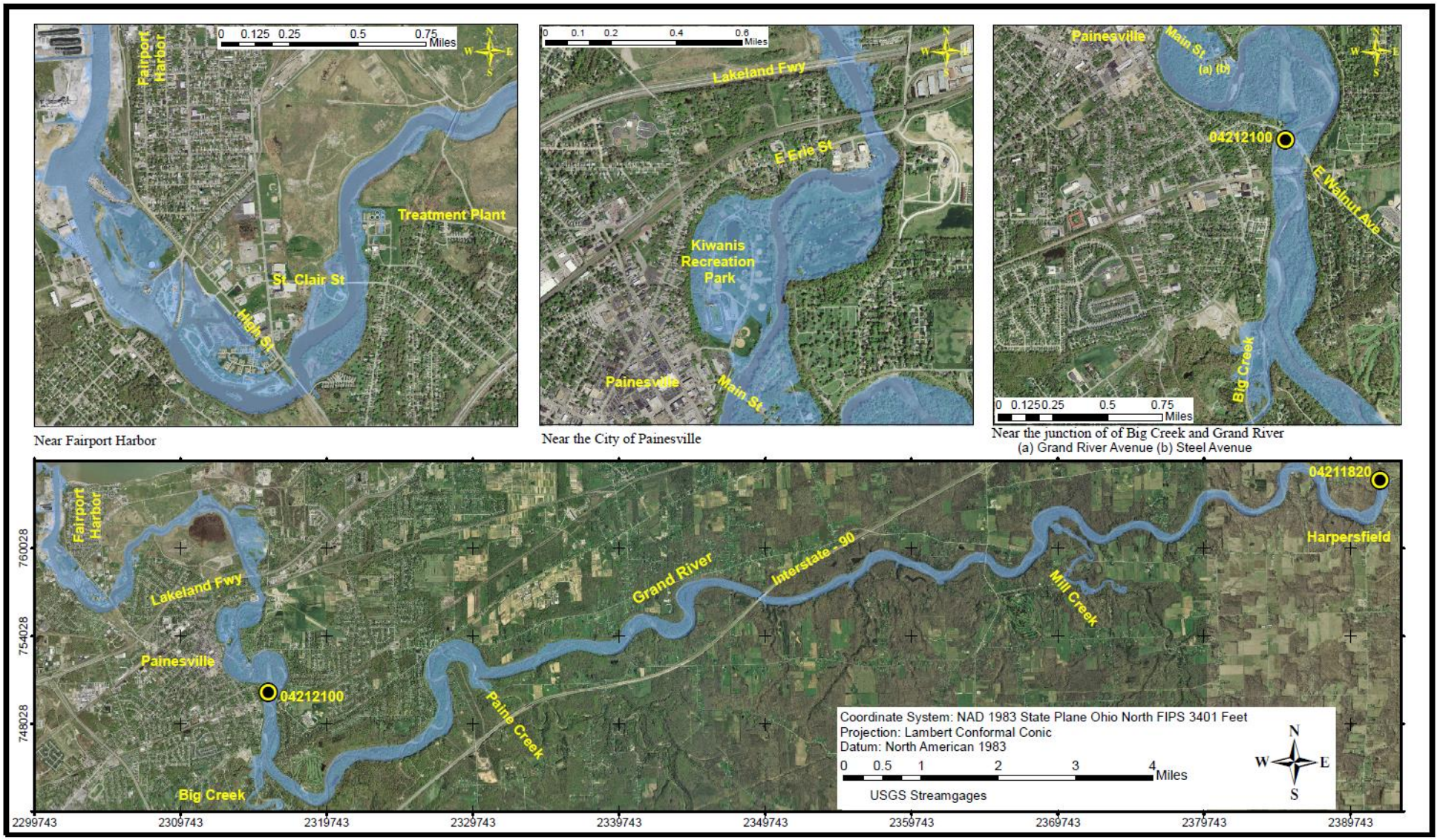

Figure 3-IX: Flood inundation map along the Grand River, for the stage of 18.00 feet, 613.59 feet NAVD 88 at 04212100 and the stage of 16.96 feet, 749.96 feet NAVD 88 at 04211820

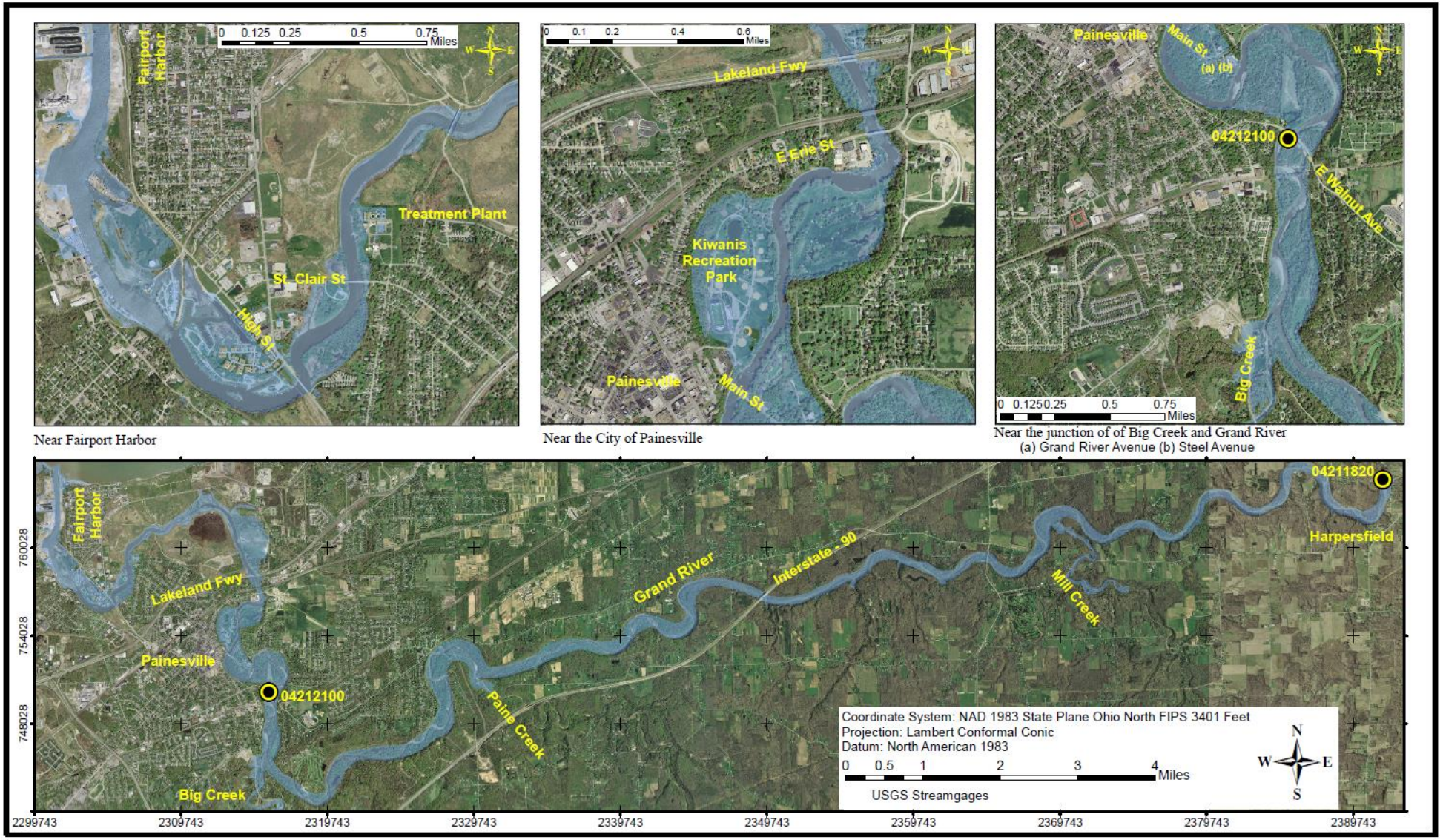

Figure 3-X: Flood inundation map along the Grand River, for the stage of 19.35 feet, 614.94 feet NAVD 88 at 04212100 and the stage of 18.10 feet, 751.10 feet NAVD 88 at 04211820

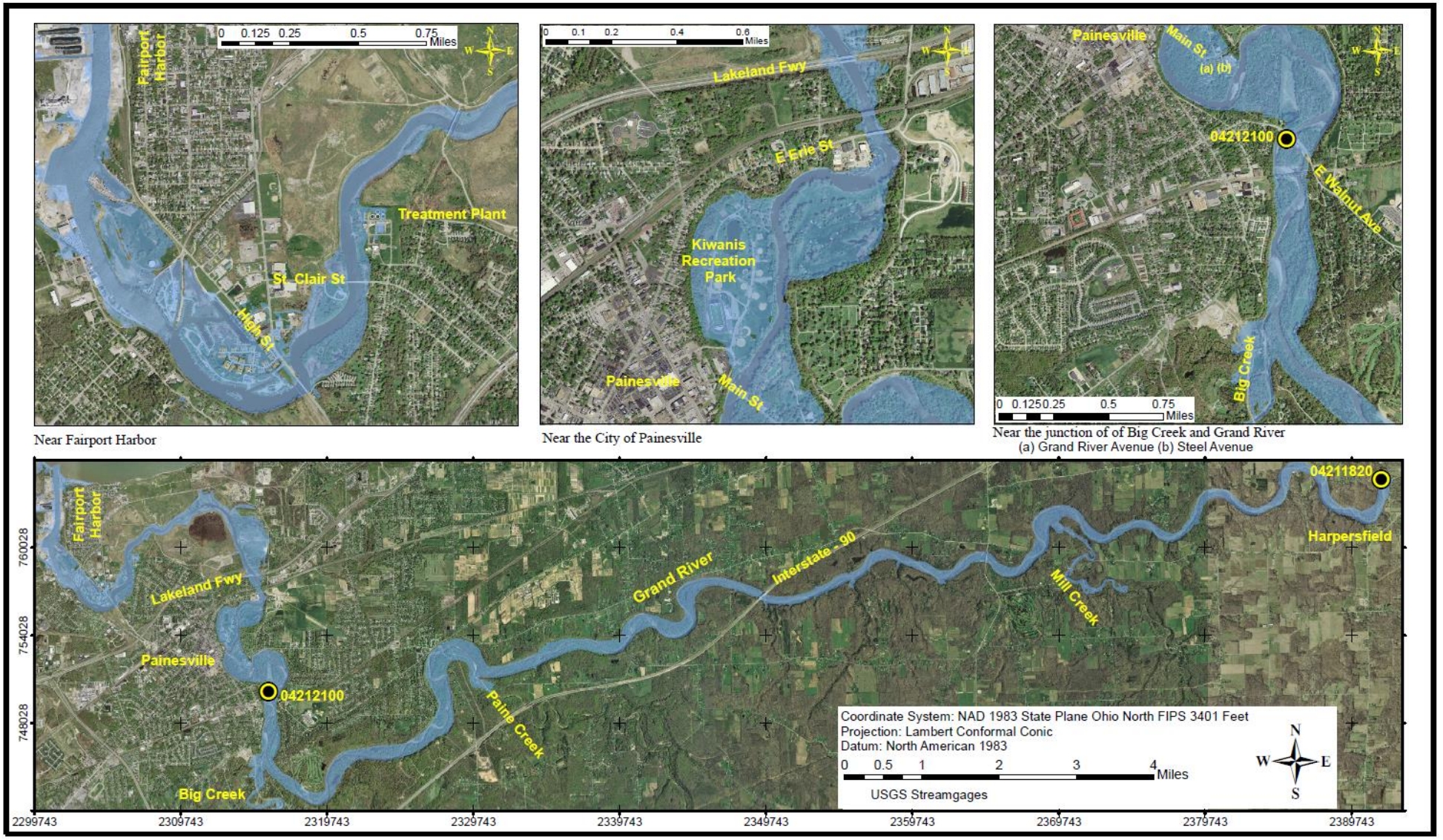

Figure 3-XI: Flood inundation map along the Grand River, for the stage of 20.00 feet, 615.59 feet NAVD 88 at 04212100 and the stage of 18.62 feet, 751.62 feet NAVD 88 at 04211820

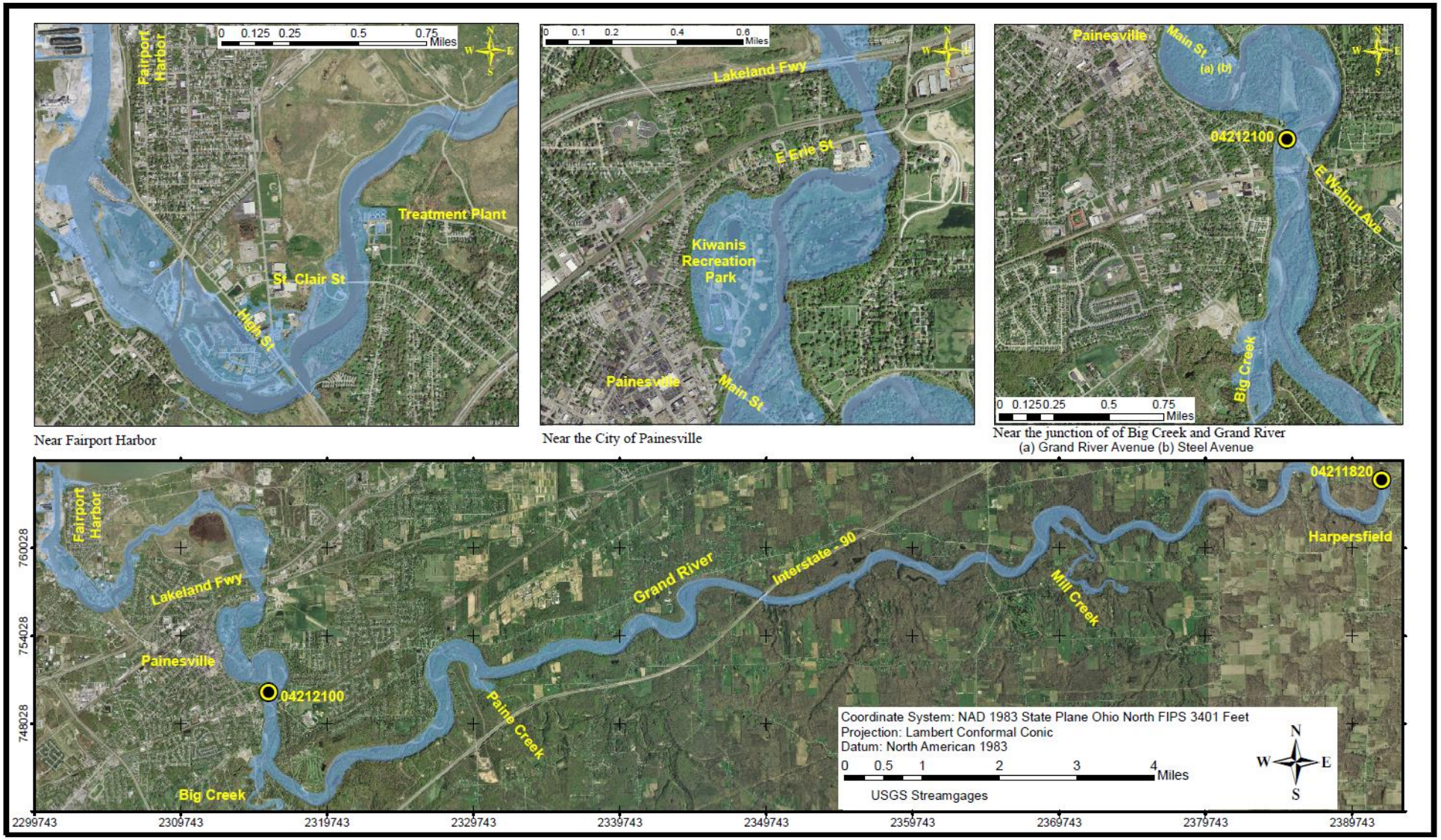

Figure 3-XII: Flood inundation map along the Grand River, for the stage of 21.00 feet, 616.59 feet NAVD 88 at 04212100 and the stage of 19.42 feet, 752.42 feet NAVD 88 at 04211820

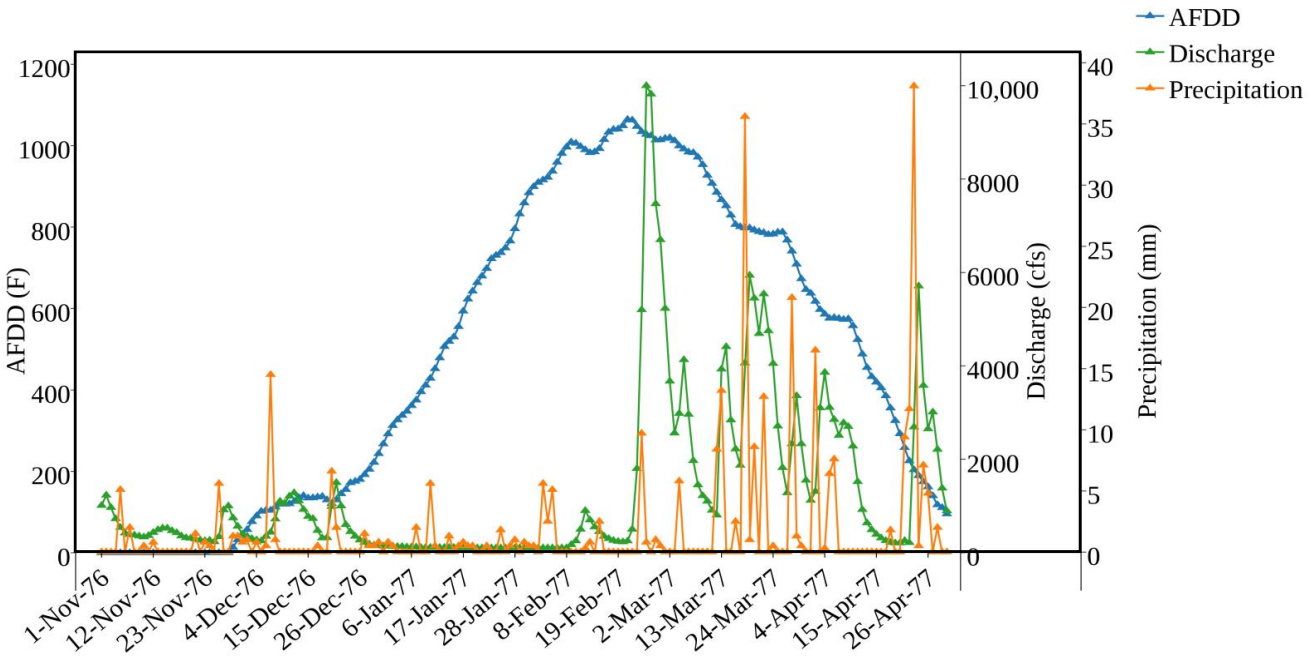

Figure 4-I: Relationship between AFDD, Discharge and Precipitation for 1976/1977

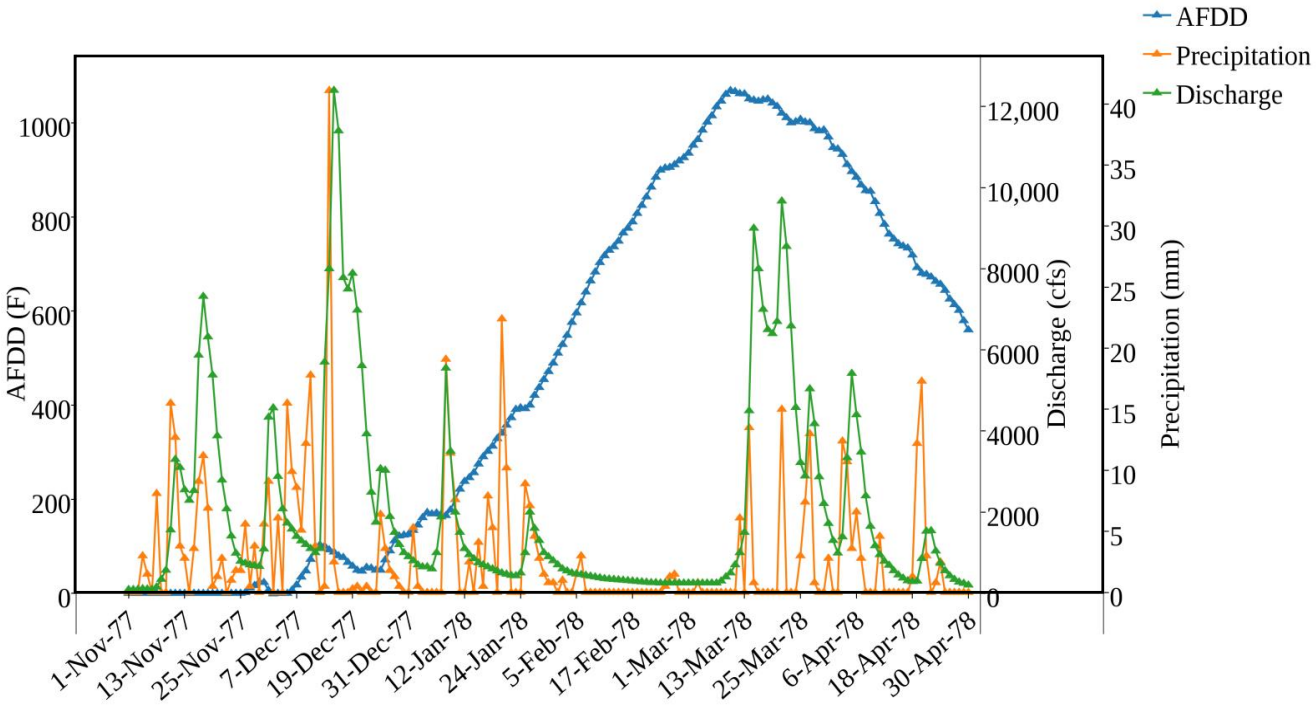

Figure 4-II: Relationship between AFDD, Discharge and Precipitation for 1977/1978

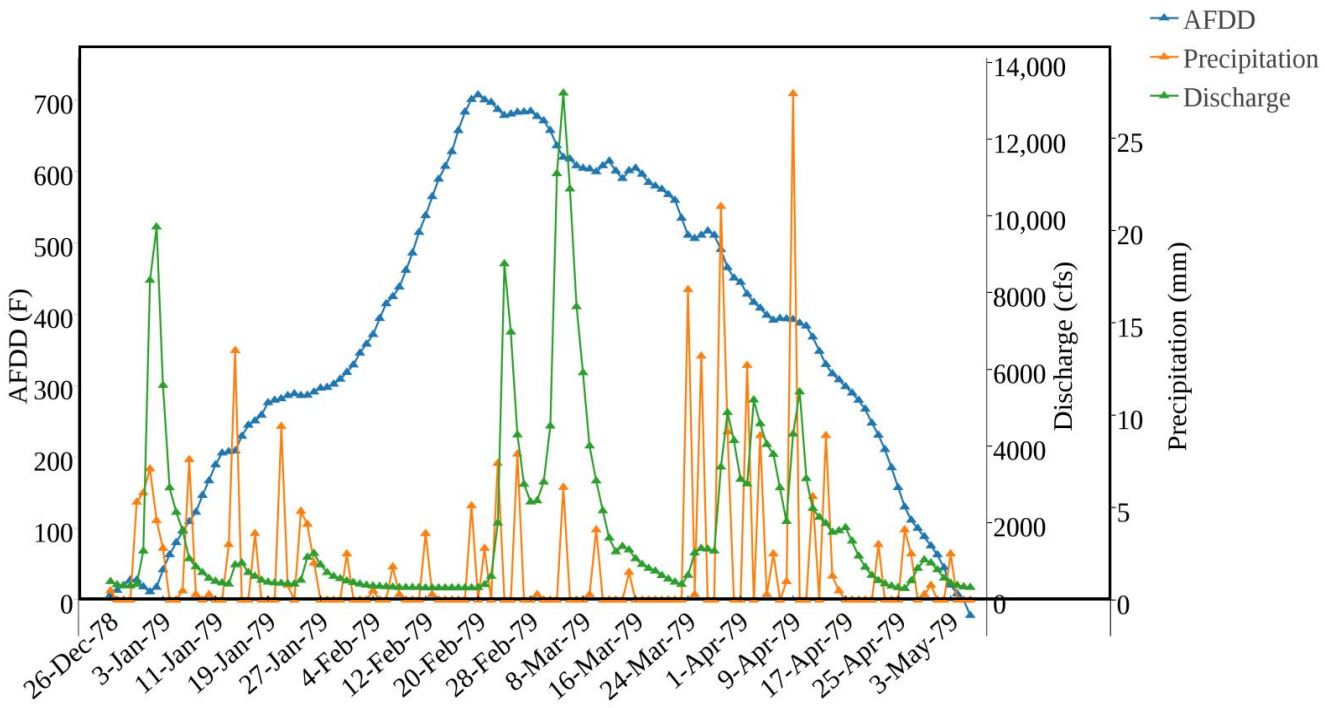

Figure 4-III: Relationship between AFDD, Discharge and Precipitation for 1978/1979

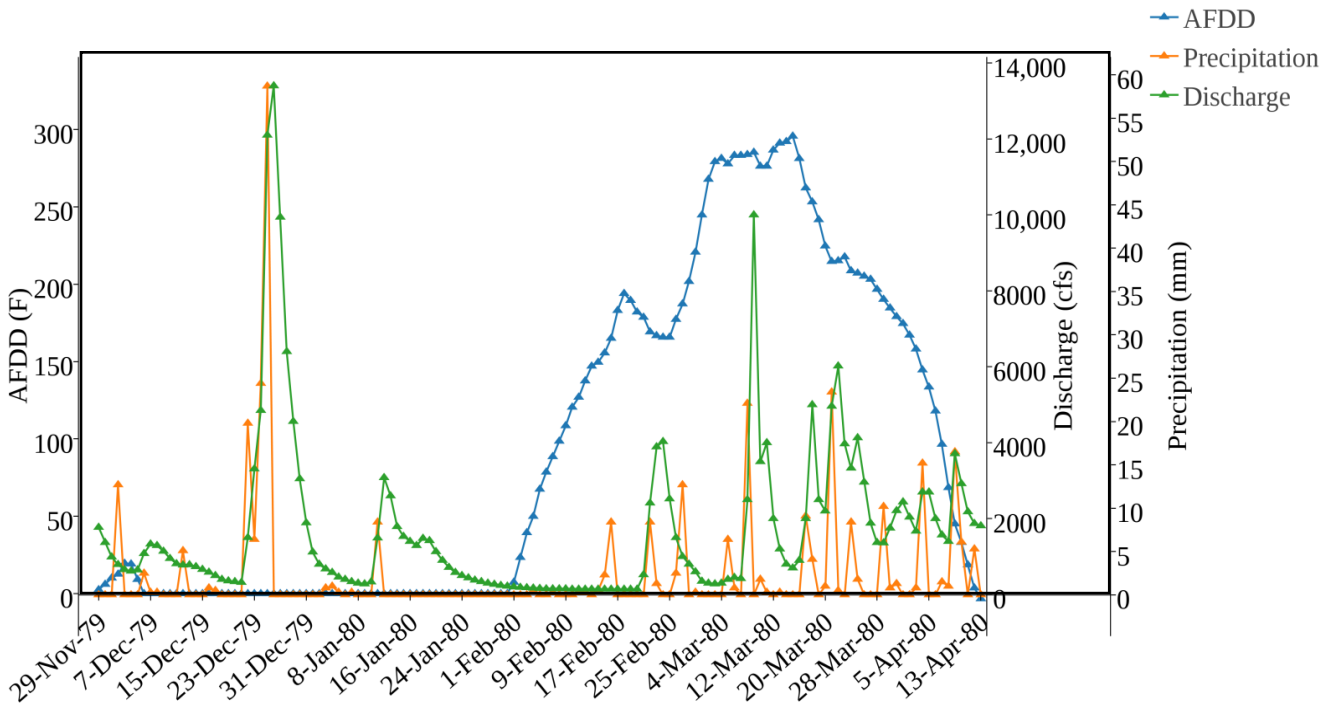

Figure 4-IV: Relationship between AFDD, Discharge and Precipitation for 1979/1980

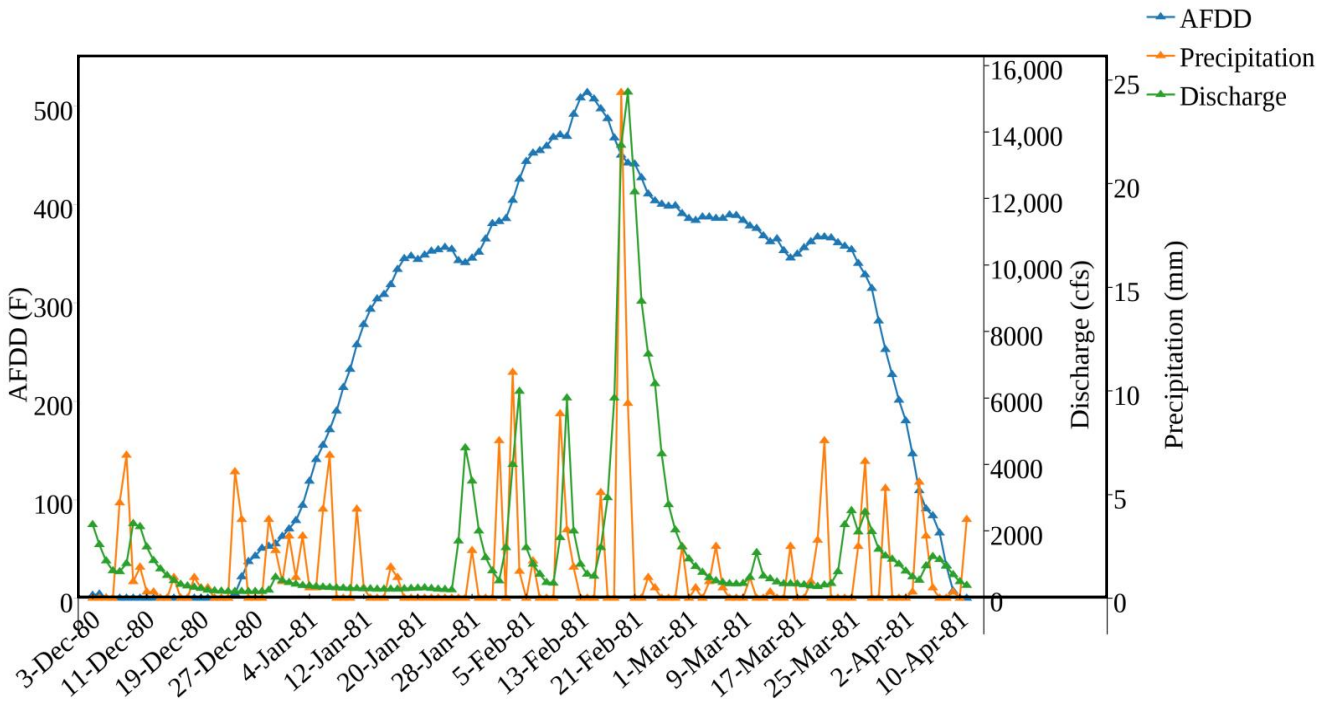

Figure 4-V: Relationship between AFDD, Discharge and Precipitation for 1980/1981

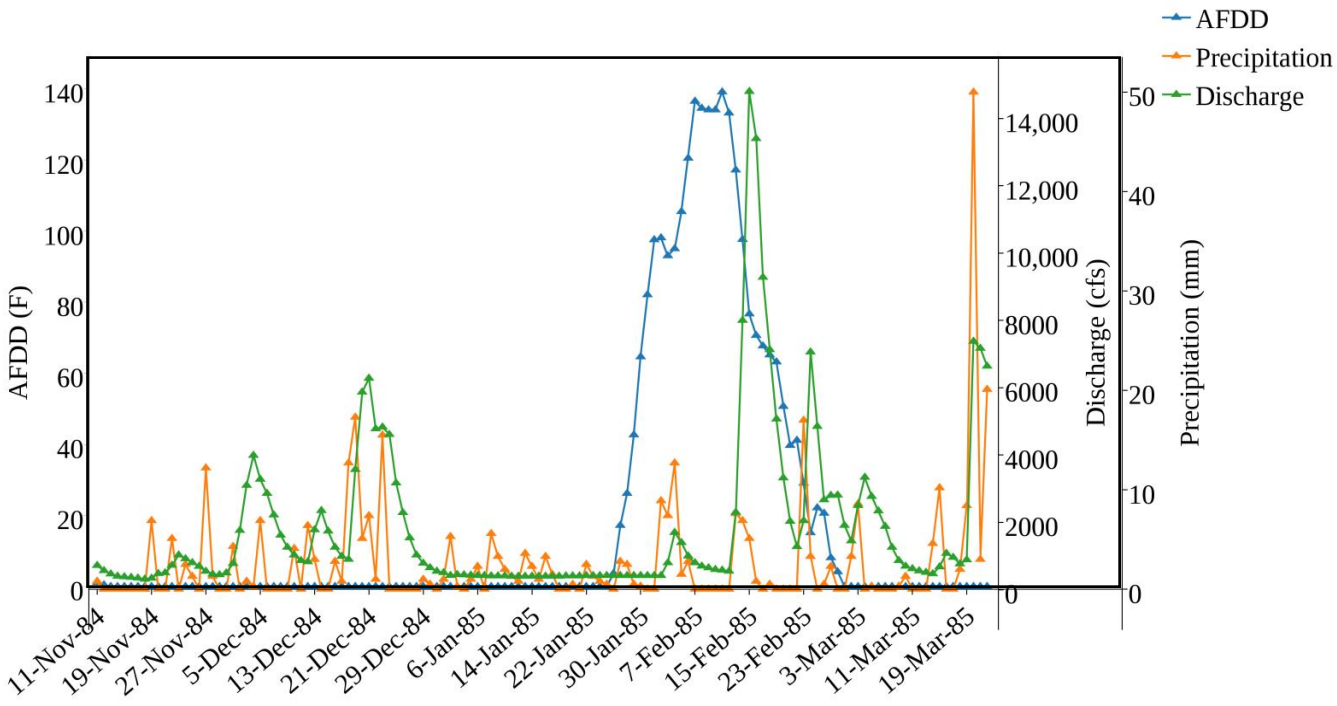

Figure 4-VI: Relationship between AFDD, Discharge and Precipitation for 1984/1985

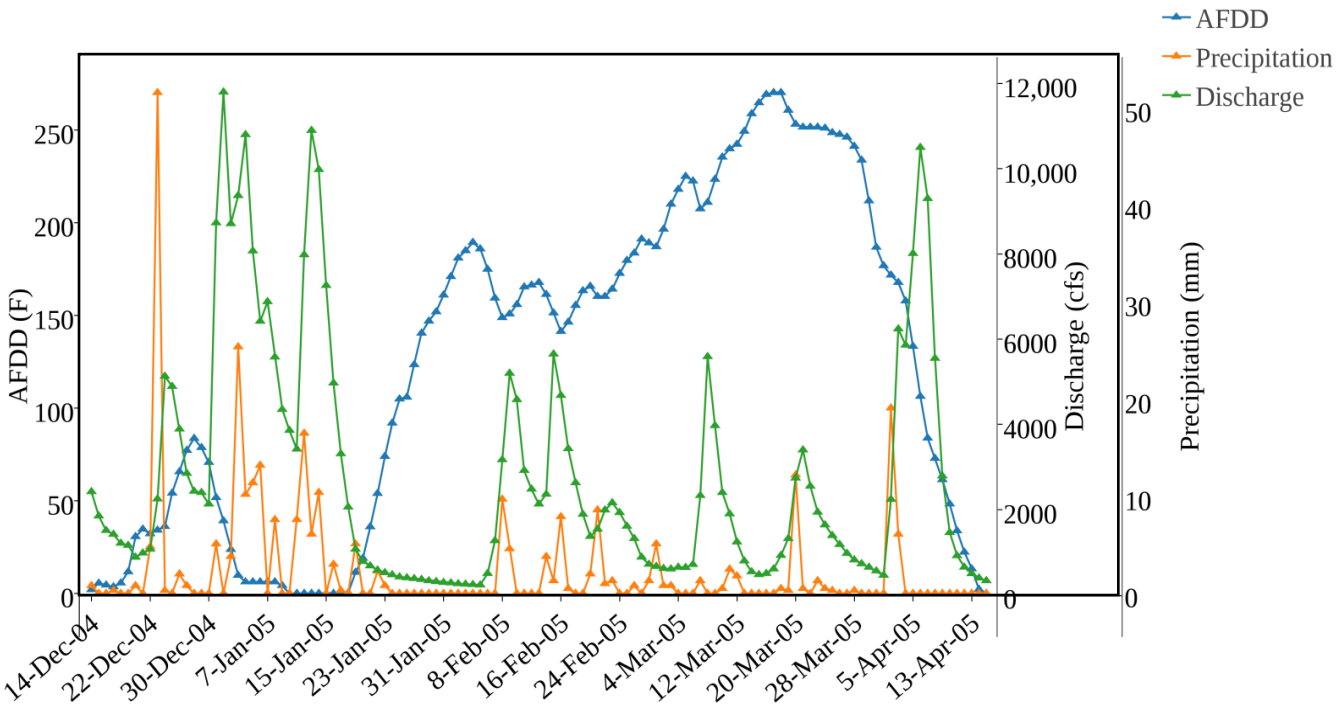

Figure 4-VII: Relationship between AFDD, Discharge and Precipitation for 2004/2005

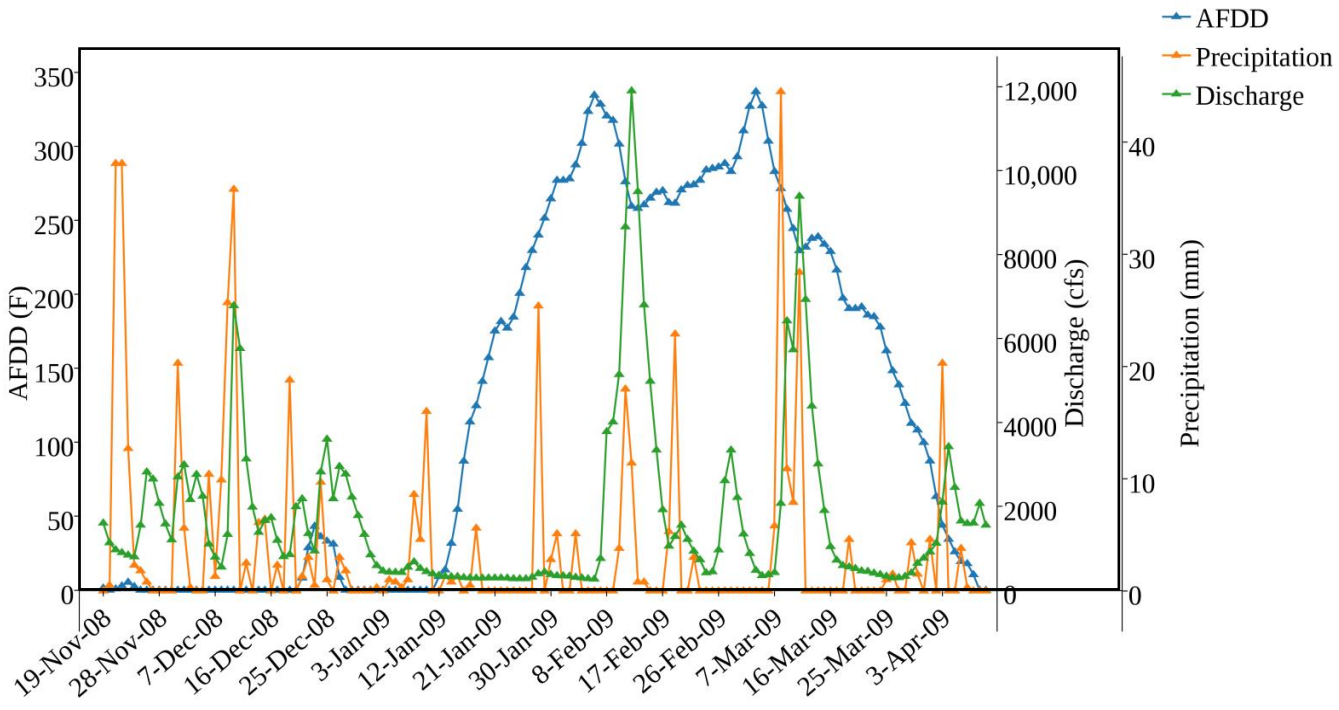

Figure 4-VIII: Relationship between AFDD, Discharge and Precipitation for 2008/2009

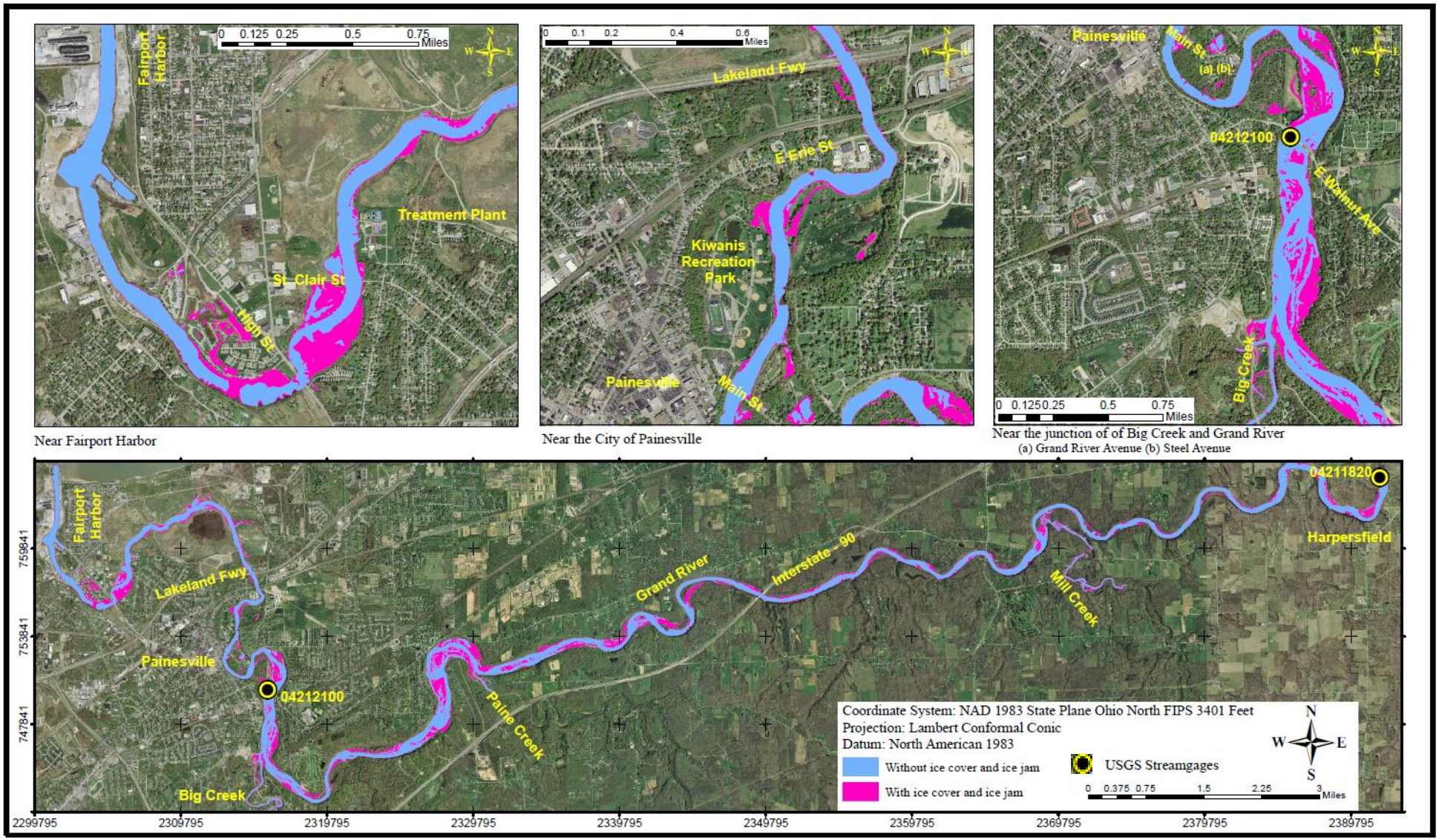

Figure 4-IX: Flood inundation Map along the Grand River considering ice cover and ice jam effects for 25 percentile winter flow.

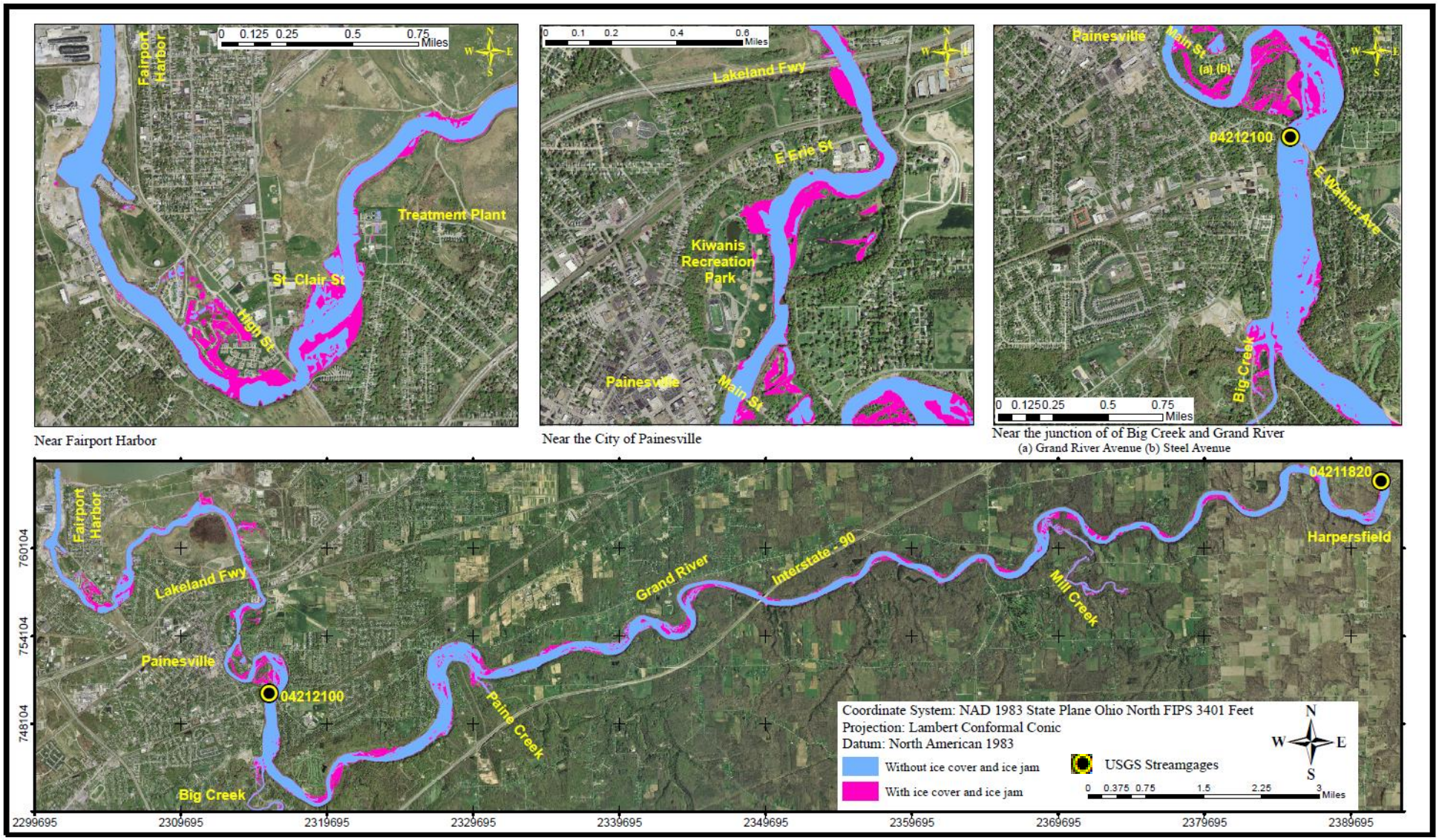

Figure 4-X: Flood inundation Map along the Grand River considering ice cover and ice jam effects for 50 percentile winter flow.

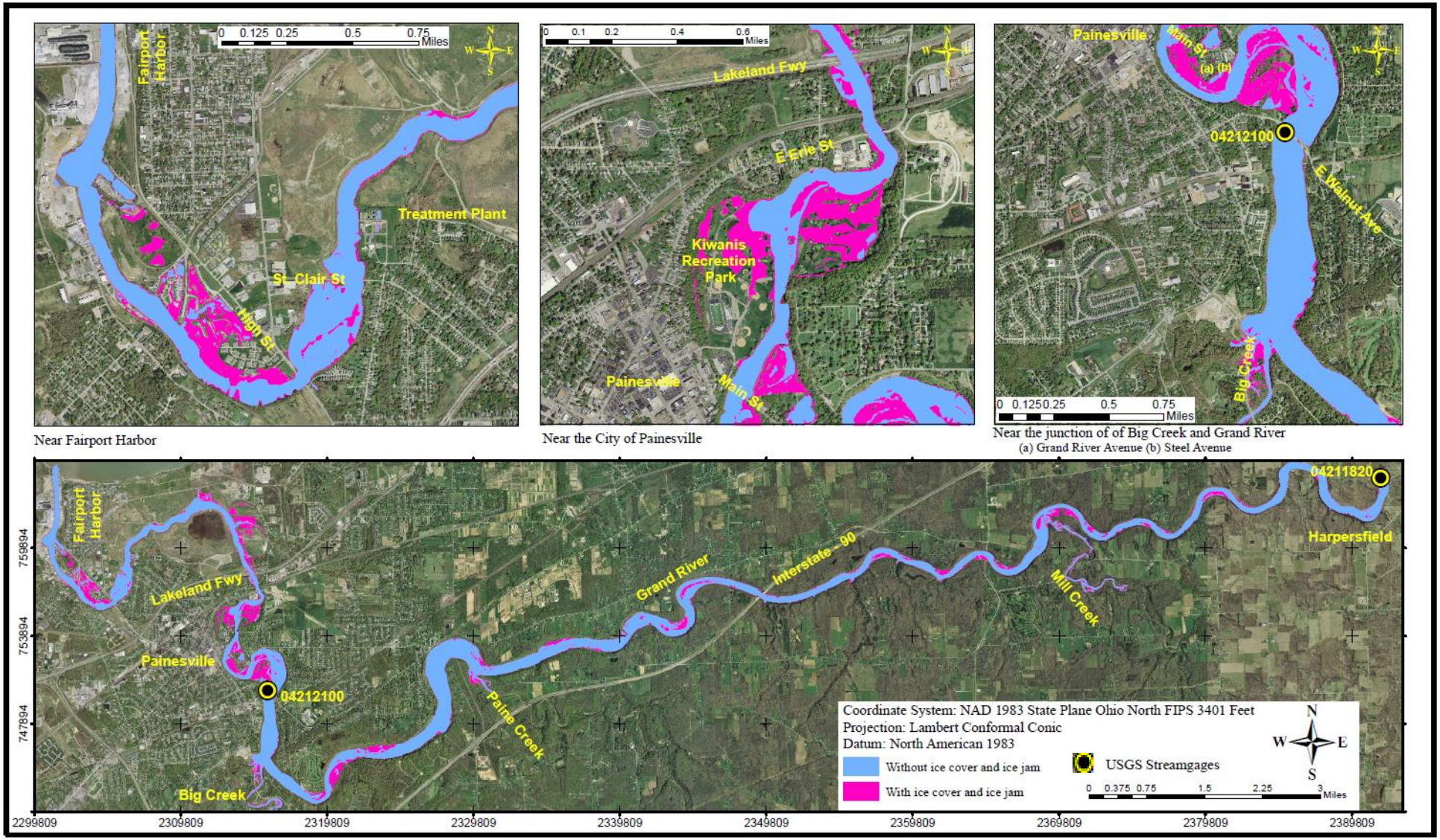

Figure 4-XI: Flood inundation Map along the Grand River considering ice cover and ice jam effects for 75 percentile winter flow.

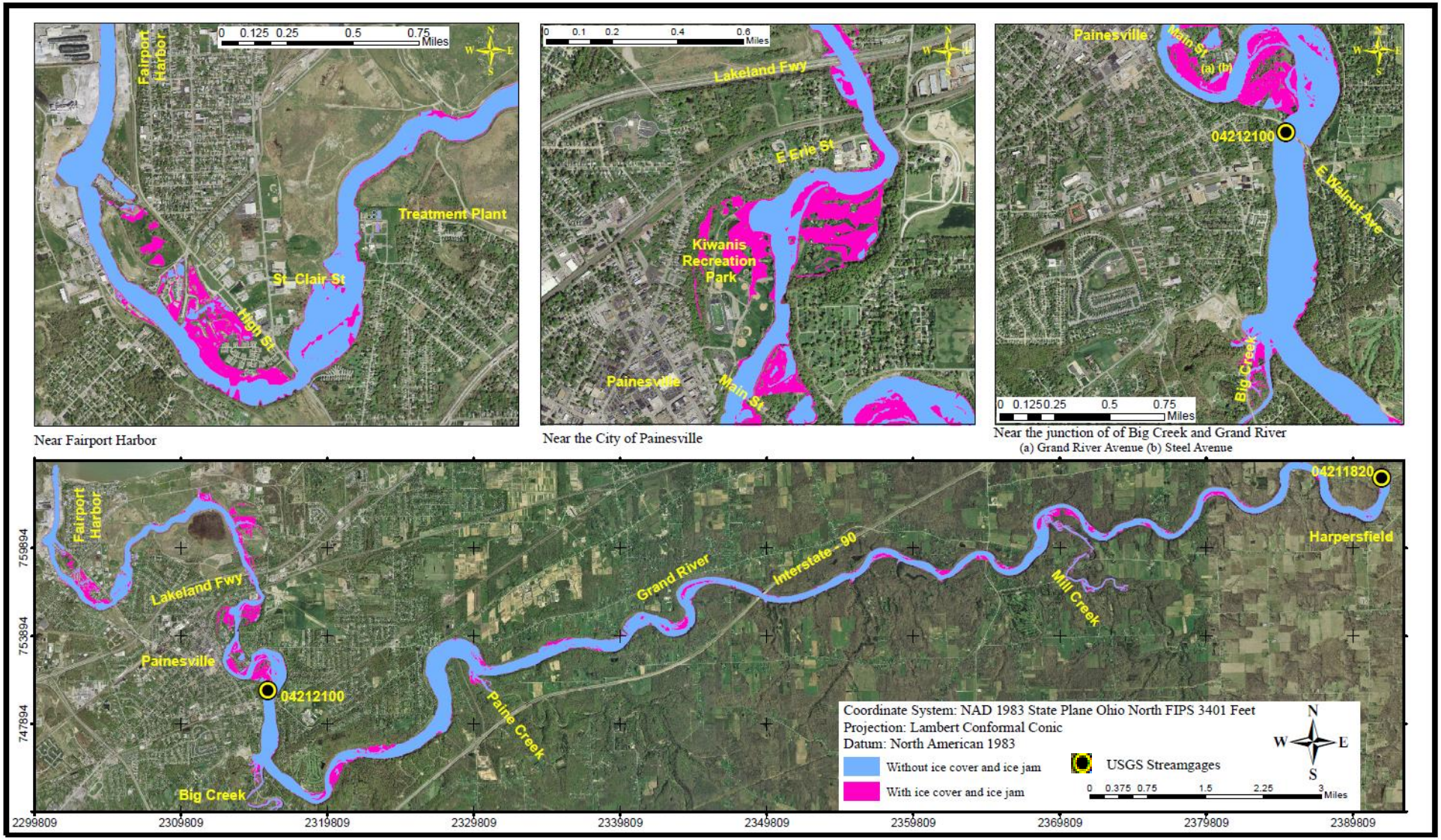

Figure 4-XII: Flood inundation Map along the Grand River considering ice cover and ice jam effects for 90 percentile winter flow.

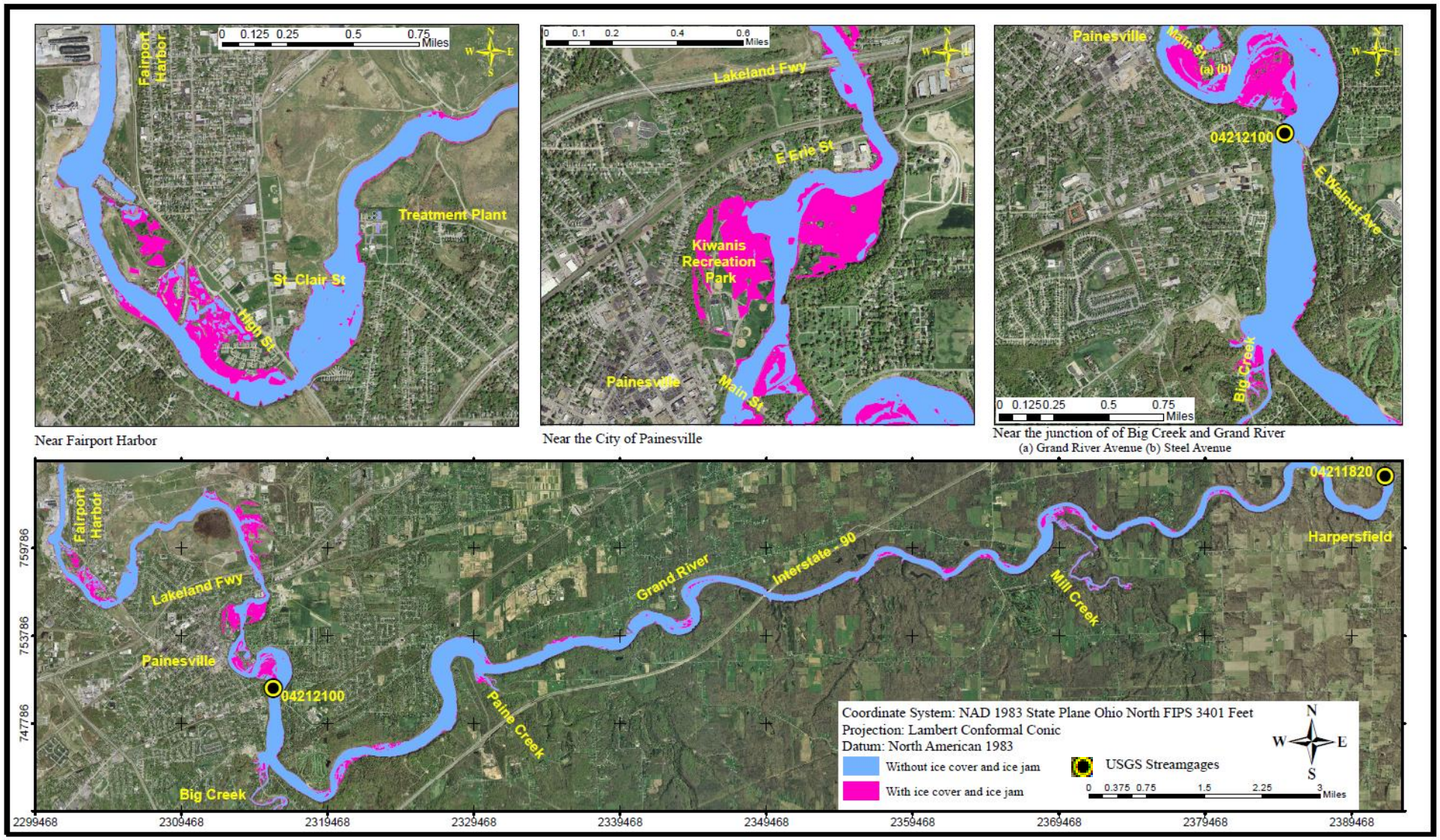

Figure 4-XIII: Flood inundation Map along the Grand River considering ice cover and ice jam effects for 100 percentile winter flow.